Large scale wavefield reconstruction via weighted matrix factorization and seismic survey design

Yijun Zhang

May, 2023

SLIM
Georgia Institute of Technology

Motivation

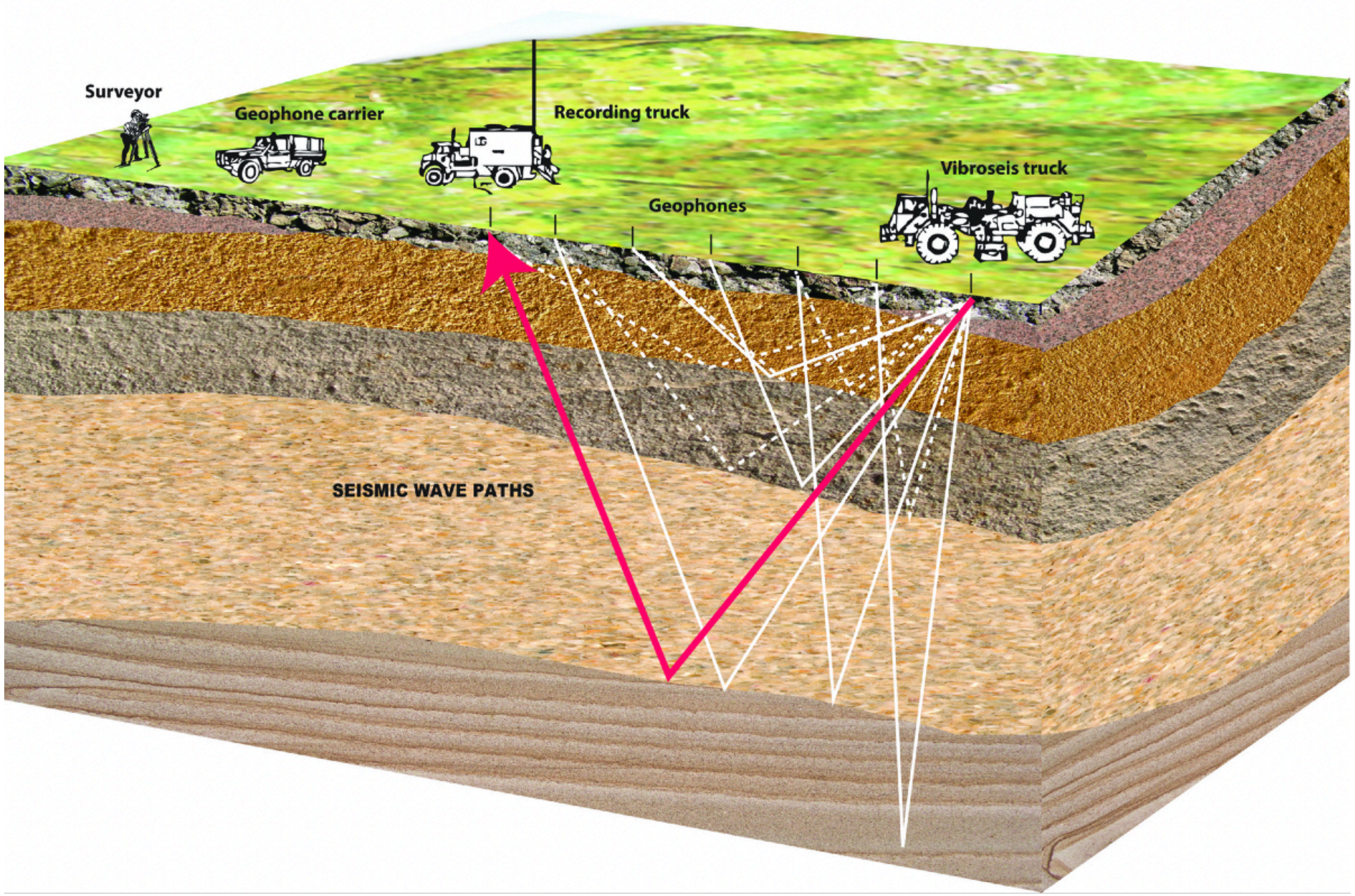

Fully sampled data

- needs for high resolution image

Seismic data

- expensive to acquire

Solution

- acquire subsampled data
- wavefield reconstruction

High-frequency wavefield recovery with weighted matrix factorizations

Chapter 2 & 3

Rajiv Kumar, Curt Da Silva, Okan Akalin, Aleksandr Y. Aravkin, Hassan Mansour, Ben Recht, and Felix J. Herrmann, “Efficient matrix completion for seismic data reconstruction”, Geophysics, vol. 80, pp. V97-V114, 2015.
Zhang, Y. et al. “High-frequency wavefield recovery with weighted matrix factorizations.” In SEG Technical Program Expanded Abstracts, 2019.

SLIM

Motivations

Fully sampled data

- needs for multiple removal, migration & FWI

Seismic data

- expensive to acquire

Conventional matrix completion

- exploits low-rank structure for recovery
- computationally efficient method
- performance degrades w/ increasing frequency

Question: Can we improve the recovered result at high frequencies?

Matrix completion

Matrix completion

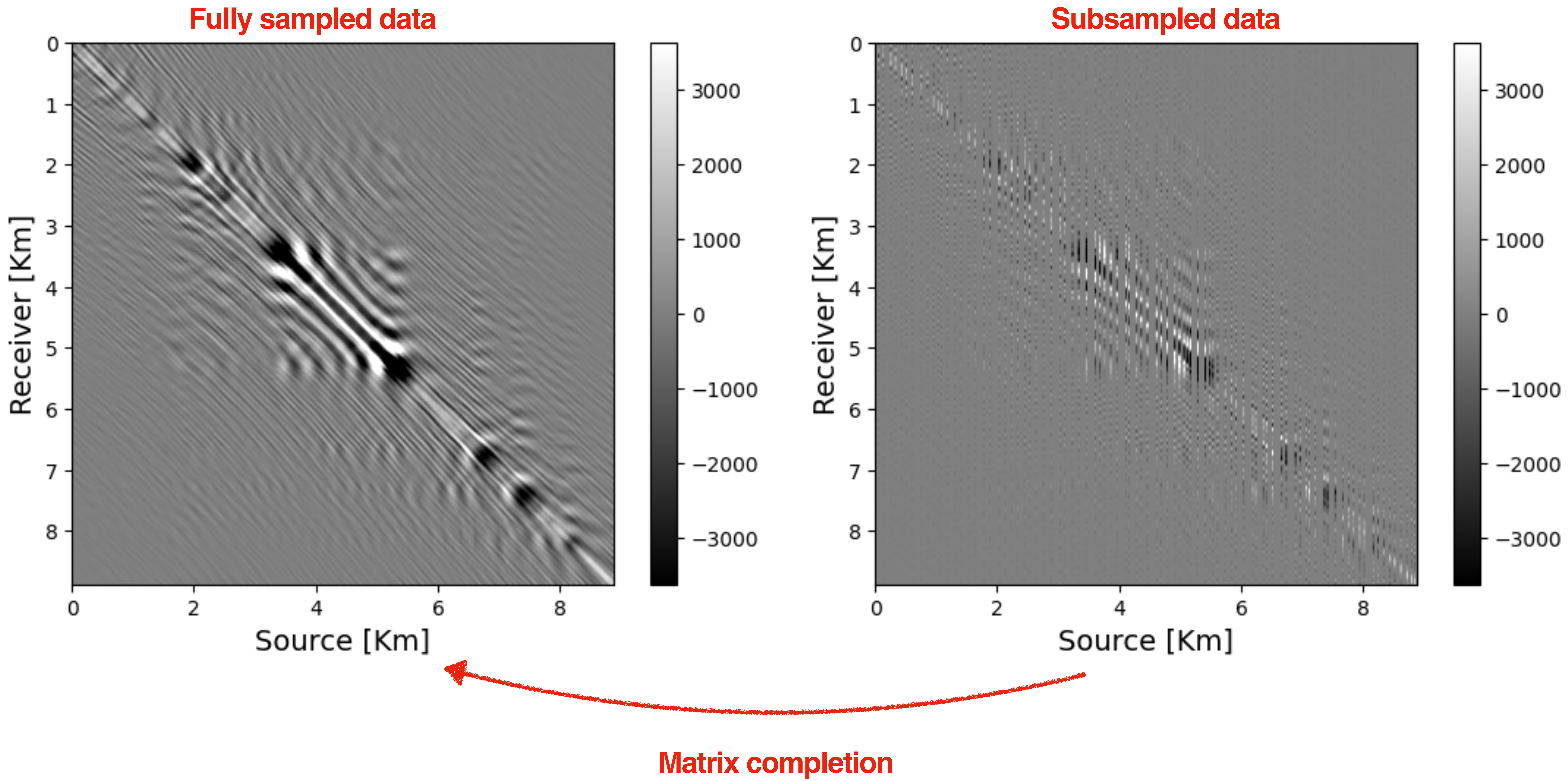

SLIM

Matrix completion

Successful matrix completion strategy

- Exploit low rank structure in “some domain”
  - fast decay of singular values
- Sample randomly
  - increase rank in “some domain”
- Optimization
  - via rank-minimization

Kumar, Rajiv. "Enabling large-scale seismic data acquisition, processing and waveform-inversion via rank-minimization." PhD diss., University of British Columbia, 2017.

SLIM

Matrix completion

Successful matrix completion strategy

- Exploit low rank structure in “some domain”
  - fast decay of singular values
- Sample randomly
  - increase rank in “some domain”
- Optimization
  - via rank-minimization

Aminzadeh, Fred, and Shivaji N. Dasgupta. "Fundamentals of Petroleum Geophysics." In *Developments in Petroleum Science*, vol. 60, pp. 37-92. Elsevier, 2013.

SLIM

Low-rank structure
(w/ 2D seismic survey)

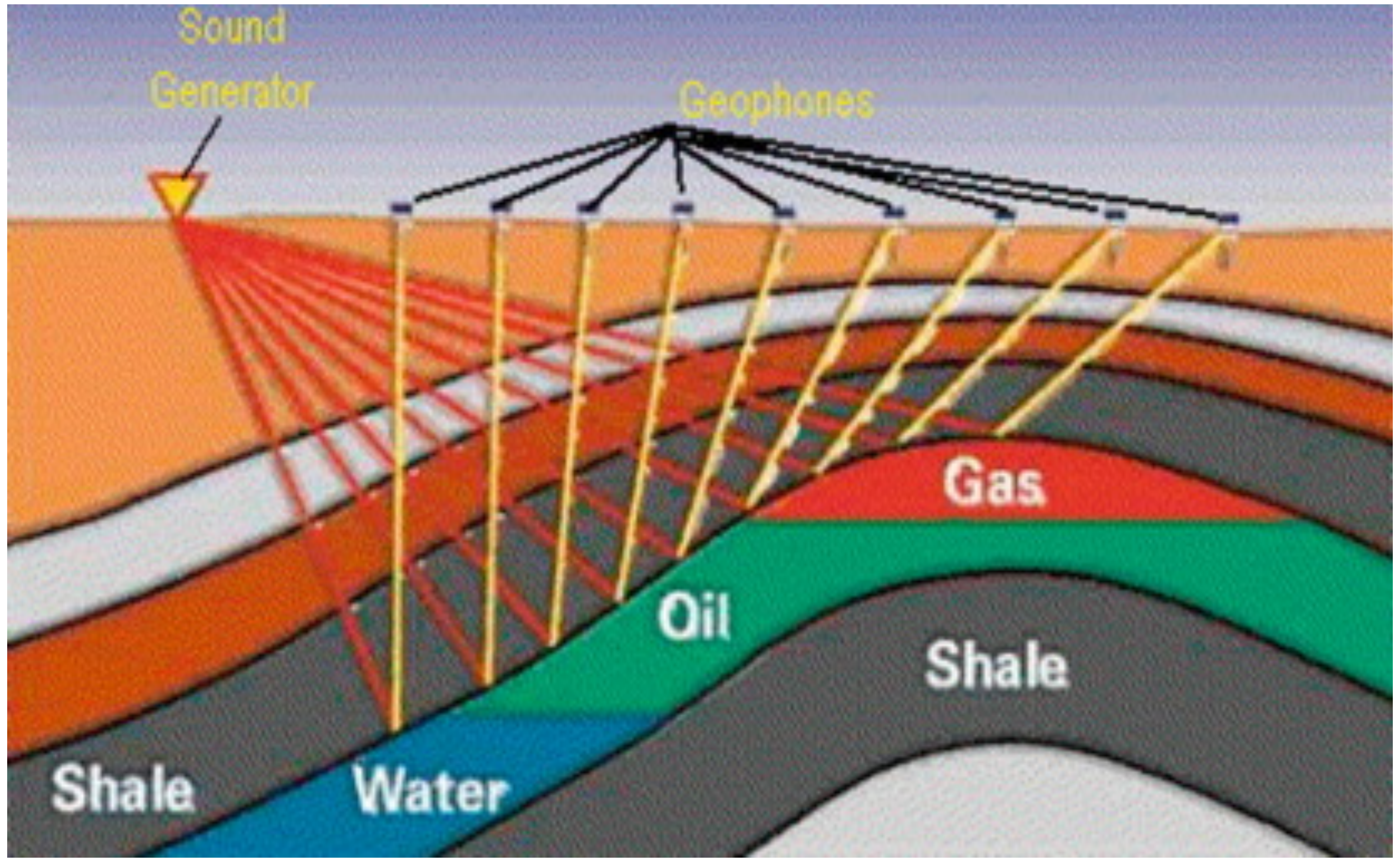

Low-rank structure

2D monochromatic slice (~10Hz) in source-receiver domain

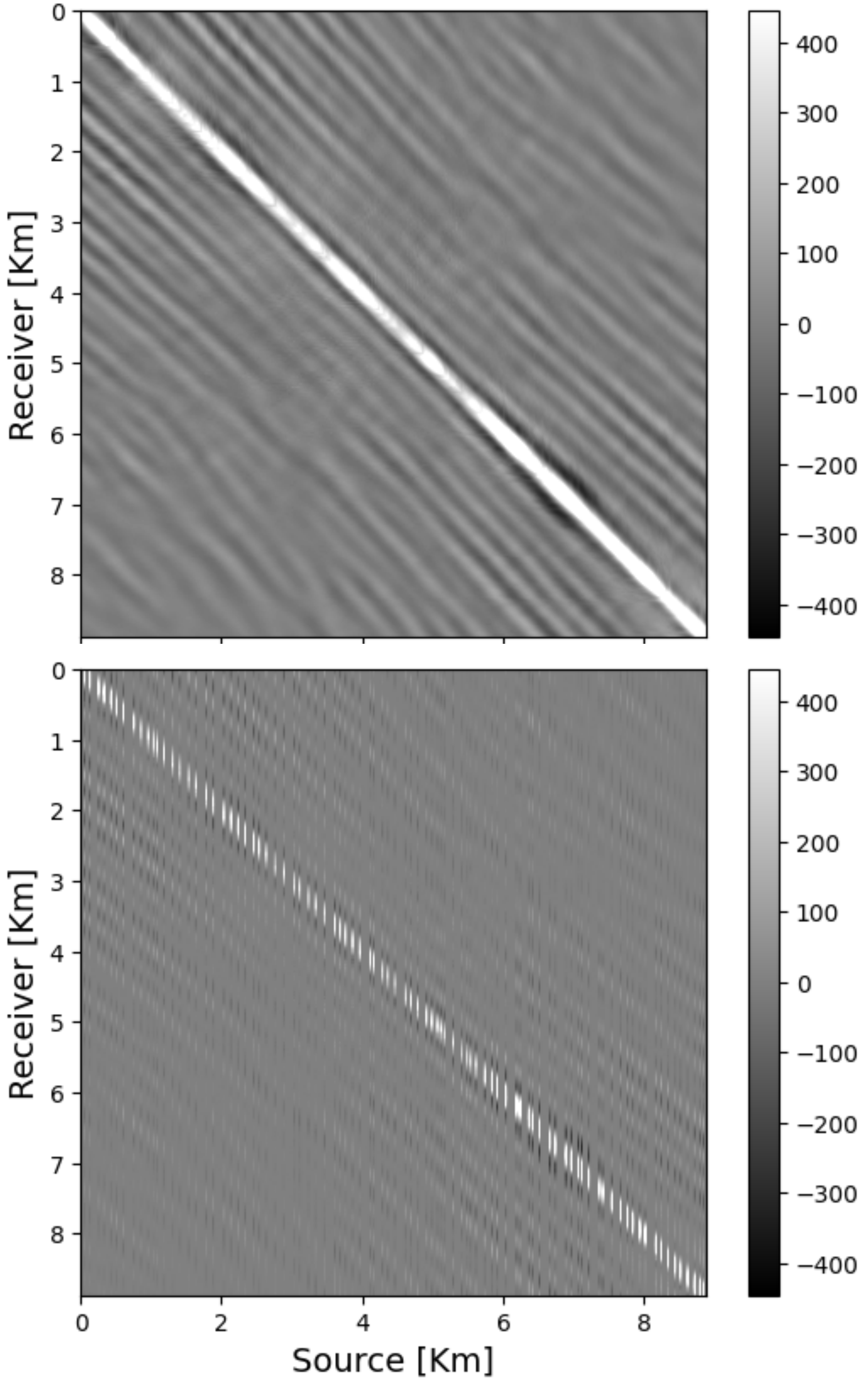

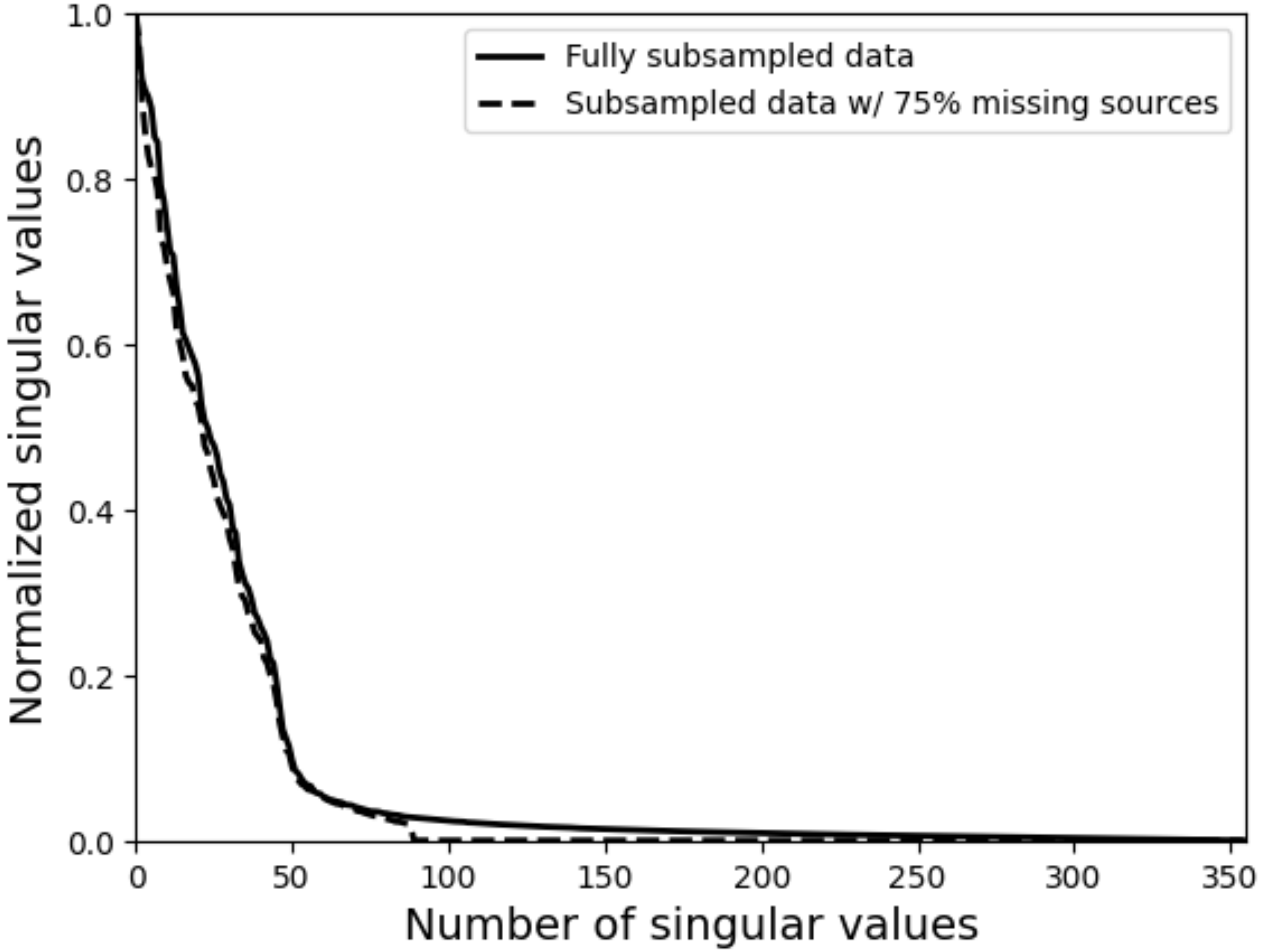

Low-rank structure

2D monochromatic slice (~10Hz) in midpoint-offset domain

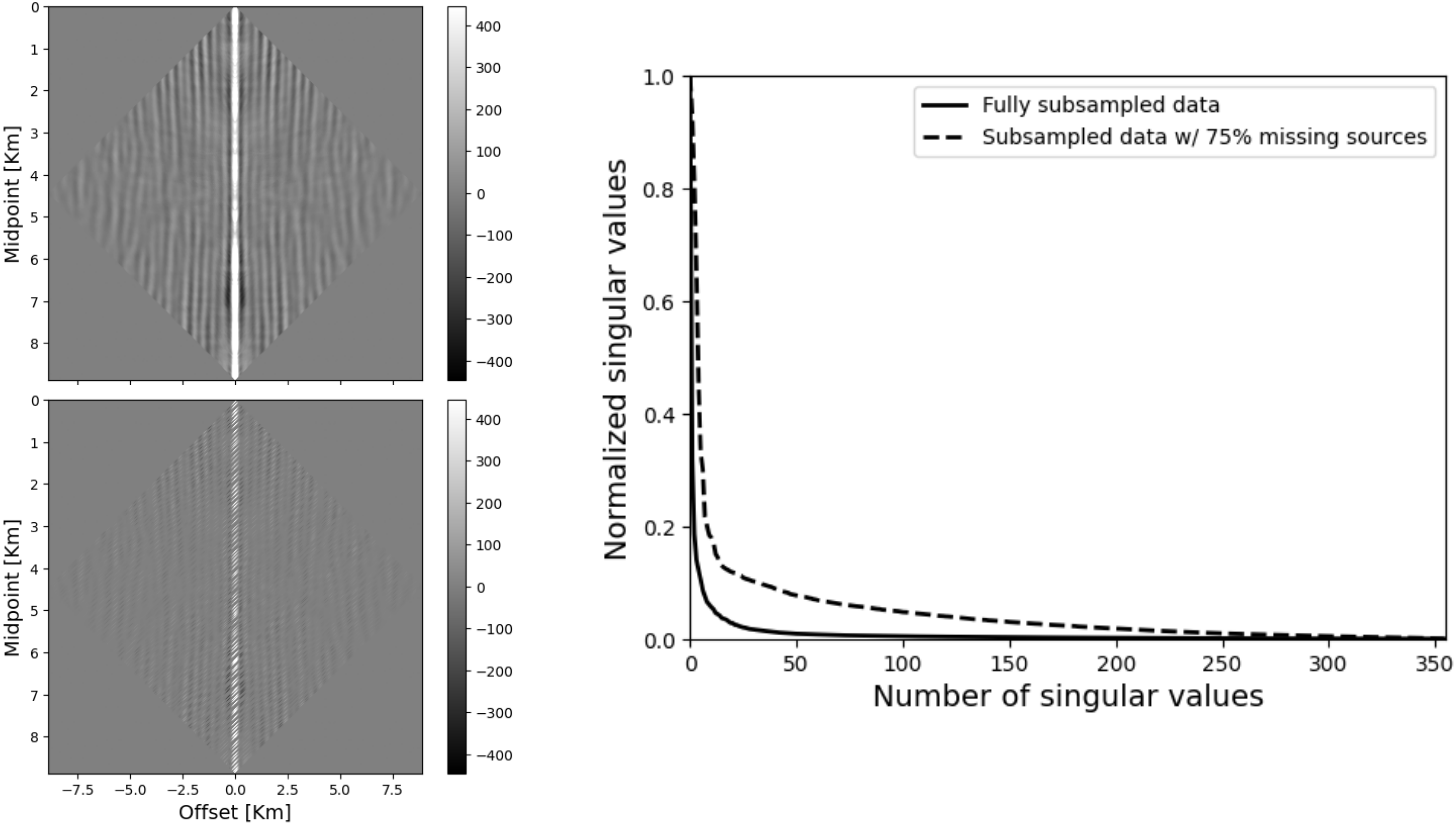

Matrix completion

Successful matrix completion strategy

- Exploit low rank structure in "some domain"
  - fast decay of singular values
- Sample randomly
  - increase rank in "some domain"
- Optimization
  - via rank-minimization

Conventional method

Rank minimization

Hard to solve

$$\underset{\mathbf{X}\in\mathbb{C}^{m\times n}}{\text{minimize}} \quad \underbrace{\text{rank}(\mathbf{X})}_{\textbf{number of singular values of X}} \quad \text{subject to} \quad \| \mathscr{A}(\mathbf{X}) - \mathbf{B} \|_F \leq \epsilon$$

- $\mathscr{A}$: acquisition mask
- $\mathbf{B} \in \mathbb{C}^{m\times n}$: observed data
- $\| \cdot \|_F$: Frobenius norm

Rajiv Kumar, Curt Da Silva, Okan Akalin, Aleksandr Y. Aravkin, Hassan Mansour, Ben Recht, and Felix J. Herrmann, "Efficient matrix completion for seismic data reconstruction", Geophysics, vol. 80, pp. V97-V114, 2015

SLIM

Conventional method

Expensive for large scale

Low-rank matrix completion

$$\underset{\mathbf{X}\in\mathbb{C}^{m\times n}}{\text{minimize}} \quad \underbrace{\|\mathbf{X}\|_*}_{\textbf{sum of singular values of } \mathbf{X}} \quad \text{subject to} \quad \|\mathscr{A}(\mathbf{X}) - \mathbf{B}\|_F \leq \epsilon$$

Low-rank matrix factorization

$$\underset{\mathbf{L},\mathbf{R}}{\text{minimize}} \quad \frac{1}{2}\left\| \begin{bmatrix}\mathbf{L}\\ \mathbf{R}\end{bmatrix} \right\|_F^2 \quad \text{subject to} \quad \|\mathscr{A}(\mathbf{L}\mathbf{R}^H) - \mathbf{B}\|_F \leq \epsilon$$

- $\mathbf{X} = \mathbf{L}\mathbf{R}^H$
- $\mathbf{L} \in \mathbb{C}^{m\times r}$
- $\mathbf{R} \in \mathbb{C}^{n\times r}$

Motivation

Matrix completion

- performance degrades w/ increasing frequency

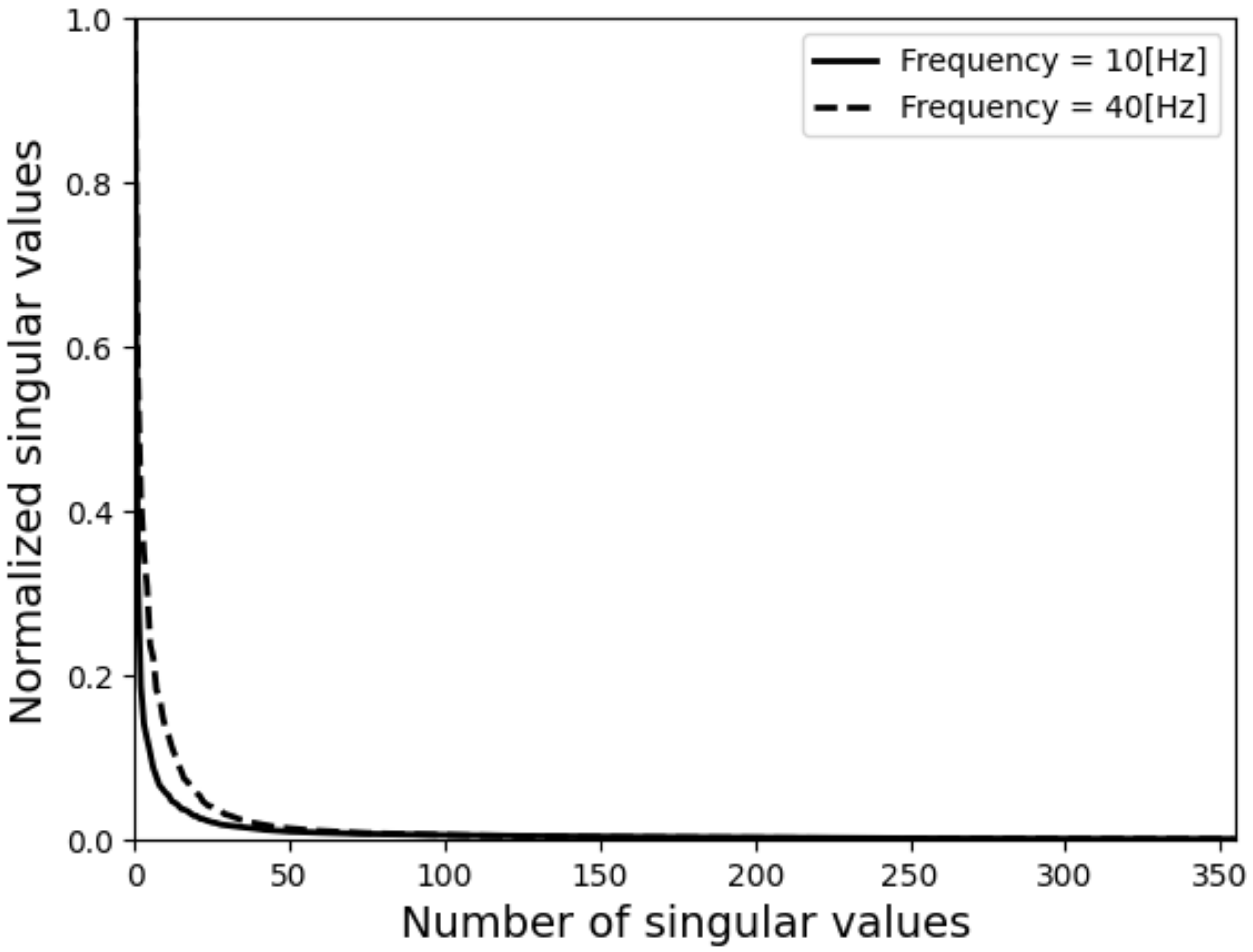

Fully sampled data

~40Hz slice

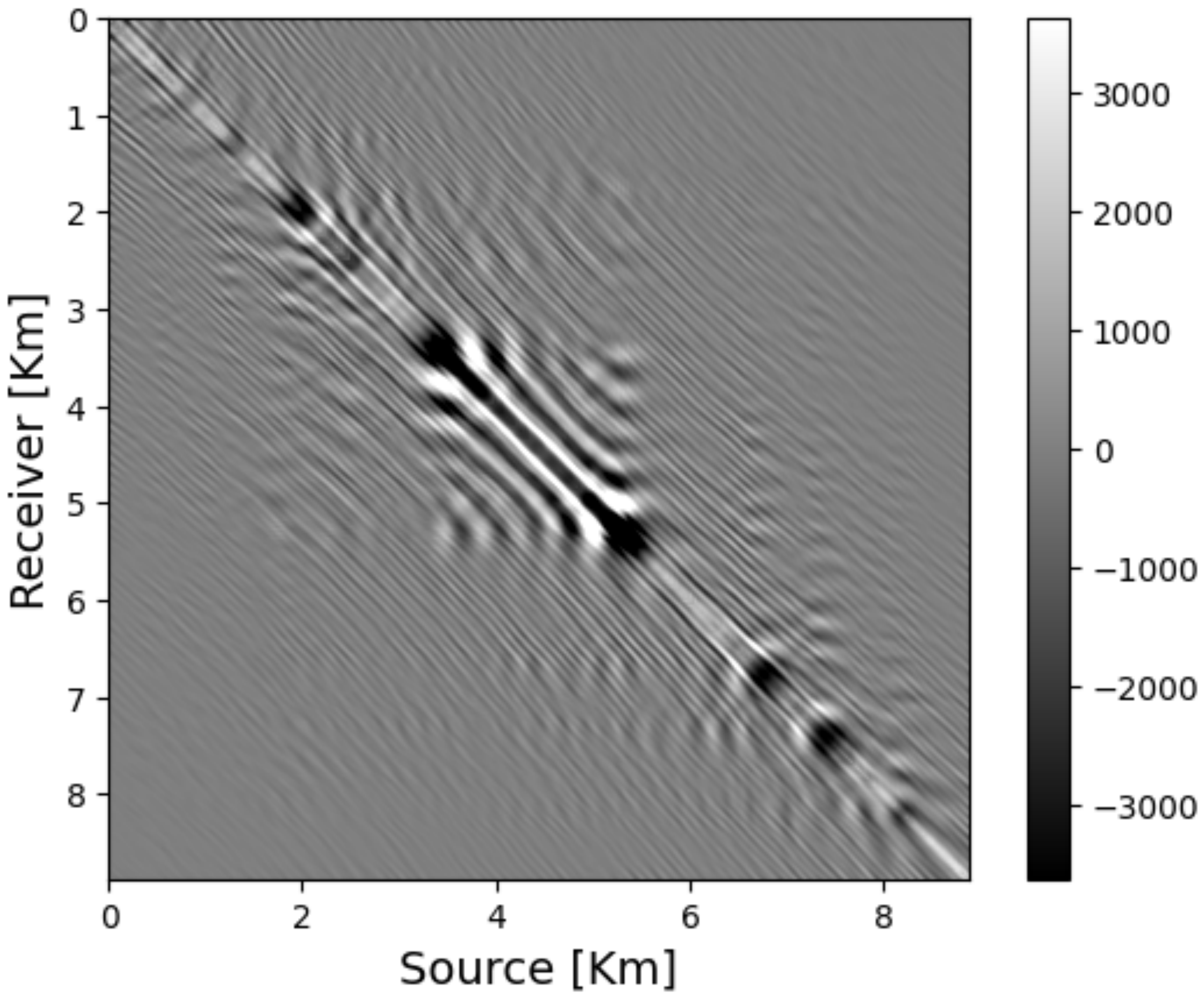

Observed data
75 % jittered subsampling

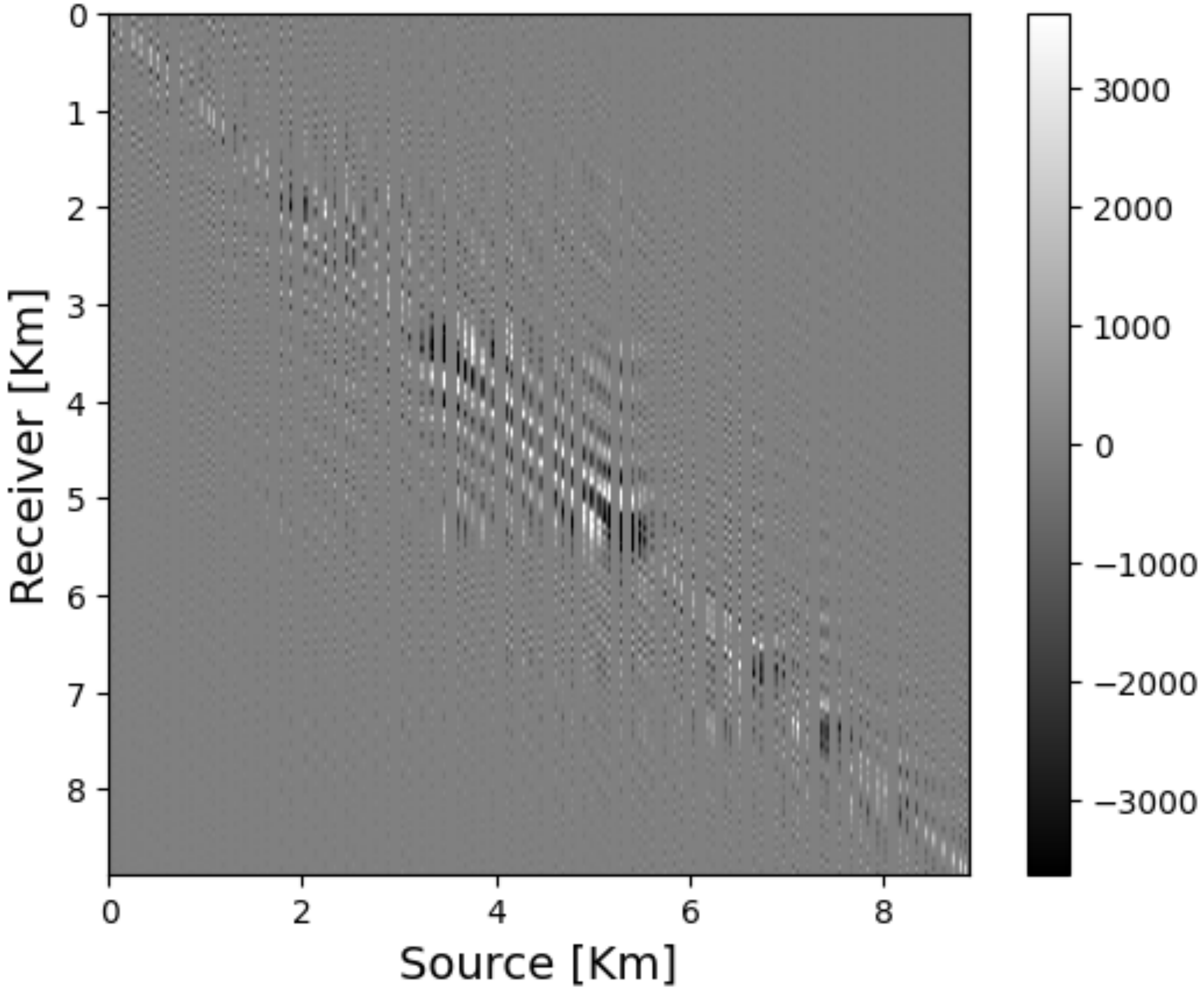

Herrmann, Felix J., and Gilles Hennenfent. "Non-parametric seismic data recovery with curvelet frames." *Geophysical Journal International* 173.1 (2008): 233-248.

Recovery
w/ conventional matrix completion

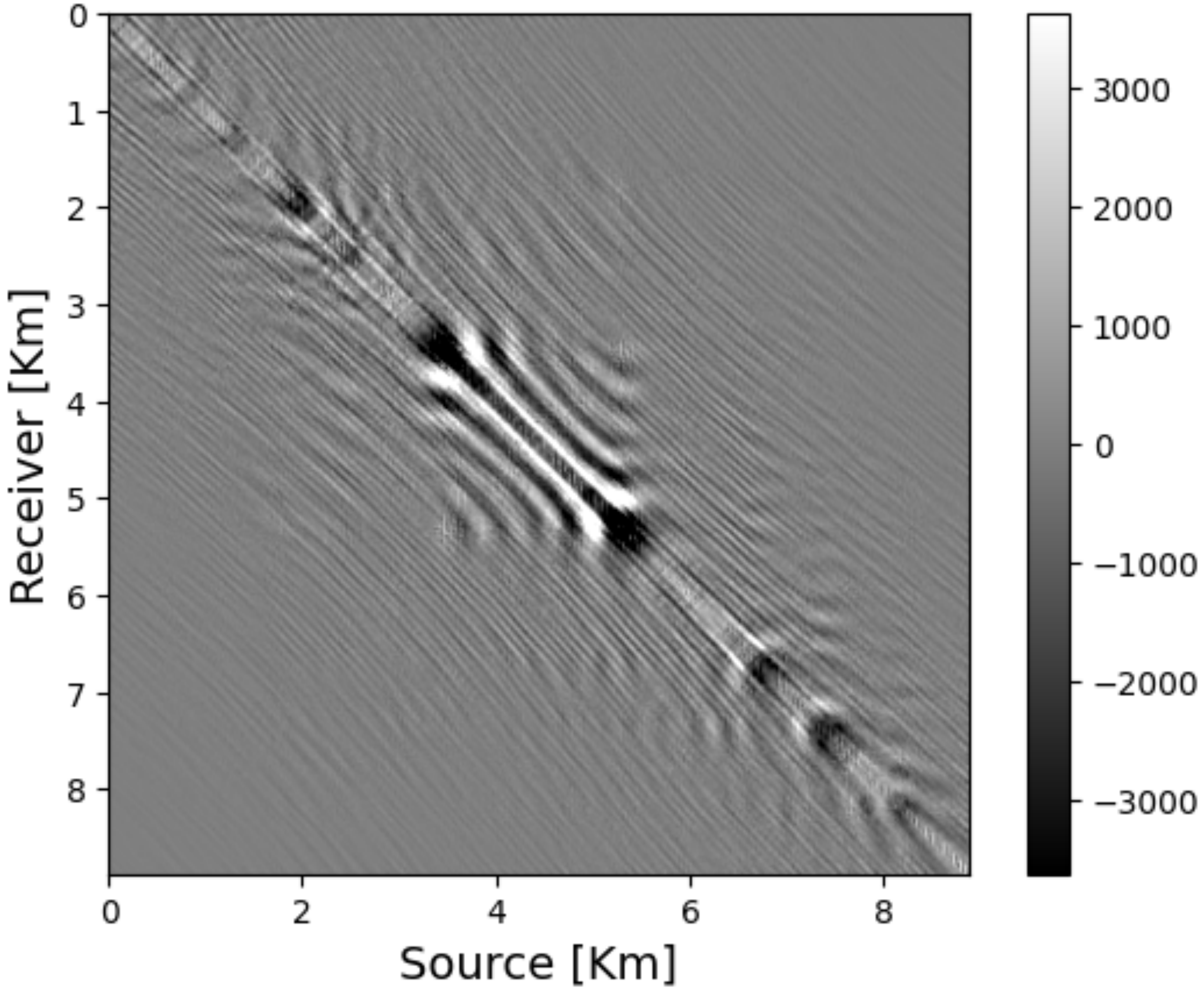

SNR = 9.49 dB
Rank = 30

Difference: True - Recovery
w/ conventional matrix completion

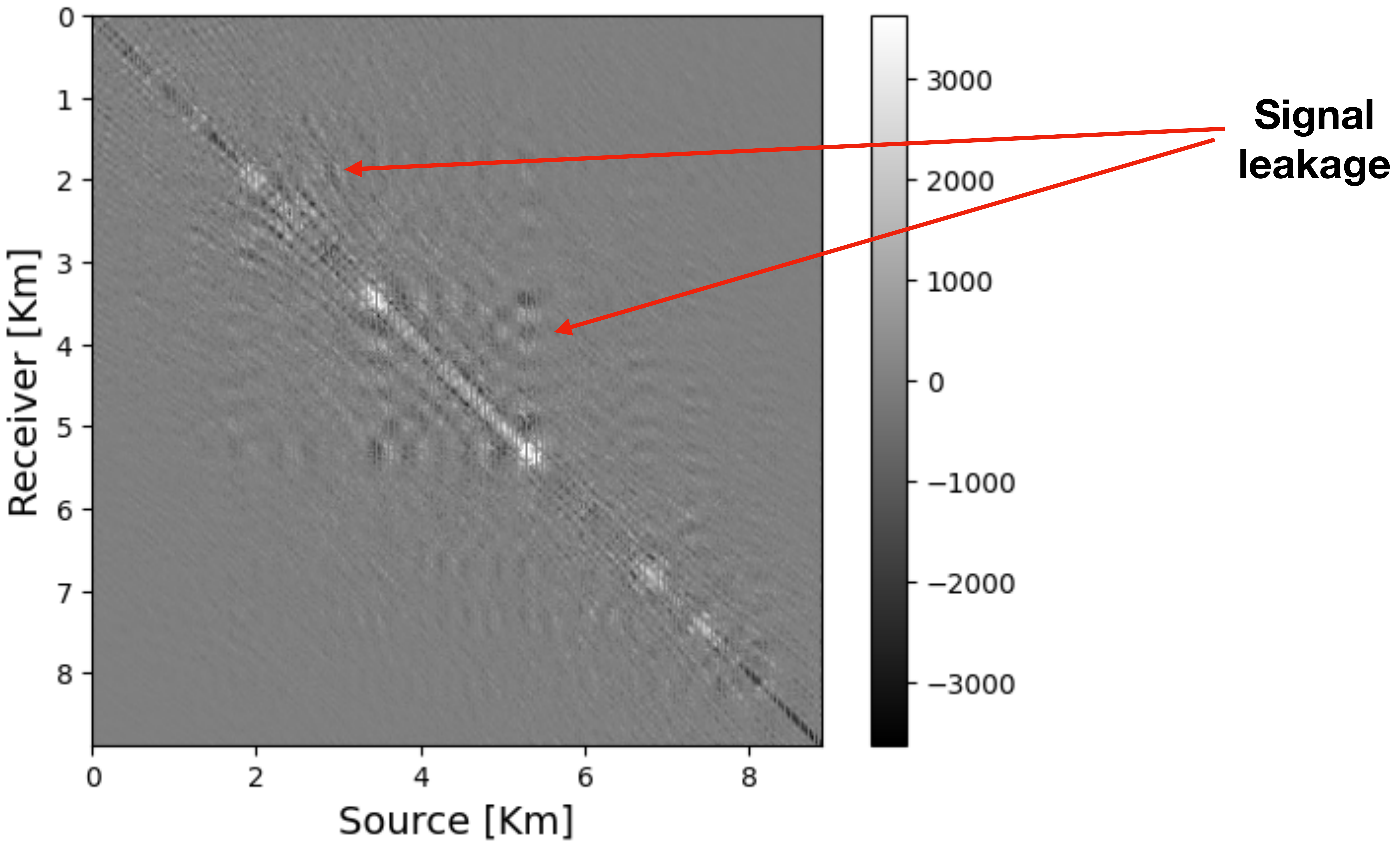

Question: Can we improve the recovered result at high frequencies?

Answer: Weighted matrix factorization

Zhang, Y. et al. “High-frequency wavefield recovery with weighted matrix factorizations.” In SEG Technical Program Expanded Abstracts, 2019.
Eftekhari, A. et al. “Weighted matrix completion and recovery with prior subspace information.” IEEE Transactions on Information Theory, 2018.

SLIM

Weighted method

Weighted matrix completion

$$\underset{\mathbf{X}\in\mathbb{C}^{m\times n}}{\text{minimize}} \quad \| \mathbf{QXW} \|_* \quad \text{subject to} \quad \| \mathscr{A}(\mathbf{X}) - \mathbf{B} \|_F \leq \epsilon$$

- $\mathbf{X}_{\text{prior}} \approx \mathbf{U\Sigma V}^H$, $\mathbf{U} \in \mathbb{C}^{m\times r}$, $\mathbf{V} \in \mathbb{C}^{n\times r}$;
- $\mathbf{X}_{\text{prior}}$ comes from neighboring frequency slice
- $\mathbf{Q} = w_1\mathbf{UU}^H + \mathbf{U}^\perp\mathbf{U}^{\perp H}$
- $\mathbf{W} = w_2\mathbf{VV}^H + \mathbf{V}^\perp\mathbf{V}^{\perp H}$
- scalars $w_1, w_2 \in (0,1]$ are weights

Smaller weights correspond to more confidence on prior information

Zhang, Y. et al. “High-frequency wavefield recovery with weighted matrix factorizations.” In SEG Technical Program Expanded Abstracts, 2019.
Eftekhari, A. et al. “Weighted matrix completion and recovery with prior subspace information.” IEEE Transactions on Information Theory, 2018.

Weighted method

Weighted matrix factorization

$$\underset{\mathbf{L},\mathbf{R}}{\text{minimize}} \quad \frac{1}{2}\left\| \begin{bmatrix} \mathbf{QL} \\ \mathbf{WR} \end{bmatrix} \right\|_F^2 \quad \text{subject to} \quad \left\| \mathscr{A}(\mathbf{L}\mathbf{R}^H) - \mathbf{B} \right\|_F \leq \epsilon$$

- expensive computation

How could this weighted technique be made more efficient?

Zhang, Yijun, et al. "Wavefield recovery with limited-subspace weighted matrix factorizations." *SEG International Exposition and Annual Meeting*. OnePetro, 2020

SLIM

Weighted method (efficient)

Weighted matrix completion

$$\underset{\bar{\mathbf{X}} \in \mathbb{C}^{m \times n}}{\text{minimize}} \quad \| \bar{\mathbf{X}} \|_* \quad \text{subject to} \quad \| \mathscr{A}(\mathbf{Q}^{-1}\bar{\mathbf{X}}\mathbf{W}^{-1}) - \mathbf{B} \|_F \leq \epsilon$$

- $\bar{\mathbf{X}} = \mathbf{QXW}; \mathbf{X} = \mathbf{Q}^{-1}\bar{\mathbf{X}}\mathbf{W}^{-1}$
- $\mathbf{Q}^{-1} = \frac{1}{w_1}\mathbf{U}\mathbf{U}^H + \mathbf{U}^{\perp}\mathbf{U}^{\perp H}$
- $\mathbf{W}^{-1} = \frac{1}{w_2}\mathbf{V}\mathbf{V}^H + \mathbf{V}^{\perp}\mathbf{V}^{\perp H}$

Weighted method (efficient)

Weighted matrix factorization

$$\underset{\bar{\mathbf{L}},\bar{\mathbf{R}}}{\text{minimize}} \quad \frac{1}{2}\left\| \begin{bmatrix} \bar{\mathbf{L}} \\ \bar{\mathbf{R}} \end{bmatrix} \right\|_F^2 \quad \text{subject to} \quad \left\| \mathcal{A}(\mathbf{Q}^{-1}\bar{\mathbf{L}}\bar{\mathbf{R}}^{\mathbf{H}}\mathbf{W}^{-1}) - \mathbf{B} \right\|_F \leq \epsilon$$

- $\bar{\mathbf{X}} = \bar{\mathbf{L}}\bar{\mathbf{R}}^{\mathbf{H}}$
- $\mathbf{X} = \mathbf{Q}^{-1}\bar{\mathbf{X}}\mathbf{W}^{-1}$

Runtime comparison

Original: Weighted method

New: Weighted method (efficient)

- same number of iterations

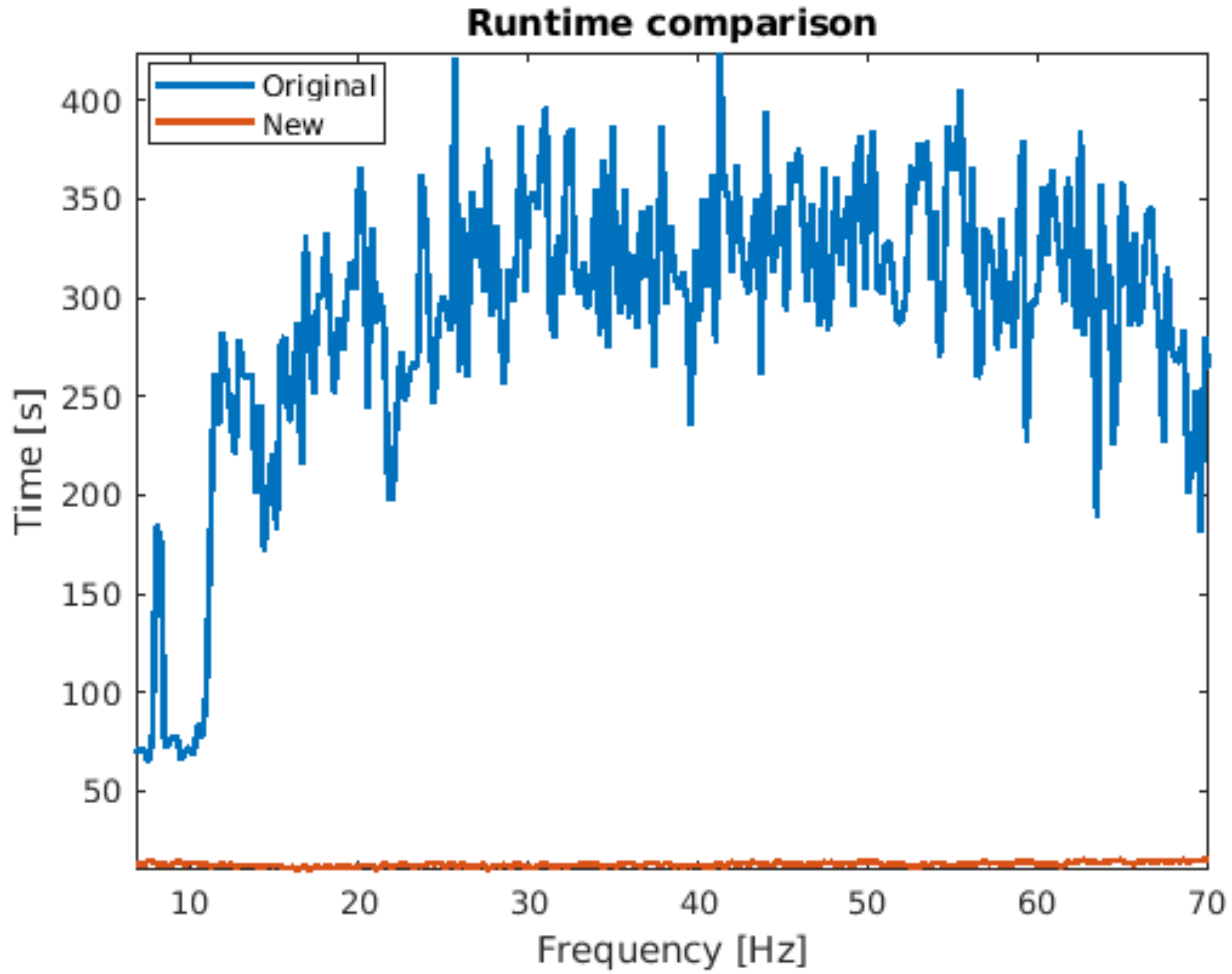

Field example

2D Field data example: Gulf of Suez

Data acquisition area: Gulf of Suez

Data dimension: $355 \times 355 \times 1024$ $(n_r \times n_s \times n_t)$

Dimension of each frequency slice: 355×355

Source sampling interval: 25 m

Receiver sampling interval: 25 m

Time sampling interval: 0.004s

Observed data: $75\ \%$ missing sources

Scenarios compared

Scenarios

- w/o using any prior information (conventional)
- using single pair prior information (pair weighted)
  - prior information comes from conventional results
- using recursive prior information (recursively weighted)

Frequency slice
(40 Hz)

Fully sampled data
~40 Hz slice

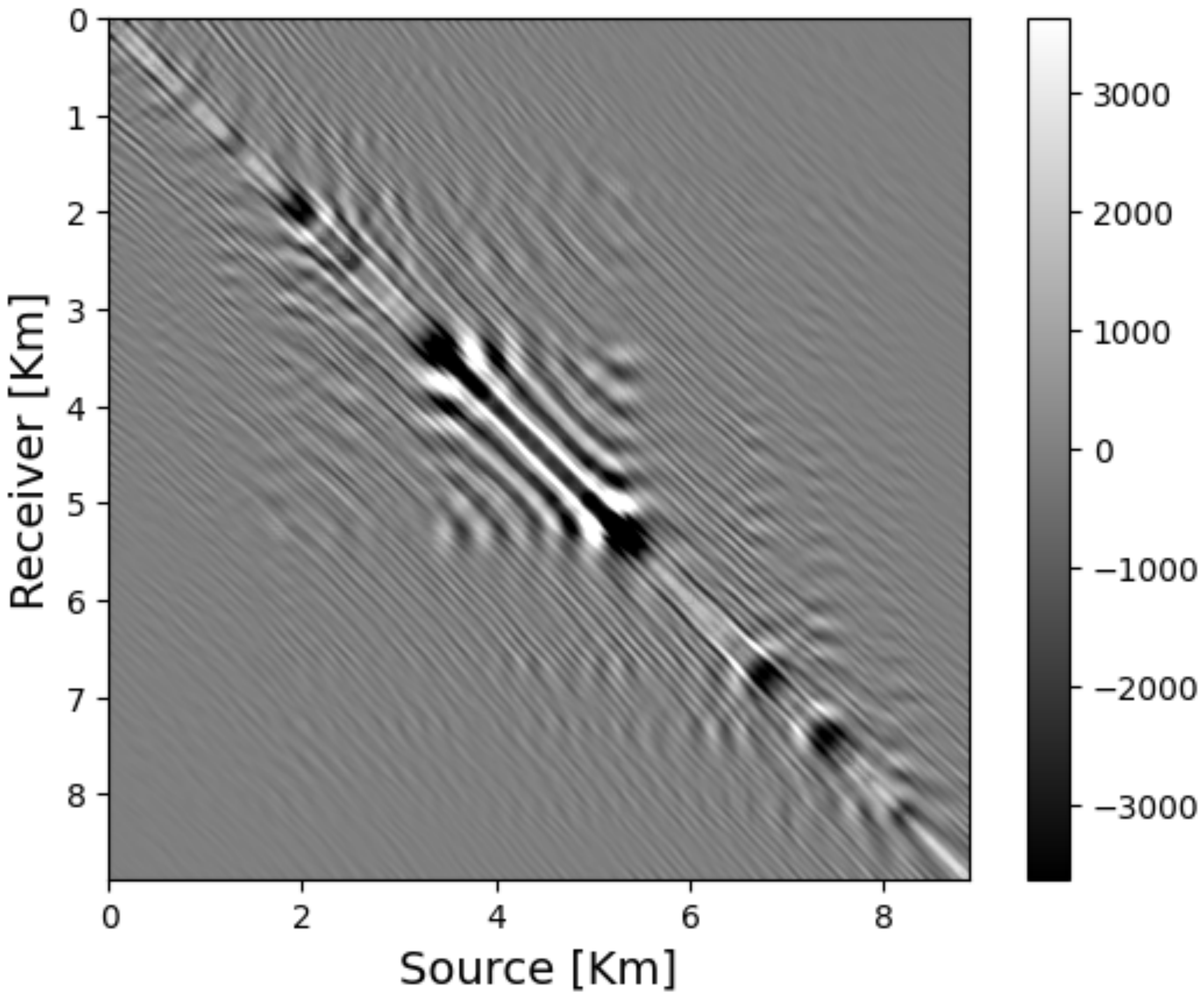

Observed data

75 % jittered subsampling

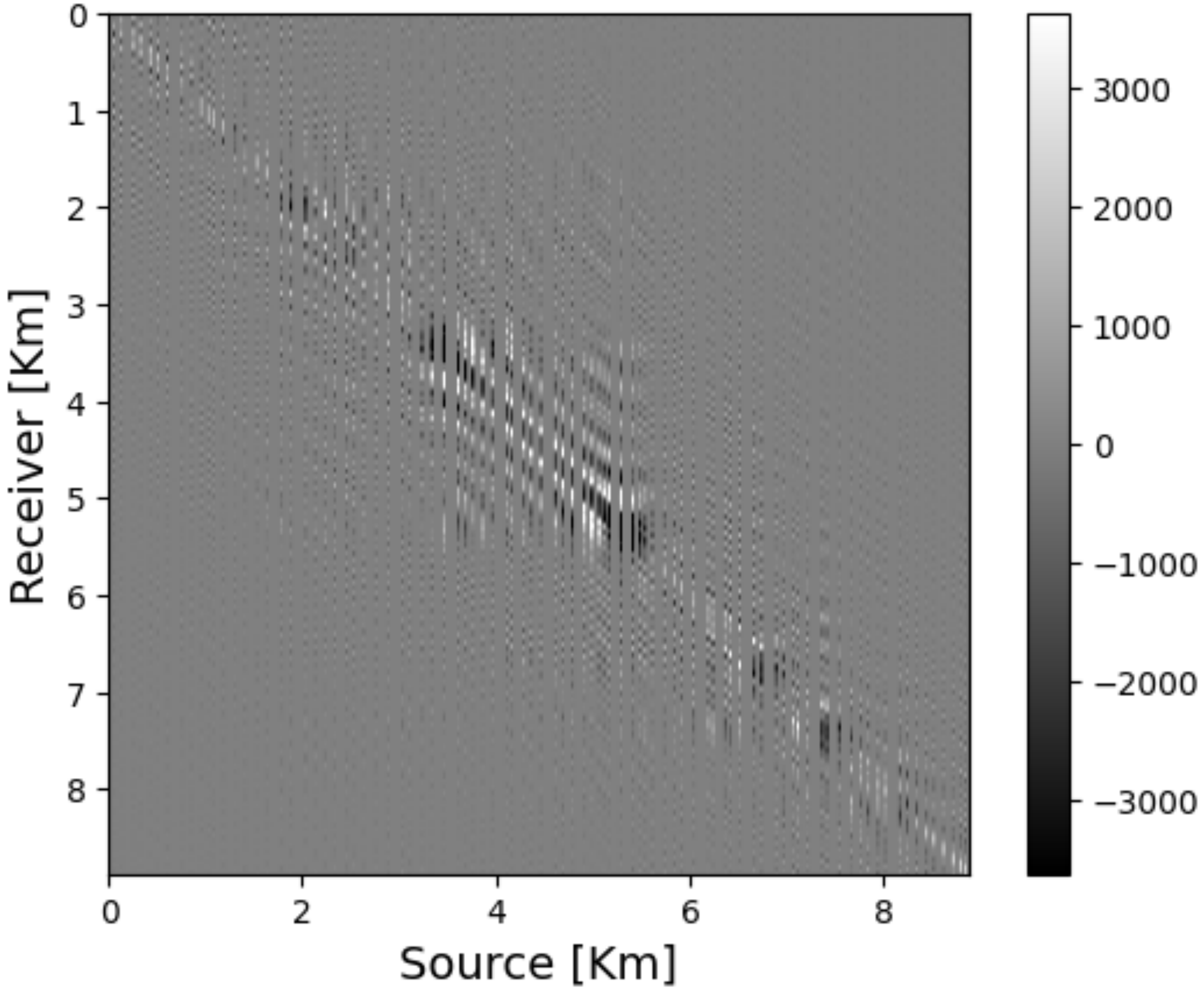

Herrmann, Felix J., and Gilles Hennenfent. "Non-parametric seismic data recovery with curvelet frames." *Geophysical Journal International* 173.1 (2008): 233-248.

Recovery
w/ conventional matrix completion

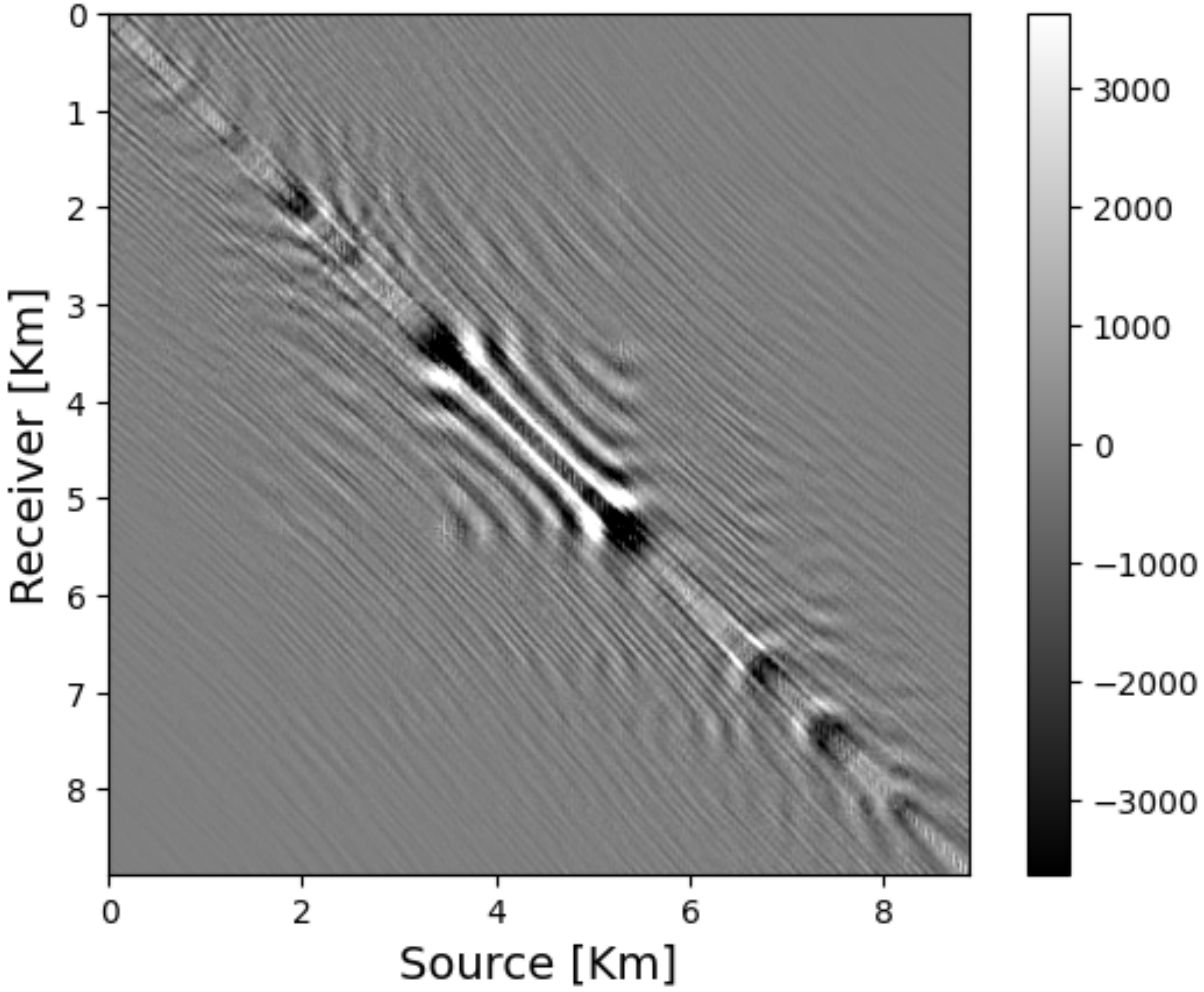

SNR = 9.49 dB
Rank = 30

Recovery
w/ pair weighted matrix completion

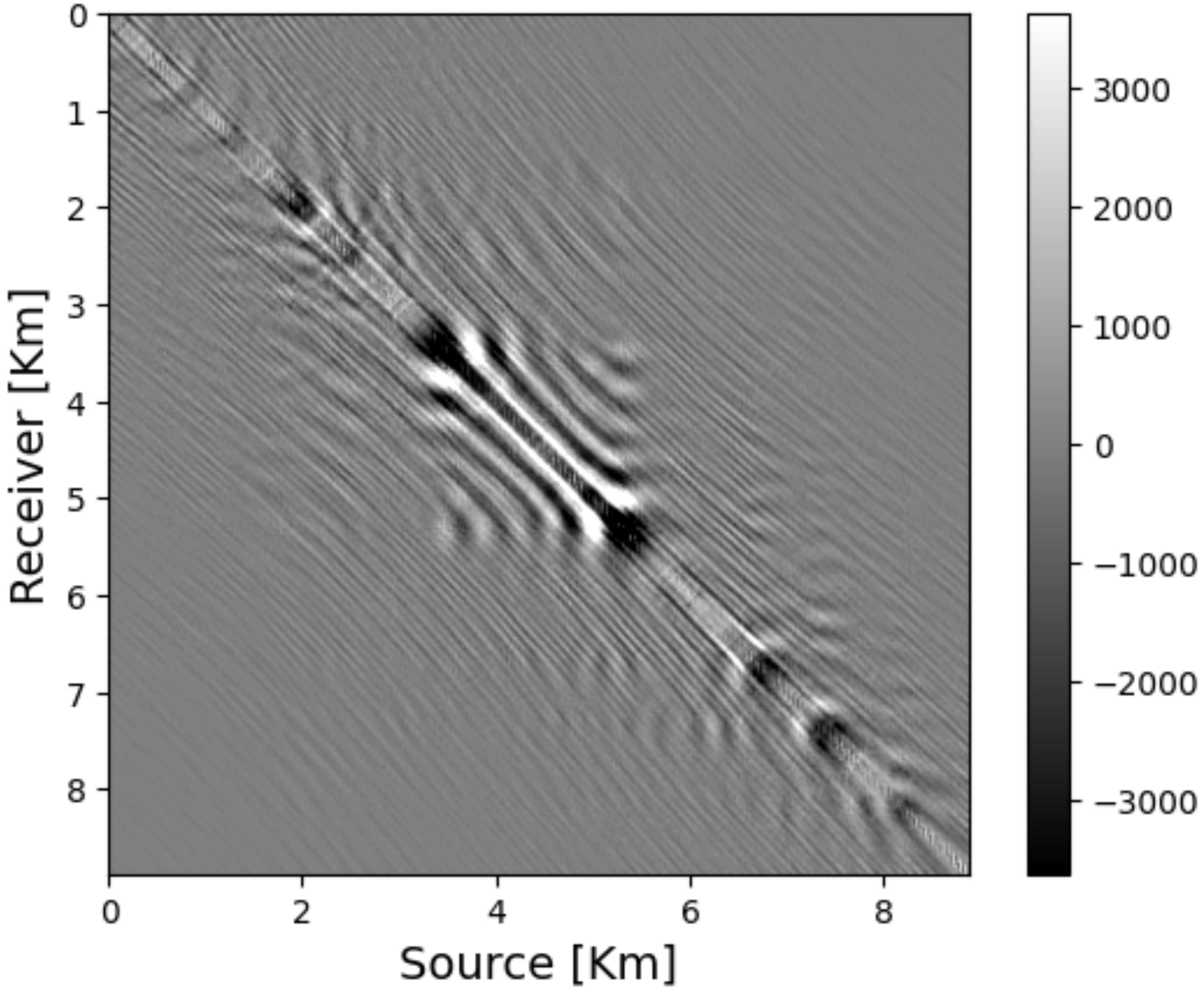

SNR = 10.34 dB
Rank = 30

Recovery
w/ recursively weighted matrix completion

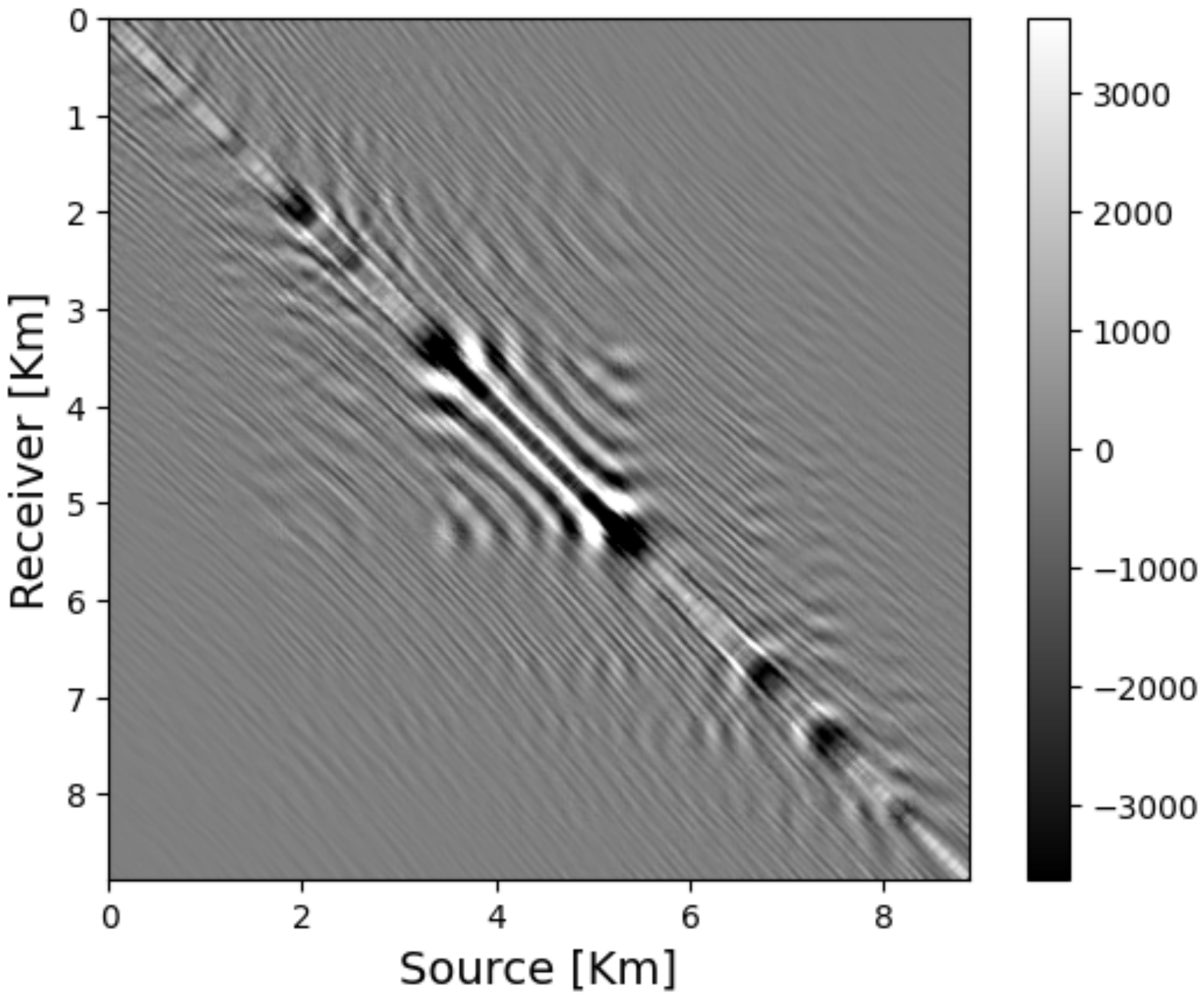

SNR = 15.92 dB
Rank = 30

Difference: True - Recovery
w/ conventional matrix completion

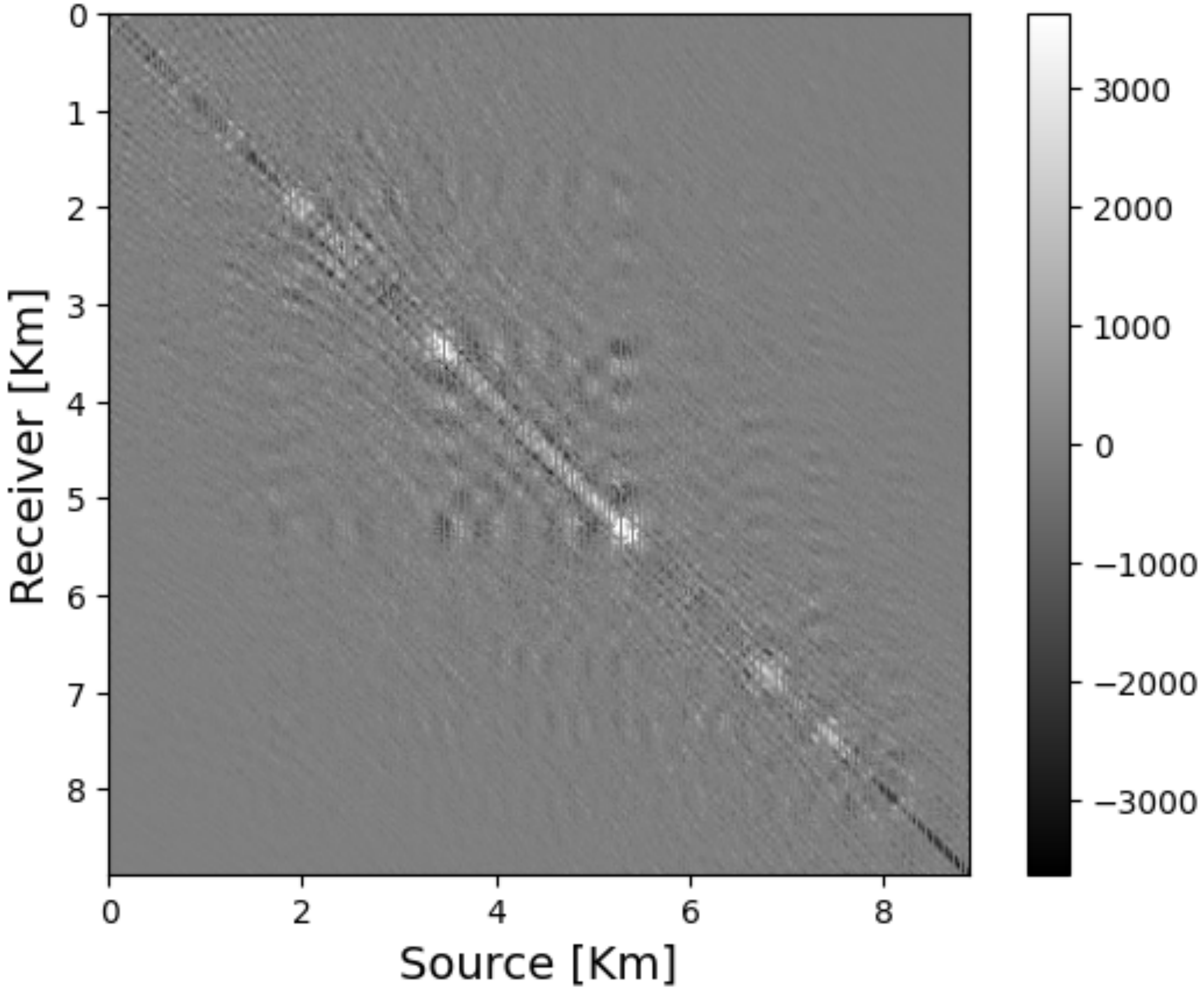

SNR = 9.49 dB
Rank = 30

Difference: True - Recovery
w/ pair weighted matrix completion

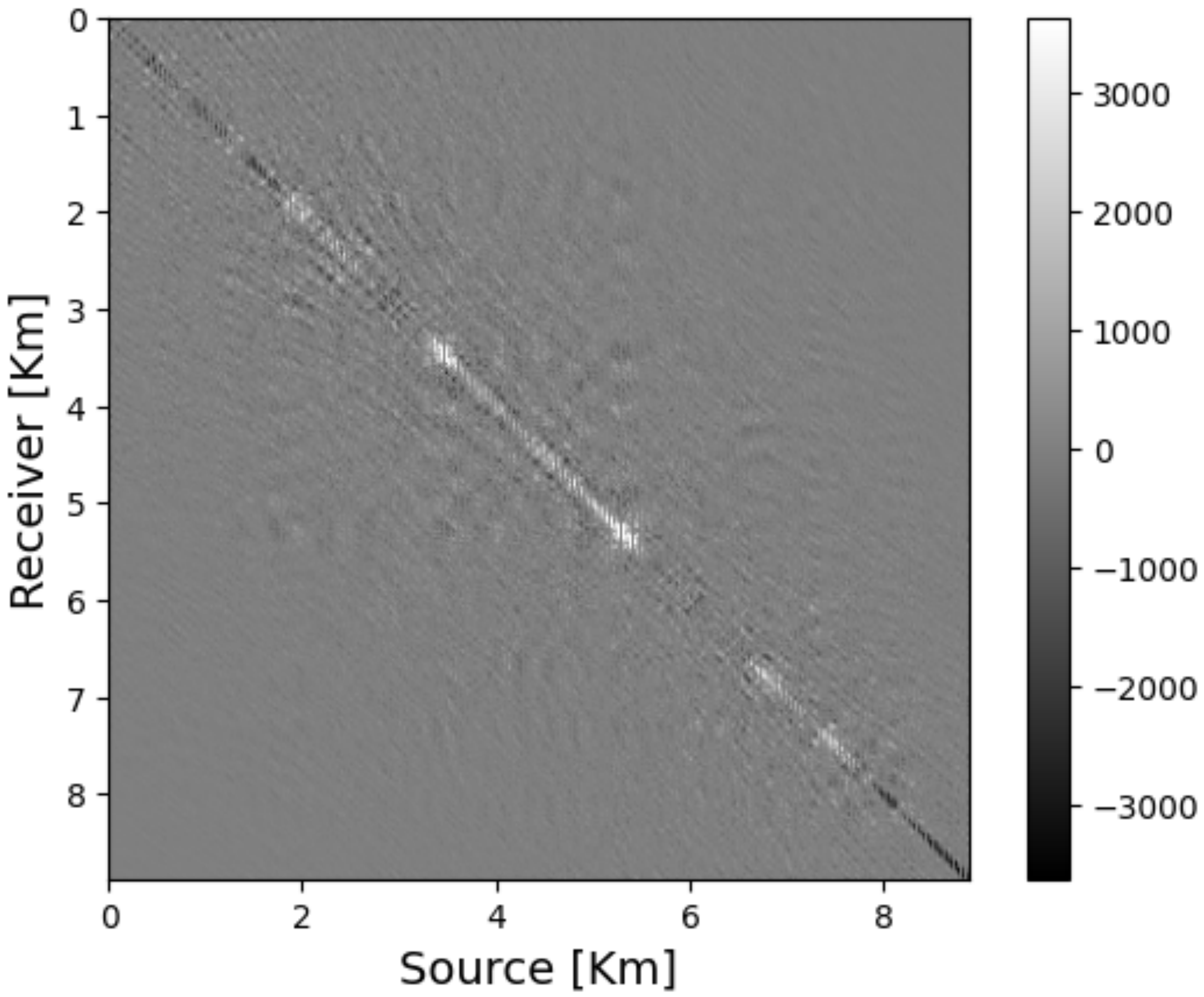

SNR = 10.34 dB
Rank = 30

Difference: True - Recovery
w/ recursively weighted matrix completion

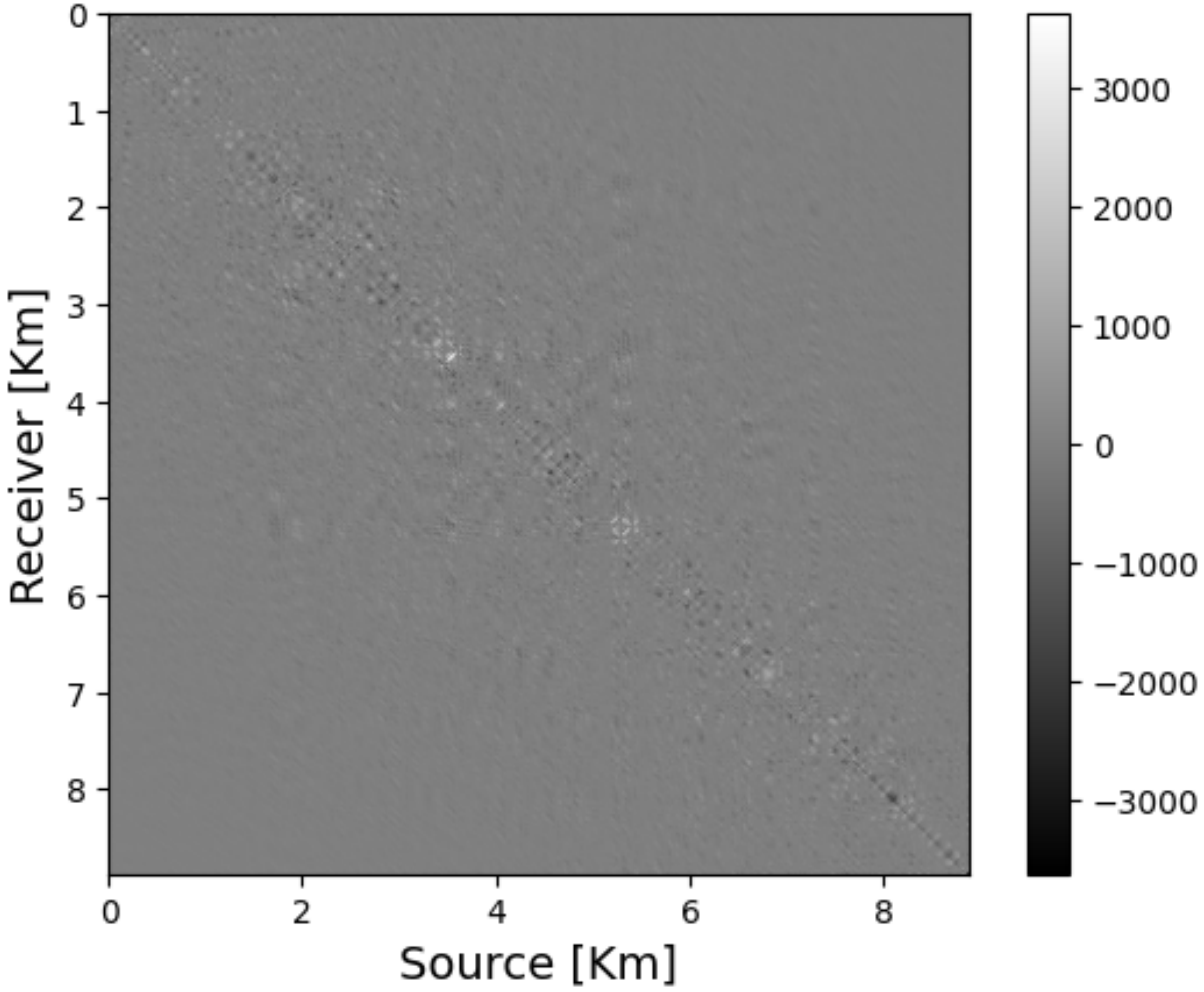

SNR = 15.92 dB
Rank = 30

Frequency slices
(7 Hz~73 Hz)

Frequencies vs. SNR
(7~73 Hz)

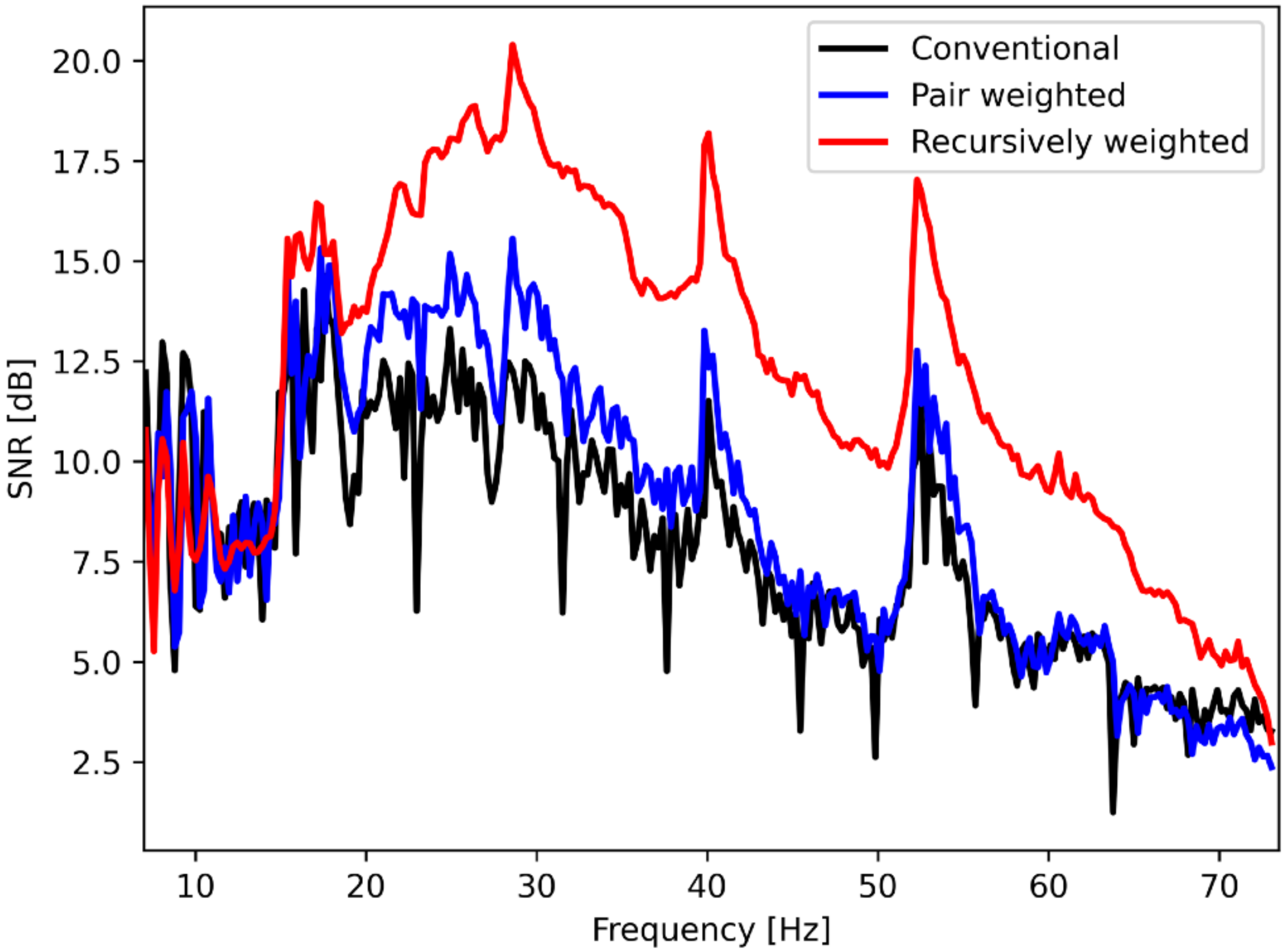

Common receiver gather

Fully sampled data

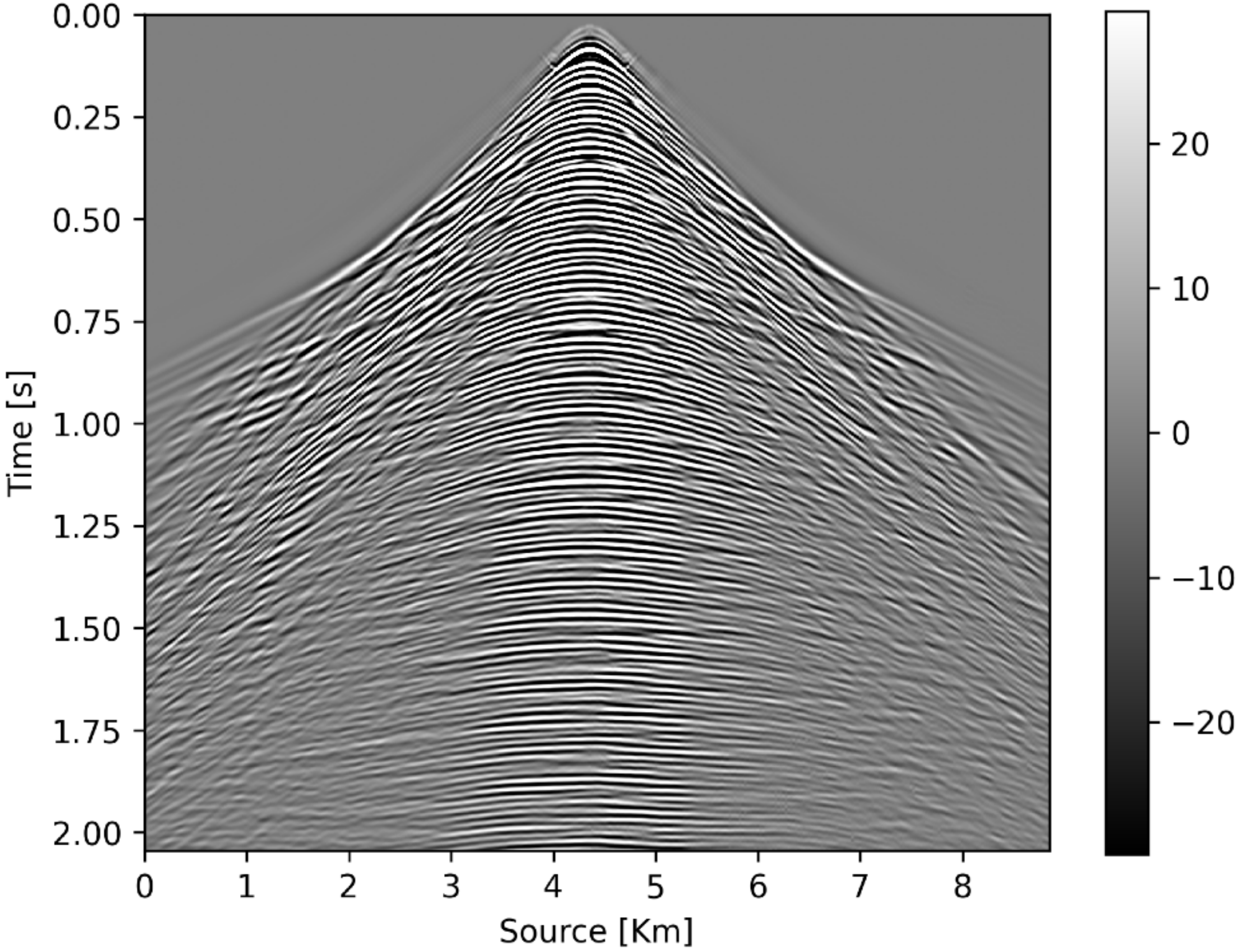

Observed data
$75\ \%$ jittered subsampling

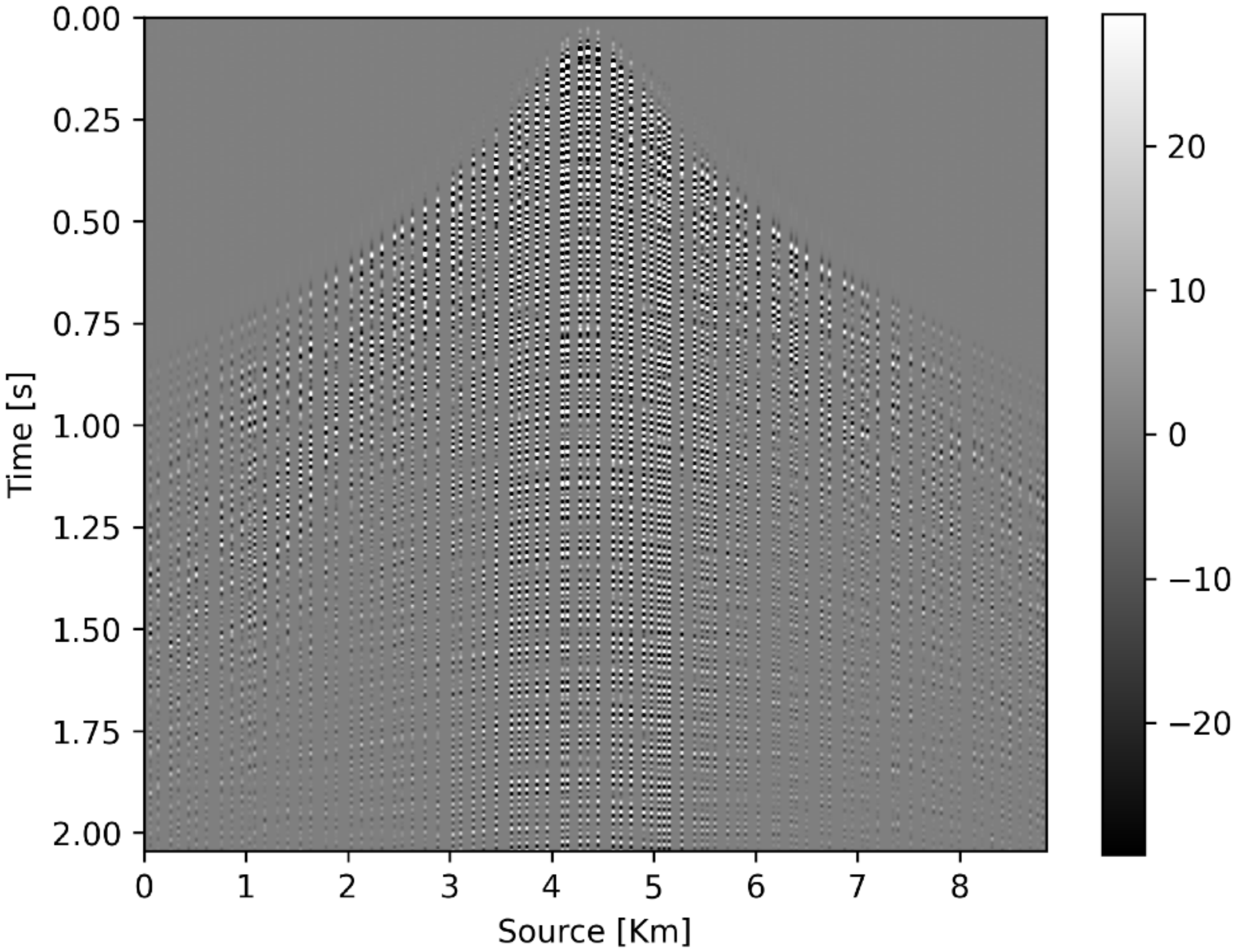

Difference: True - Recovery
w/ conventional matrix completion

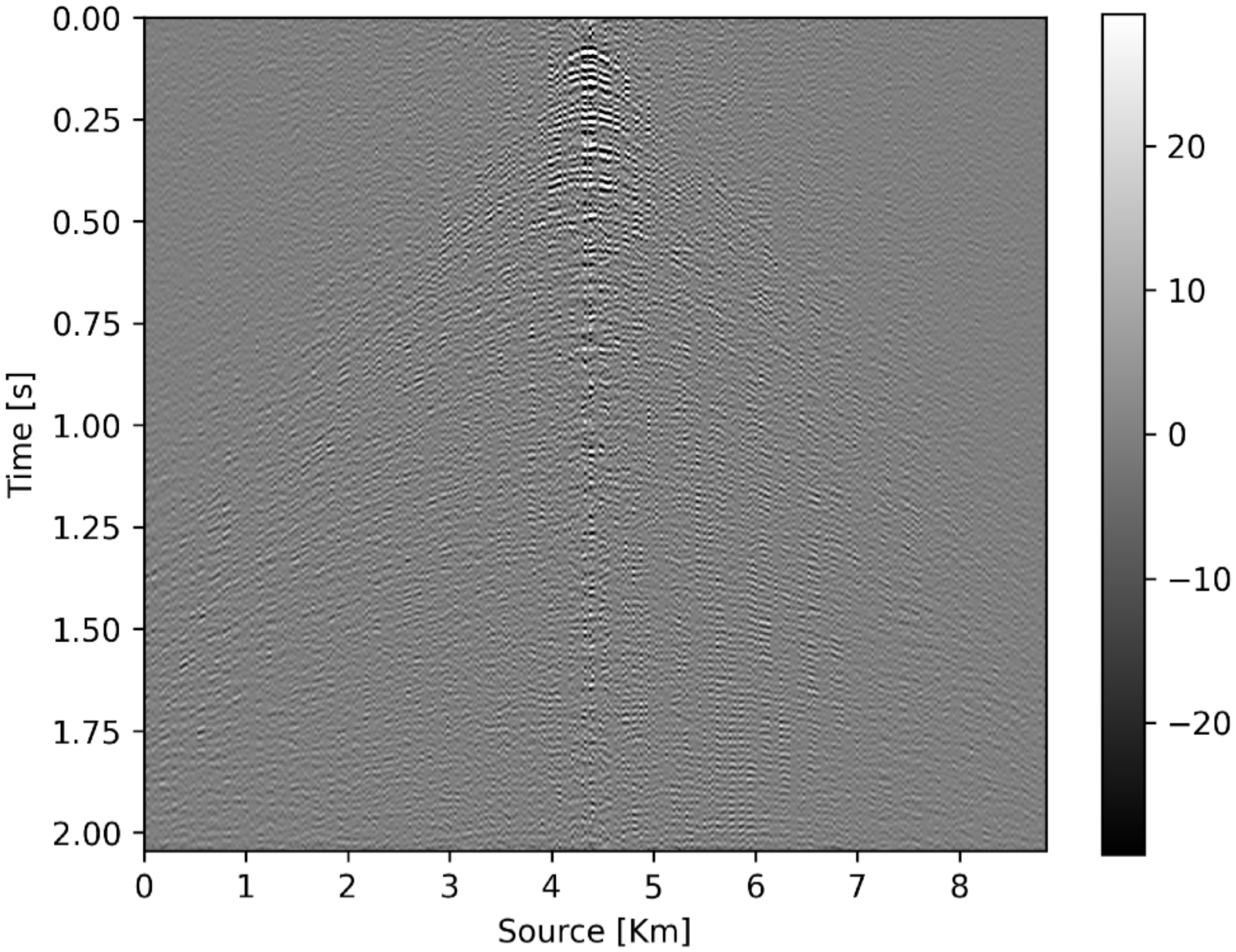

SNR = 7.00 dB
Rank = 30

Difference: True - Recovery
w/ pair weighted matrix completion

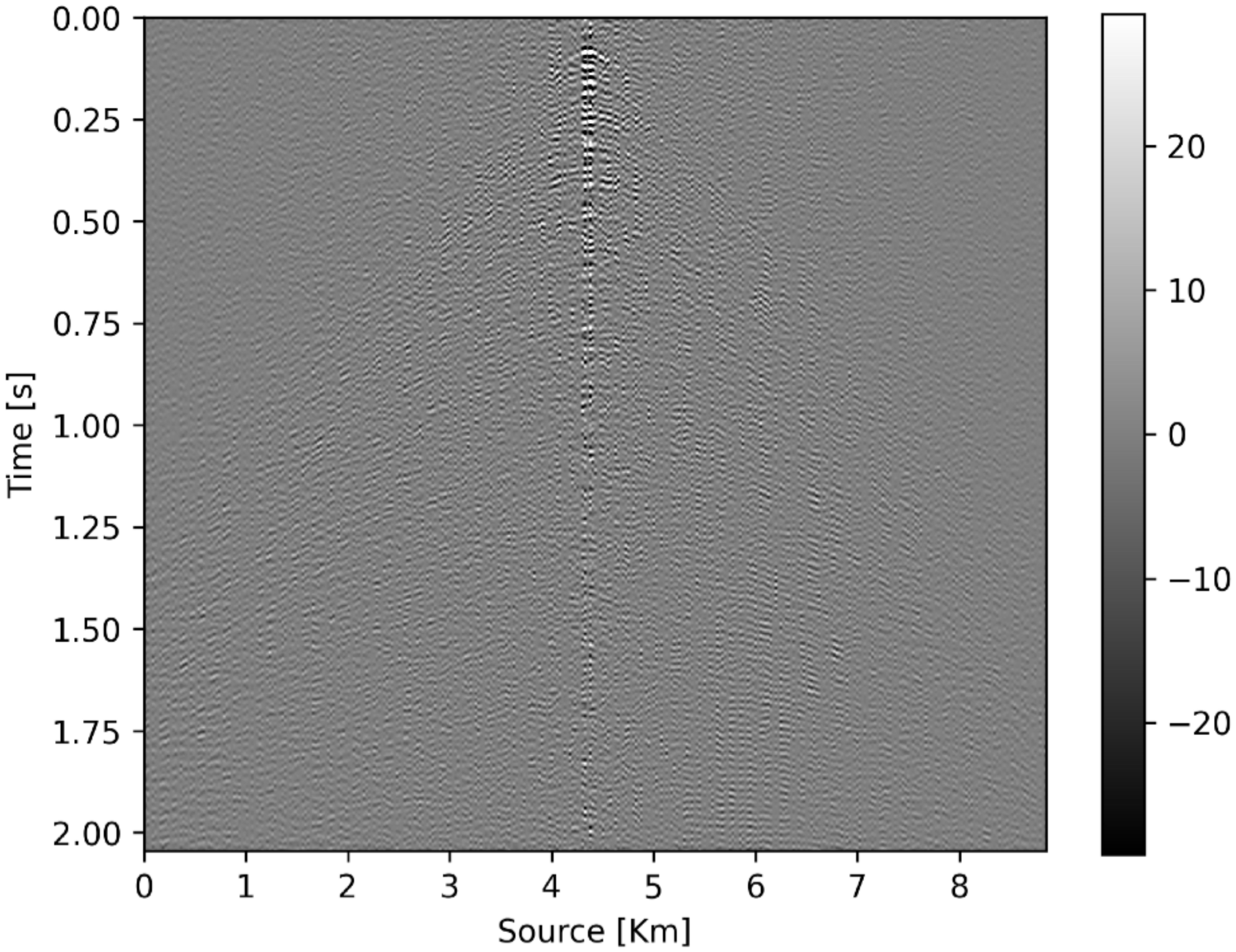

SNR = 7.78 dB
Rank = 30

Difference: True - Recovery
w/ recursively weighted matrix completion

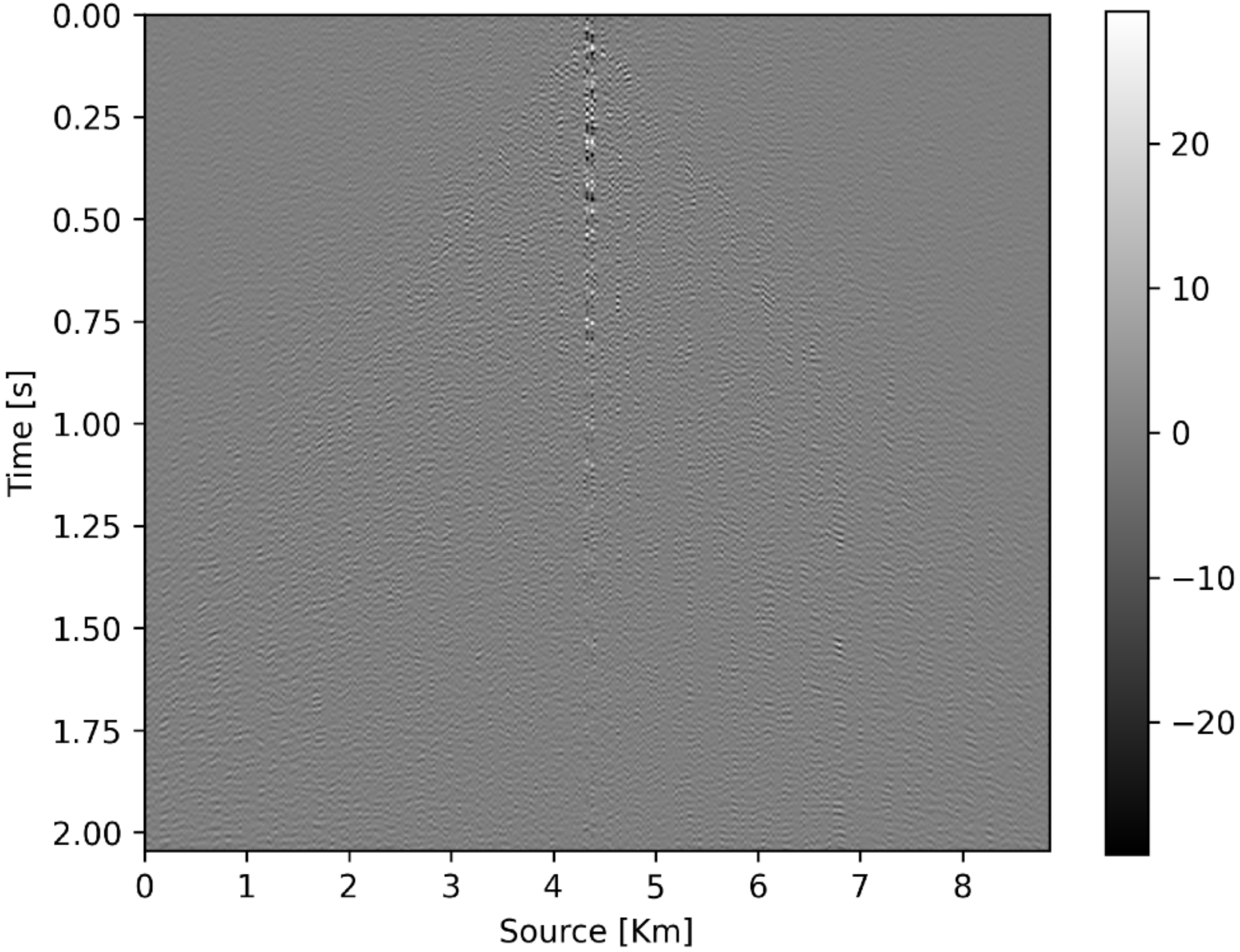

SNR = 11.88 dB
Rank = 30

Contributions

Proposed recursively weighted matrix completion

Proposed efficient weighted matrix completion

Conclusions

The proposed recursive weighted strategy

- improves SNR at higher frequencies

The efficient weighted method

- reduce the computational time w/ same number of iterations

A simulation-free seismic survey design by maximizing the spectral gap

Chapter 6

Oscar Lopez, Rajiv Kumar, Nick Moldoveanu and Felix J. Herrmann, “Graph Spectrum Based Seismic Survey Design”, 2020.
Mosher, C. C., S. T. Kaplan, and F. D. Janiszewski. "Non-uniform optimal sampling for seismic survey design." *74th EAGE Conference and Exhibition incorporating EUROPEC 2012*. European Association of Geoscientists & Engineers, 2012.

Motivation

Seismic data

- expensive to acquire

Subsampling

- increasingly employed in seismic data acquisition
- reduce costs

Uniform & jittered sample design

- suboptimal & not flexible — i.e., impossible to add constraints

Simulation-based seismic acquisition design

- expensive & time consuming

Goal: propose a simulation-free seismic survey design

Oscar Lopez, Rajiv Kumar, Nick Moldoveanu and Felix J. Herrmann, “Graph Spectrum Based Seismic Survey Design”, 2020.
Bhojanapalli, Srinadh, and Prateek Jain. "Universal matrix completion." *International Conference on Machine Learning*. PMLR, 2014.
Burnwal, Shantanu Prasad, and Mathukumalli Vidyasagar. "Deterministic completion of rectangular matrices using asymmetric ramanujan graphs: Exact and stable recovery." *IEEE Transactions on Signal Processing* 68 (2020): 3834-3848.

Motivation

Matrix completion

- reconstructs fully sampled wavefields from sparse seismic data
- computationally efficient

Spectral gap of a subsampling mask (binary mask)

- distance between the first & second singular values
- an indicator for the connectivity of a graph
- a cheap metric to predict performance of an acquisition design
- maximizing the spectral gap favors reconstruction via matrix completion

Binary mask
(2D acquisition & towed array)

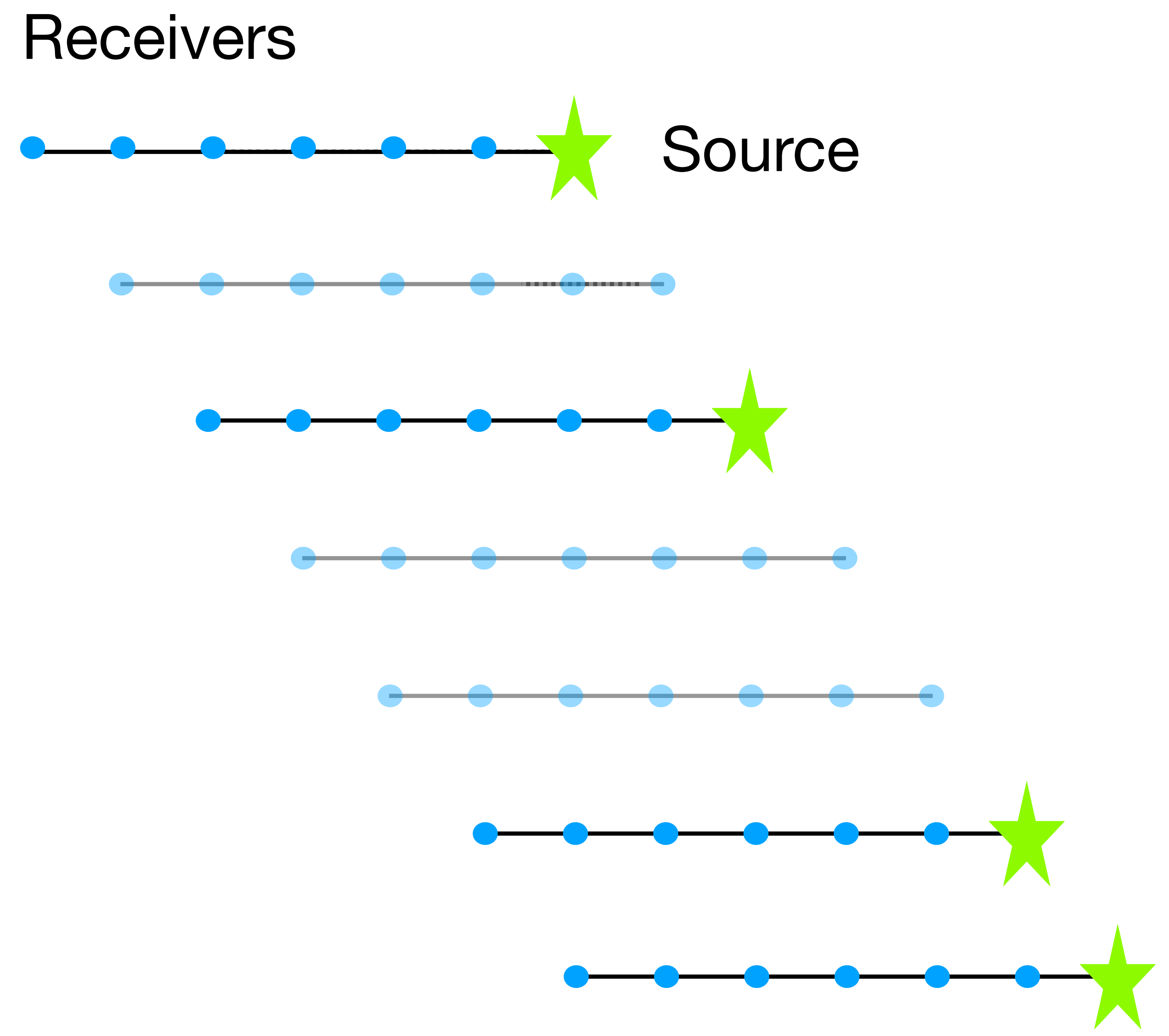

Sampling matrix in source-receiver domain

Receivers (rows) × Sources (columns)

1	0	1	0	0	1	1
1	0	1	0	0	1	1
1	0	1	0	0	1	1
1	0	1	0	0	1	1
1	0	1	0	0	1	1
1	0	1	0	0	1	1
1	0	1	0	0	1	1

Sources

Oscar Lopez, Rajiv Kumar, Nick Moldoveanu and Felix J. Herrmann, “Graph Spectrum Based Seismic Survey Design”, 2020.
Bhojanapalli, Srinadh, and Prateek Jain. "Universal matrix completion." *International Conference on Machine Learning*. PMLR, 2014.

SLIM ML4Seismic

Motivation

relationship between reconstruction quality & sampled matrix

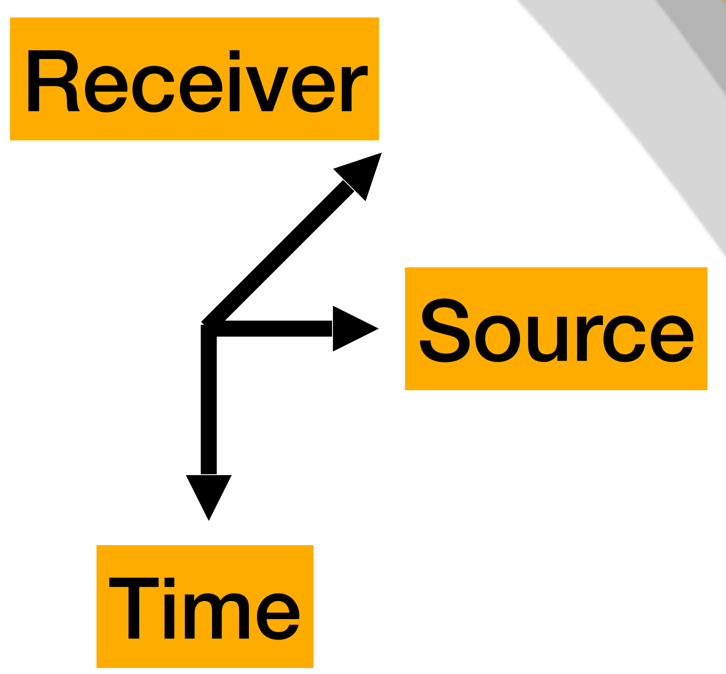

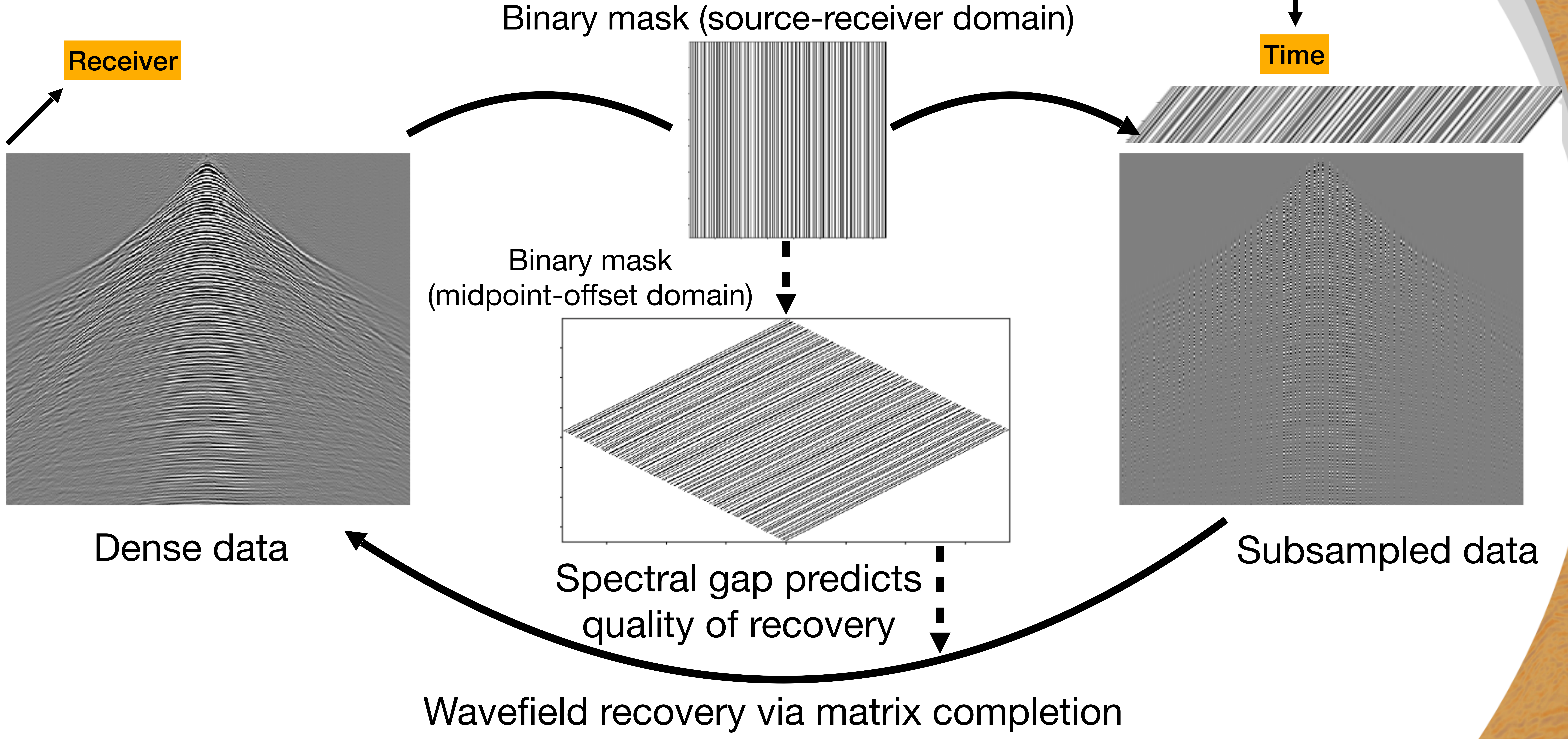

Motivation

relationship between reconstruction quality & sampling matrix

$$\rho = \frac{\sigma_2(M)}{\sigma_1(M)}$$ spectral gap ratio

- $\sigma_1(\,.\,)$ first singular value
- $\sigma_2(\,.\,)$ second singular value

Toy test: an average of 30 independent experiments

optimized subsampling

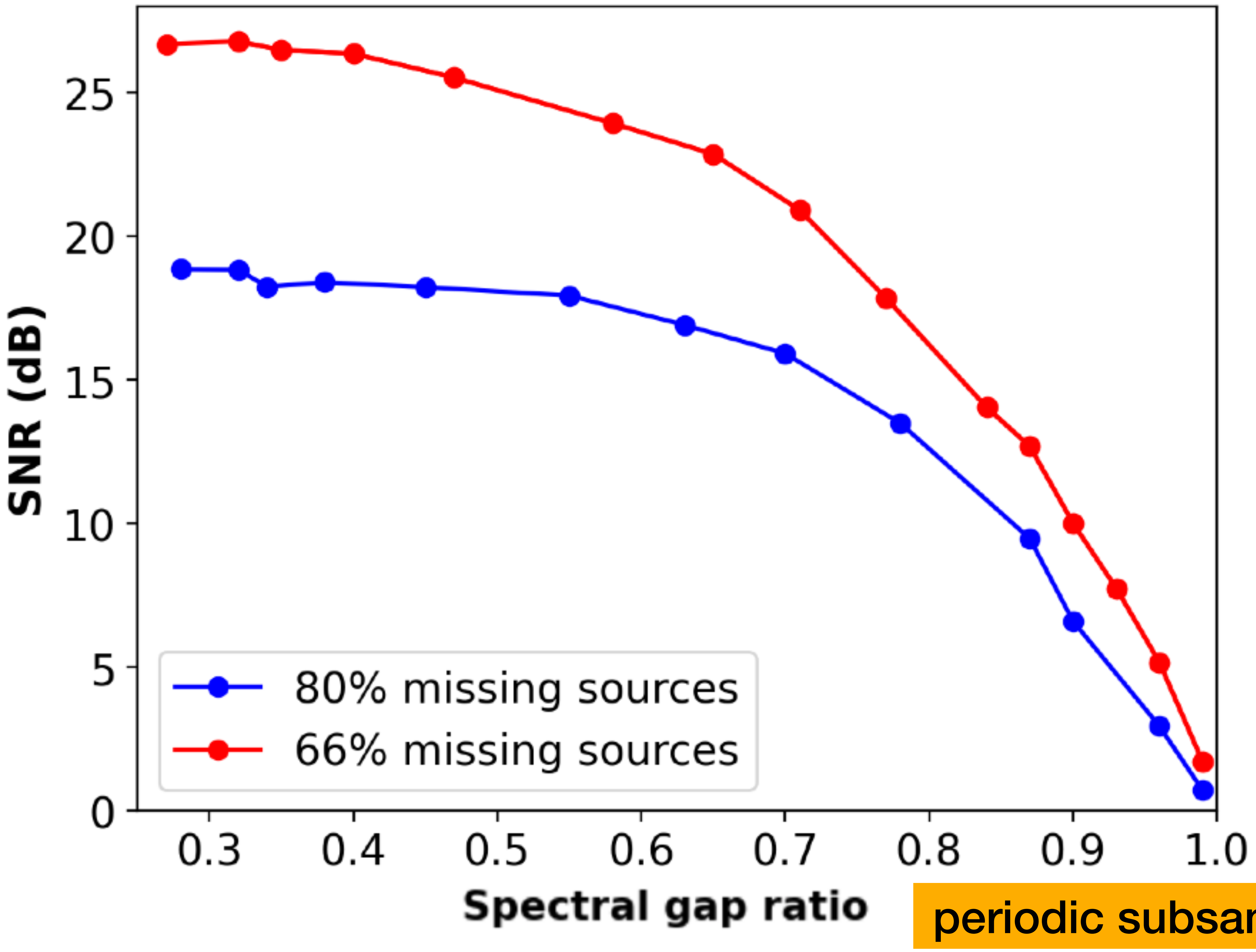

periodic subsampling

Large signal to noise ratio (SNR) corresponds to small spectral gap ratio

Oscar Lopez, Rajiv Kumar, Nick Moldoveanu and Felix J. Herrmann, “Graph Spectrum Based Seismic Survey Design”, 2020.
Bhojanapalli, Srinadh, and Prateek Jain. "Universal matrix completion." *International Conference on Machine Learning*. PMLR, 2014.

Motivation

relationship between reconstruction quality & sampling matrix

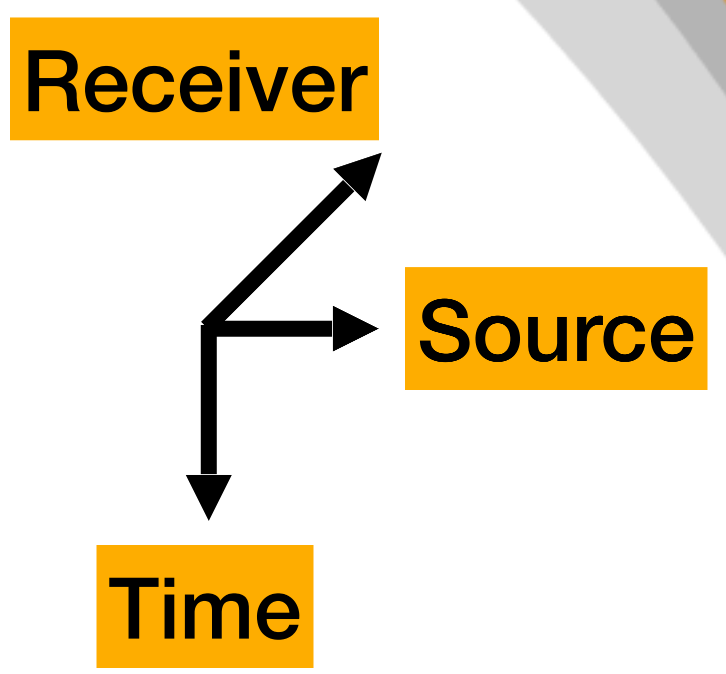

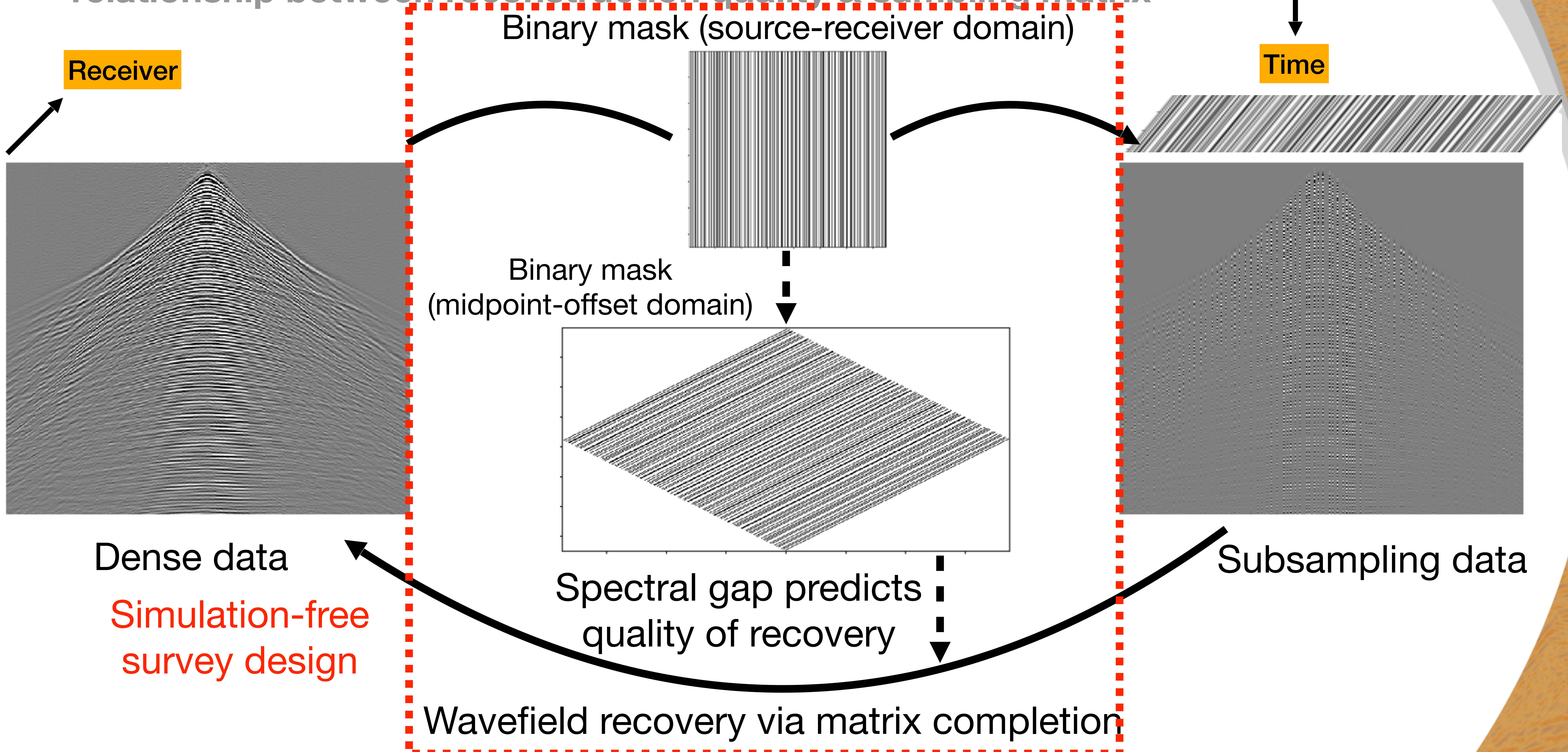

Optimization problem

2D acquisition & 1 vintage

Given n_s source locations & subsampling ratio r, find $m = \lfloor n_s \times r \rfloor \times n_r$ subsampling masks M

$$\underset{M}{\text{minimize}} \frac{\sigma_2(\mathcal{S}(M))}{\sigma_1(\mathcal{S}(M))} \quad \text{subject to } \| M \|_0 = m \cap M \in \mathcal{J} \cap M \in \{0,1\}^{n_s \times n_r}.$$

- $\mathcal{S}$: an operator transforms data from source-receiver to midpoint-offset domain
- n_r : # of receivers.
- $\mathcal{J}$: a set of all possible subsampling masks

Stylized example

Optimal ρ w/ simulated annealing
w/ single vintage

Mask dimension: 300 x 300

Subsampling ratio: 25%

Source & receiver sampling interval: 12.5 m

Optimize the ρ of a given initial subsampling mask:

- jittered subsampling

Subsampled mask
jittered subsampling

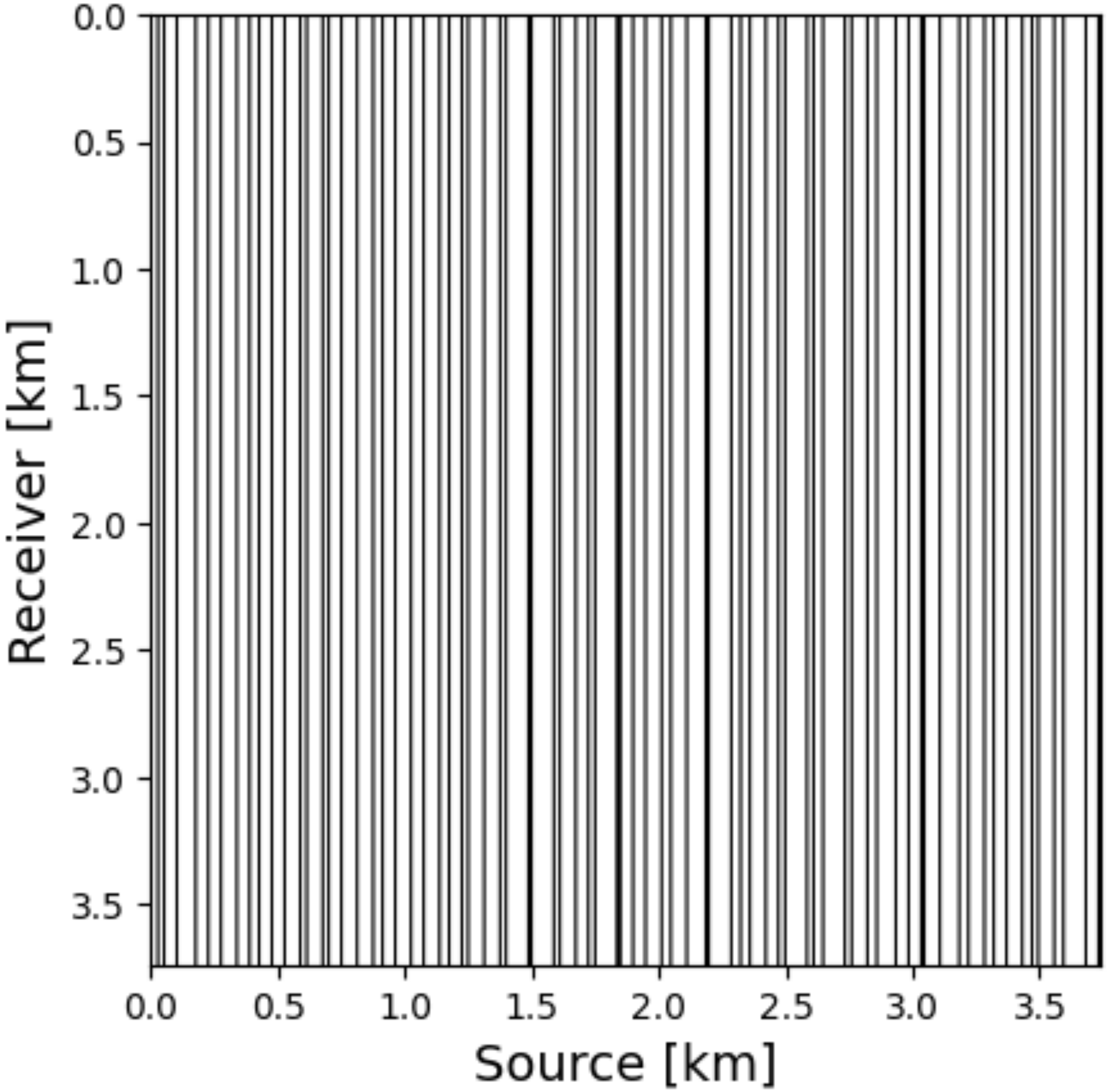

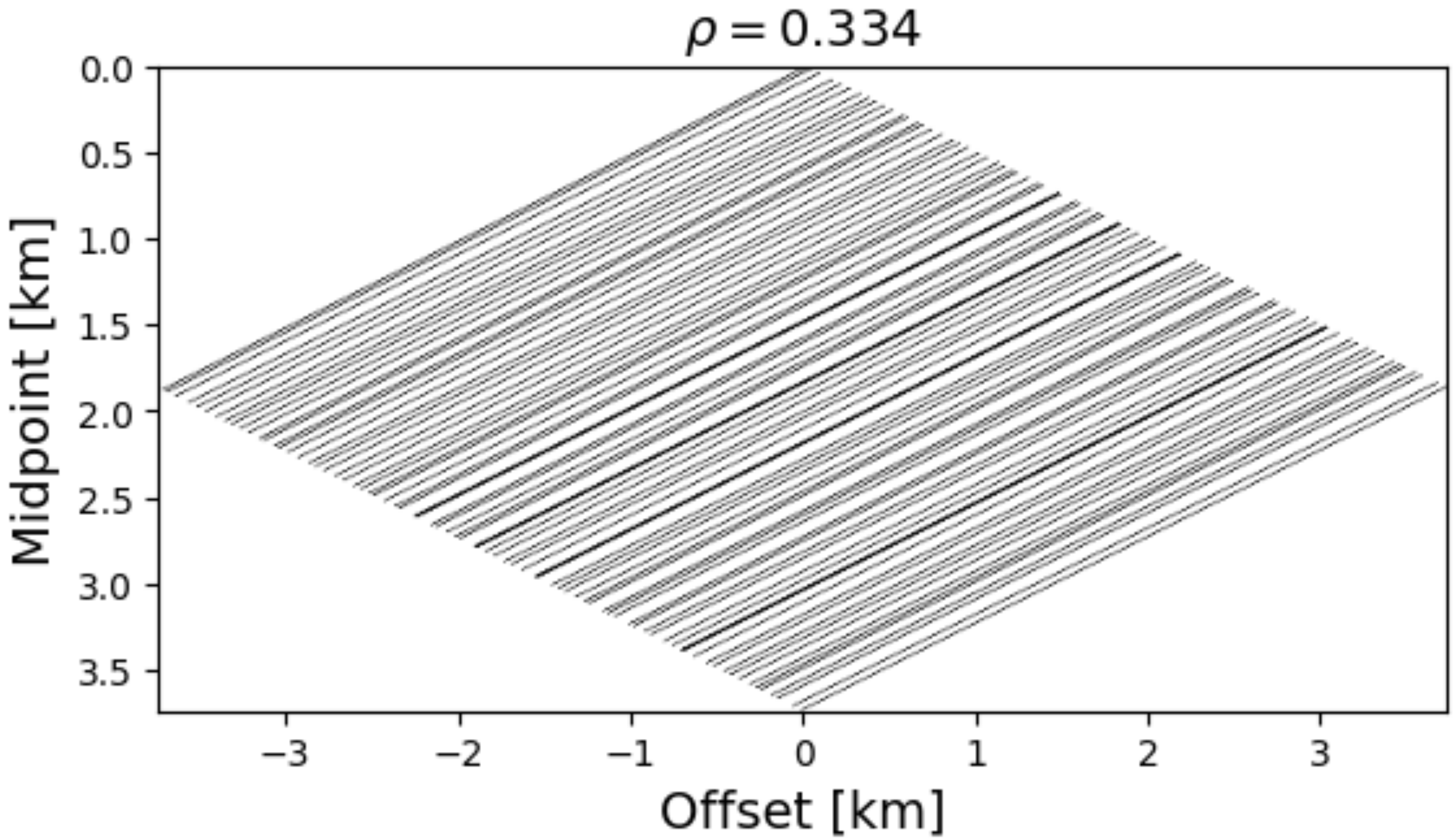

Proposed subsampling mask

optimized output produced by SA algorithm

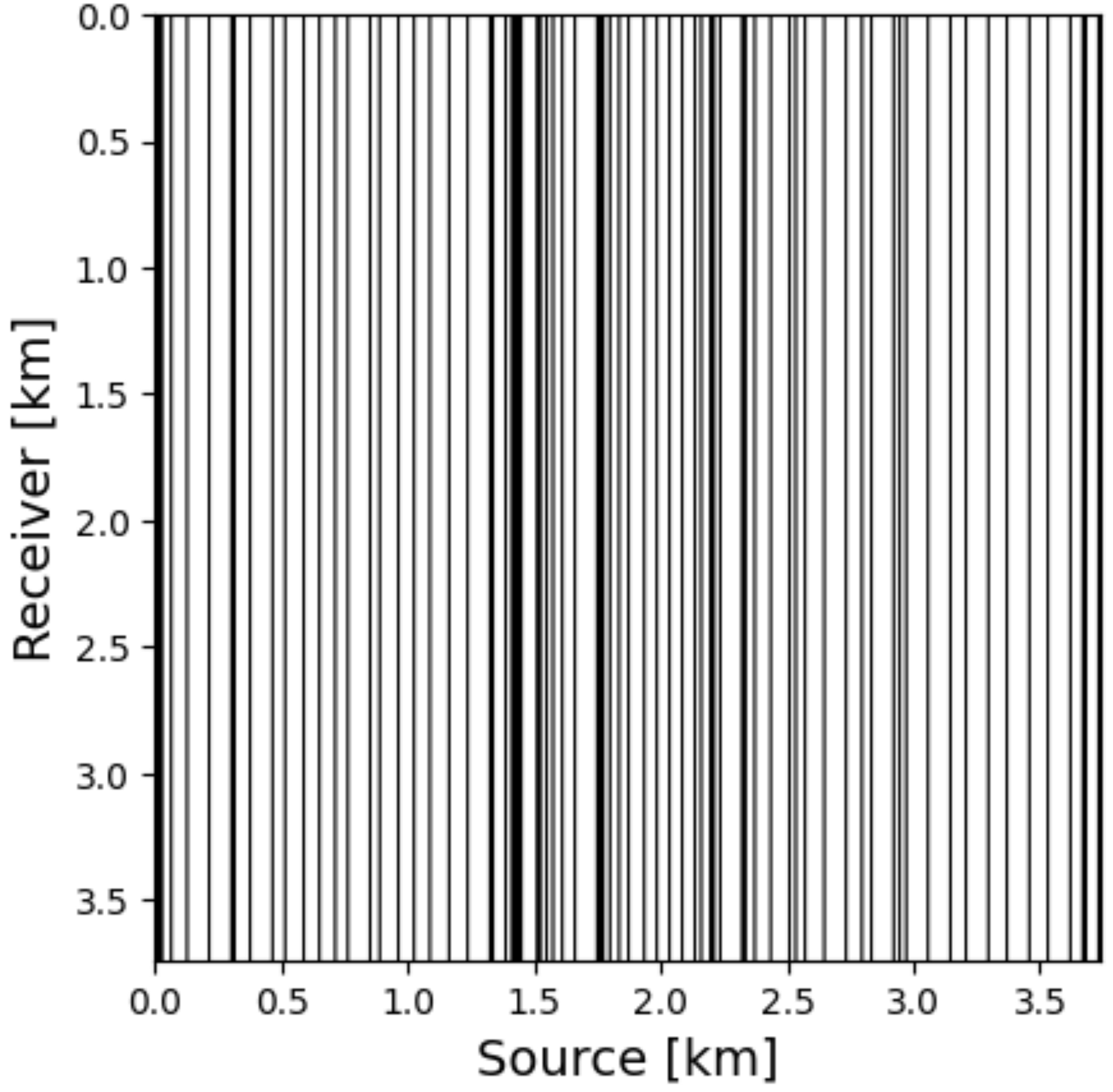

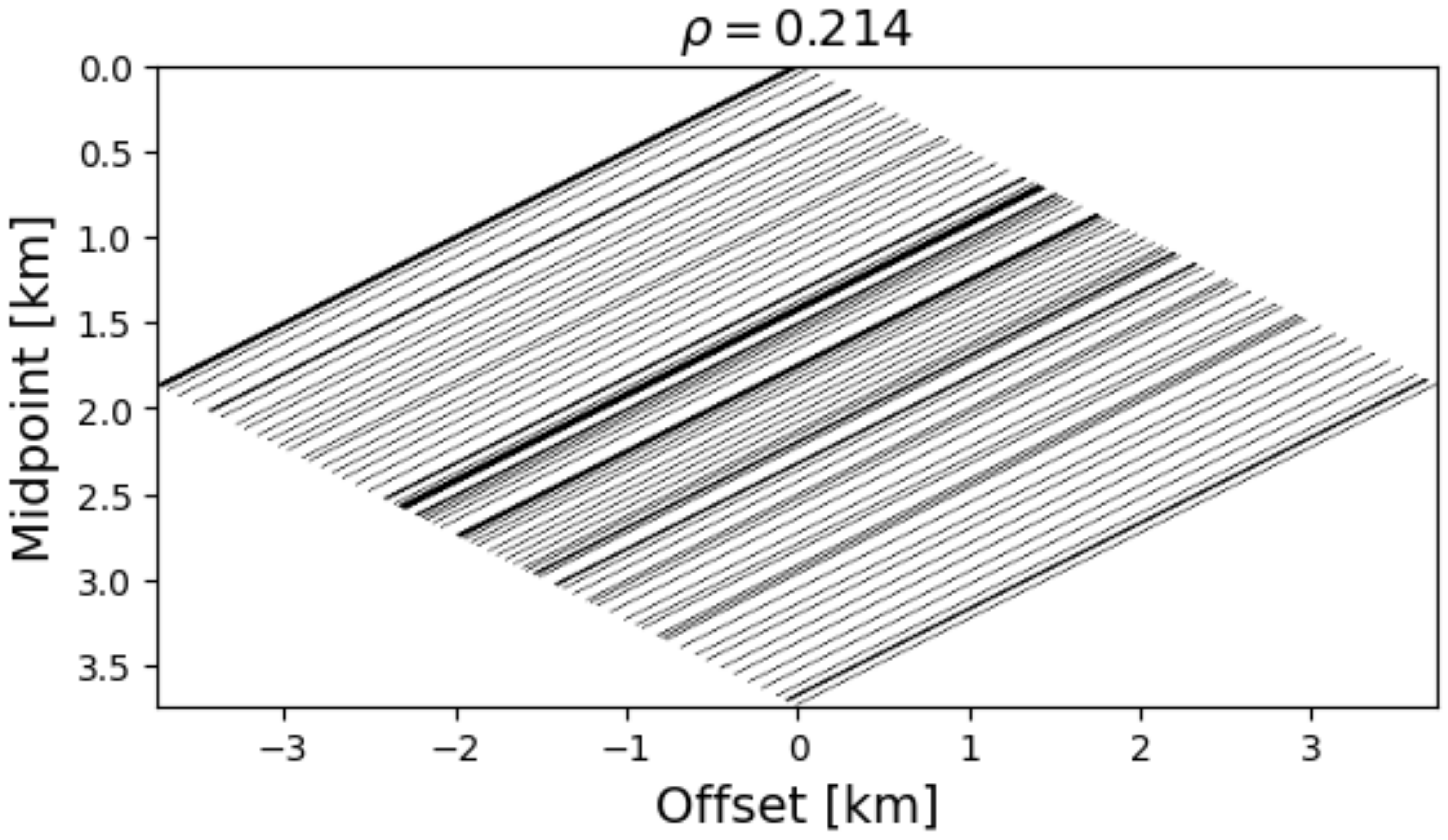

Synthetic example
jittered vs. optimized

Zhang, Yijun, Shashin Sharan, Oscar Lopez, and Felix J. Herrmann. "Wavefield recovery with limited-subspace weighted matrix factorizations." In *SEG International Exposition and Annual Meeting*. OnePetro, 2020.

Test masks via LR matrix completion

2D synthetic Compass dataset

Data dimension: 300 x 300 x 1024 $(n_r \times n_s \times n_t)$

Dimension of each frequency slice: 300 x 300

Source sampling interval: 12.5 m

Receiver sampling interval: 12.5 m

Time sampling interval: 0.002 s

Animation

jittered (SNR = 14.16 dB) vs optimized (SNR = 14.42 dB)

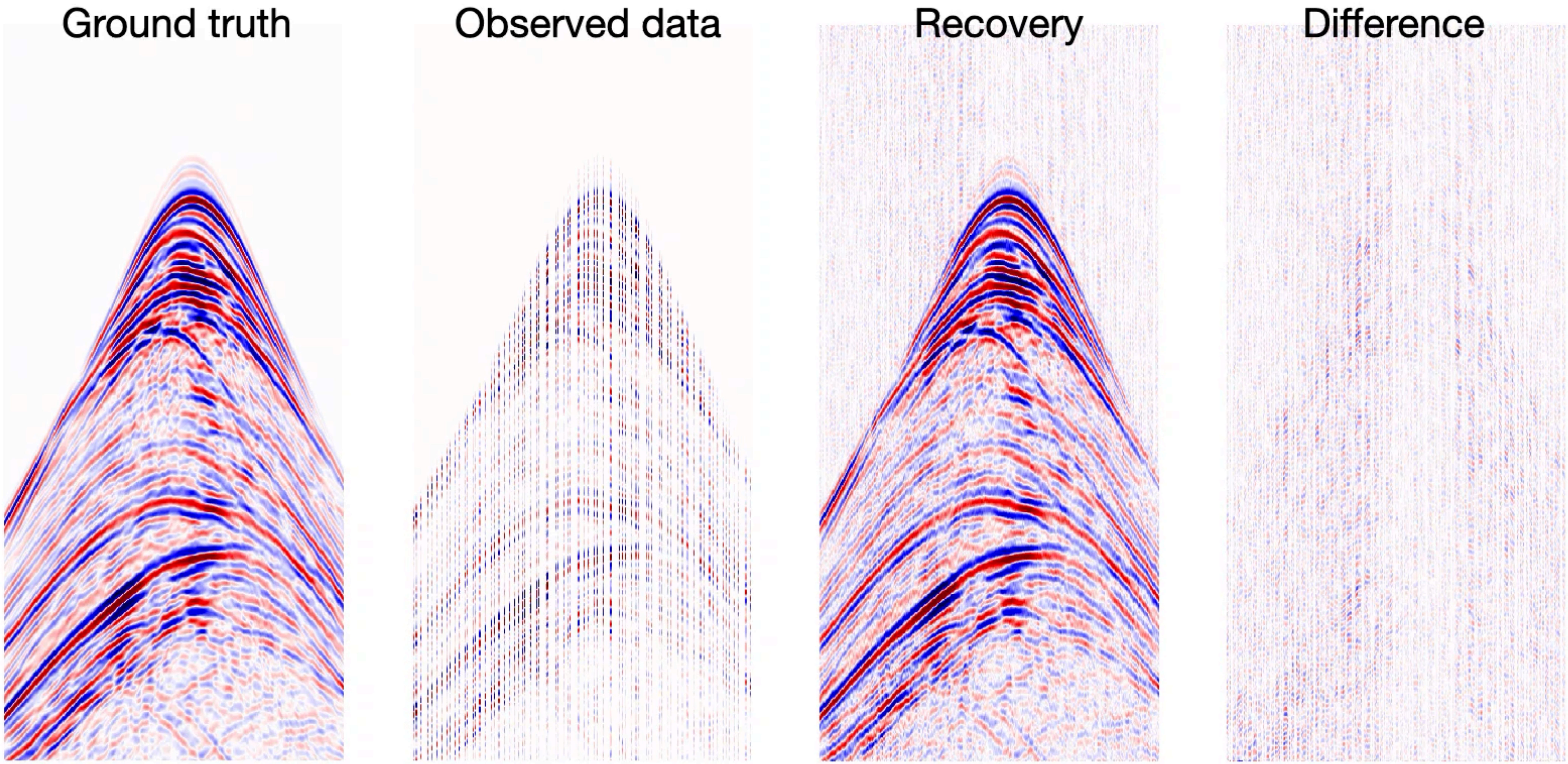

Optimization problem

3D acquisition & 1 vintage

Given n_s source locations & subsampling ratio r, find $m = \lfloor n_s \times r \rfloor \times n_r$ subsampling masks M

$$\underset{M}{\text{minimize}} \frac{\sigma_2(\mathcal{S}(M))}{\sigma_1(\mathcal{S}(M))} \qquad \text{subject to } \| M \|_0 = m \cap M \in \mathcal{J} \cap M \in \{0,1\}^{n_s \times n_r}.$$

- $\mathcal{S}$: an operator transforms data from canonical to non-canonical organization
- n_r : # of receivers.
- $\mathcal{J}$: a set of all possible subsampling masks

Method

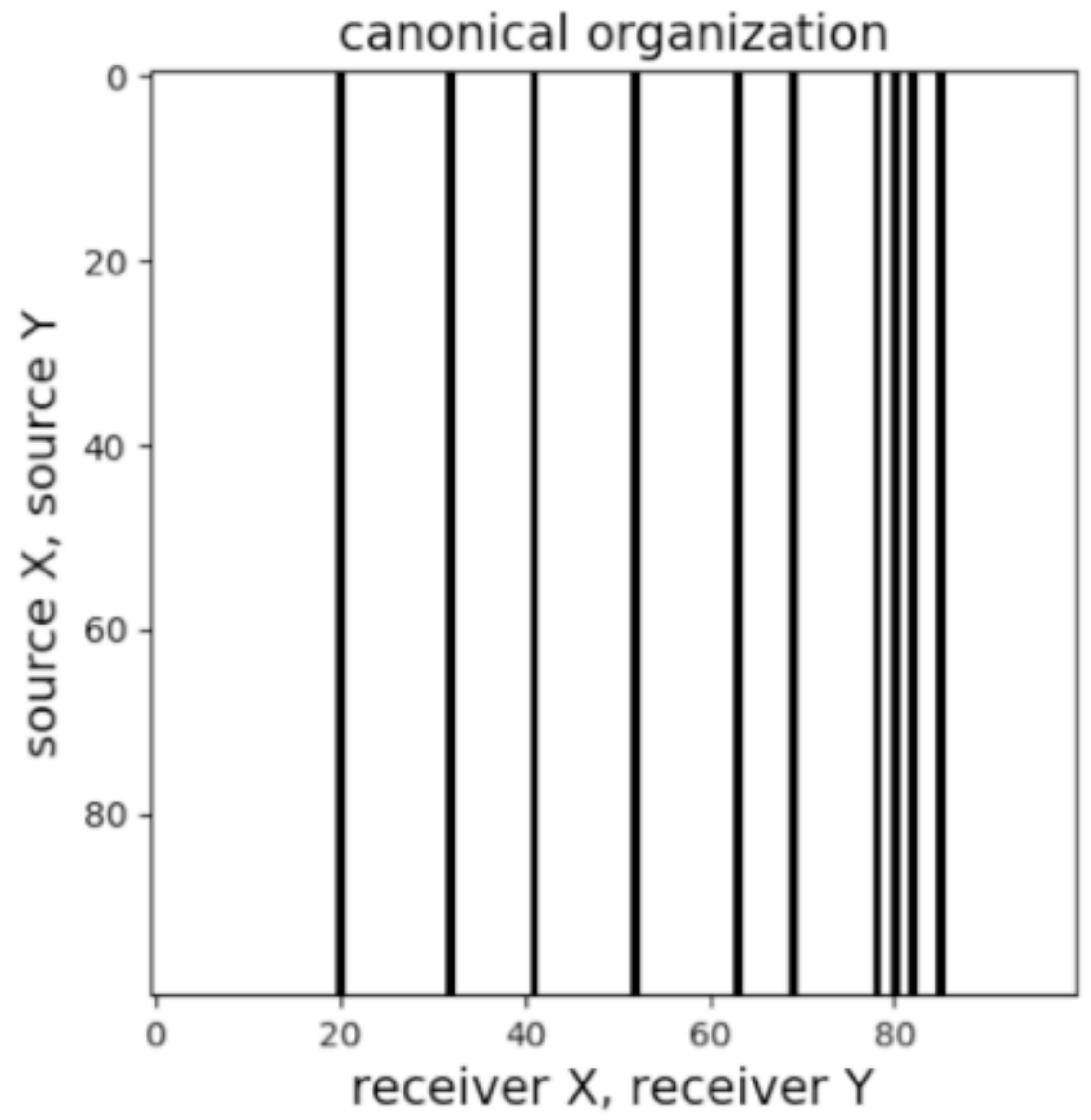

pick a row

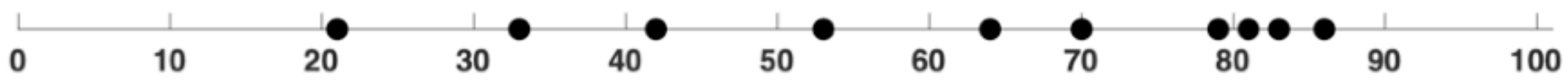

permutation

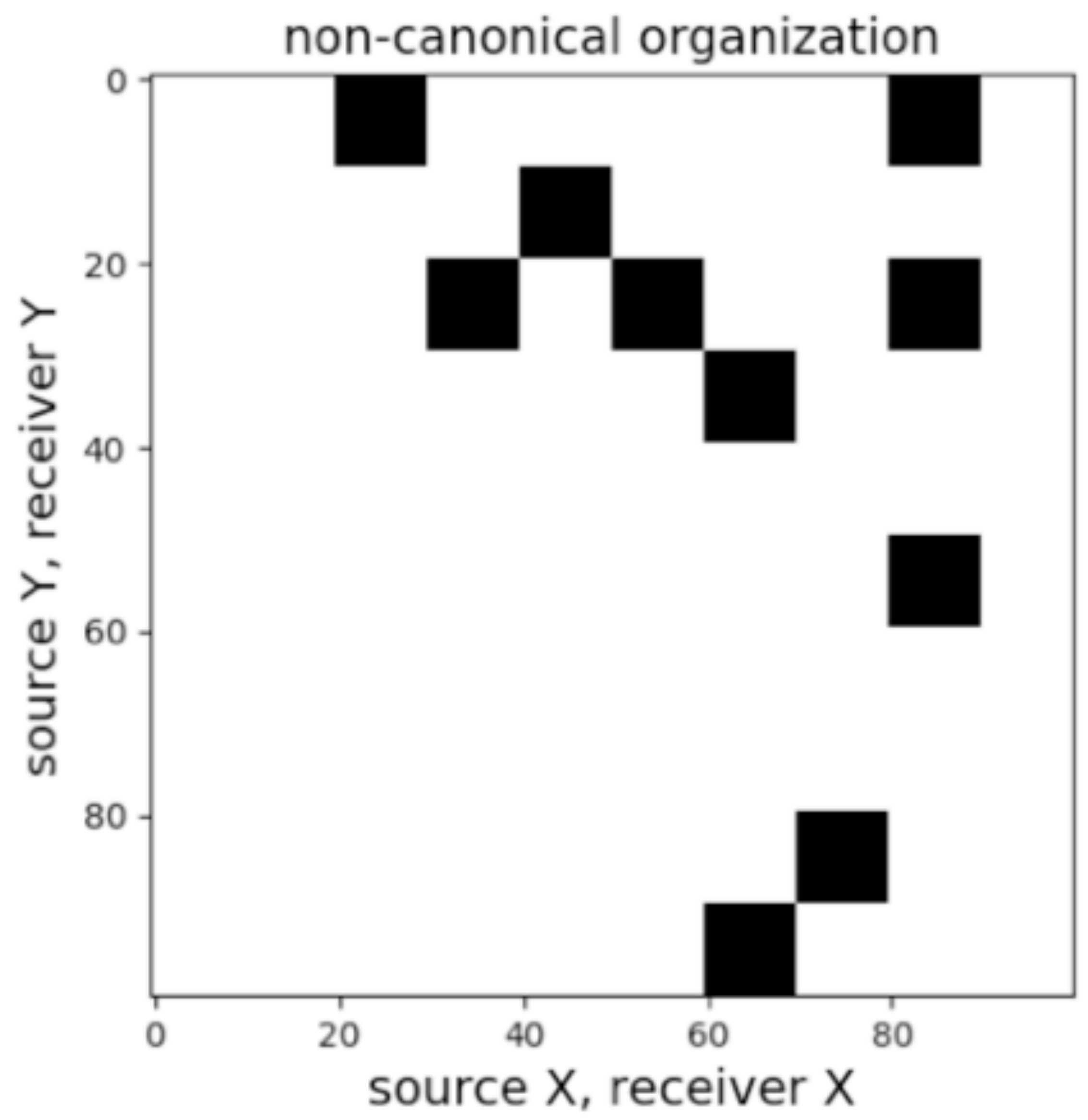

same spectral gap ratio
0.689

permutation

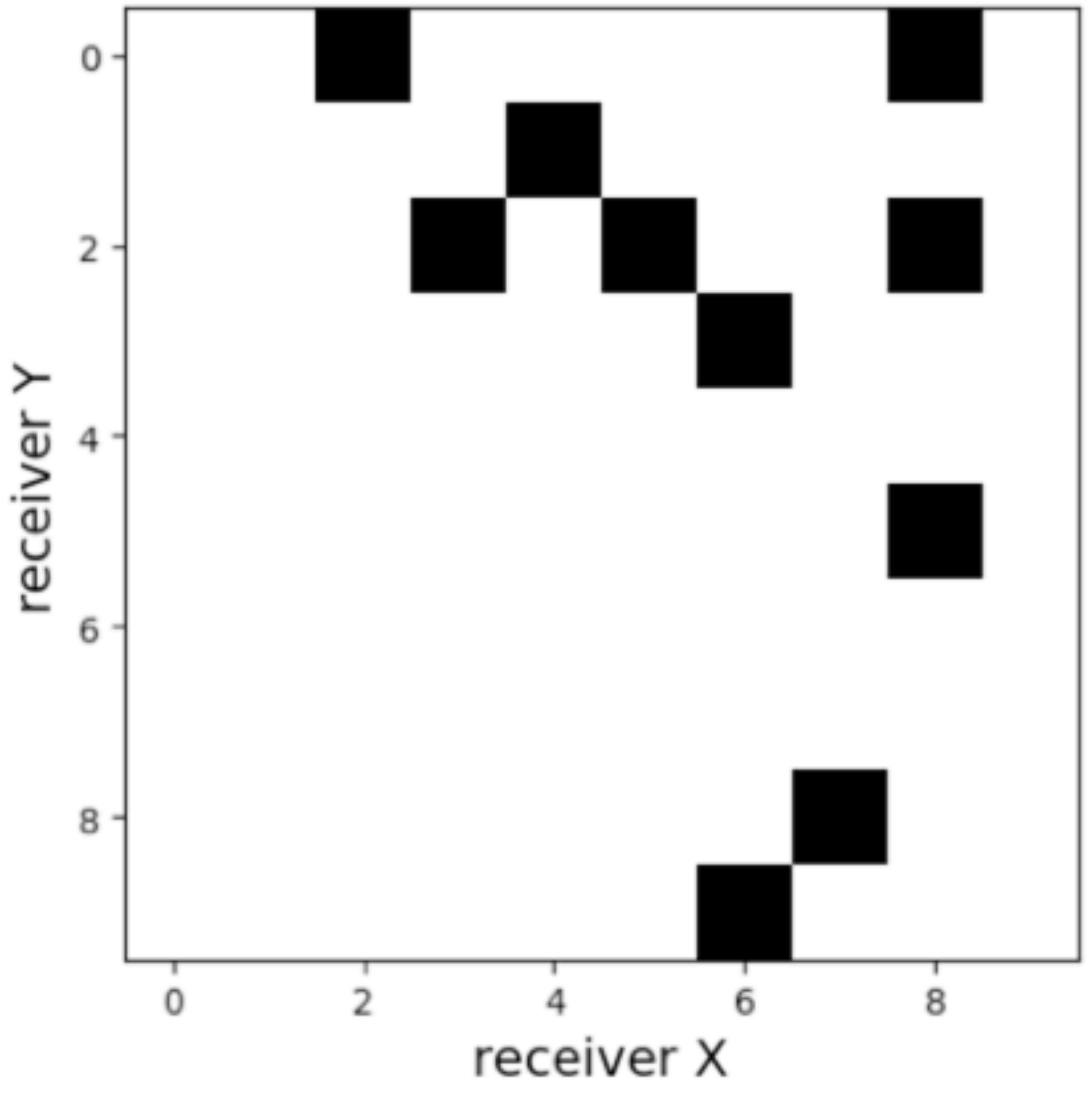

implement optimization

Zhang, Yijun, Shashin Sharan, Oscar Lopez, and Felix J. Herrmann. "Wavefield recovery with limited-subspace weighted matrix factorizations." In *SEG International Exposition and Annual Meeting*. OnePetro, 2020.

Test masks via LR matrix completion

3D synthetic Compass dataset

Data dimension: 10k x 1681 x 501 ($n_r \times n_s \times n_t$)

Frequency slice: 16.8Hz

Source sampling interval: 150 m

Receiver sampling interval: 25 m

Time sampling interval: 0.01 s

Comparison

	observed	recovery	error	SNR
jittered 0.507				**10.88dB**
proposed 0.328				**12.27dB**

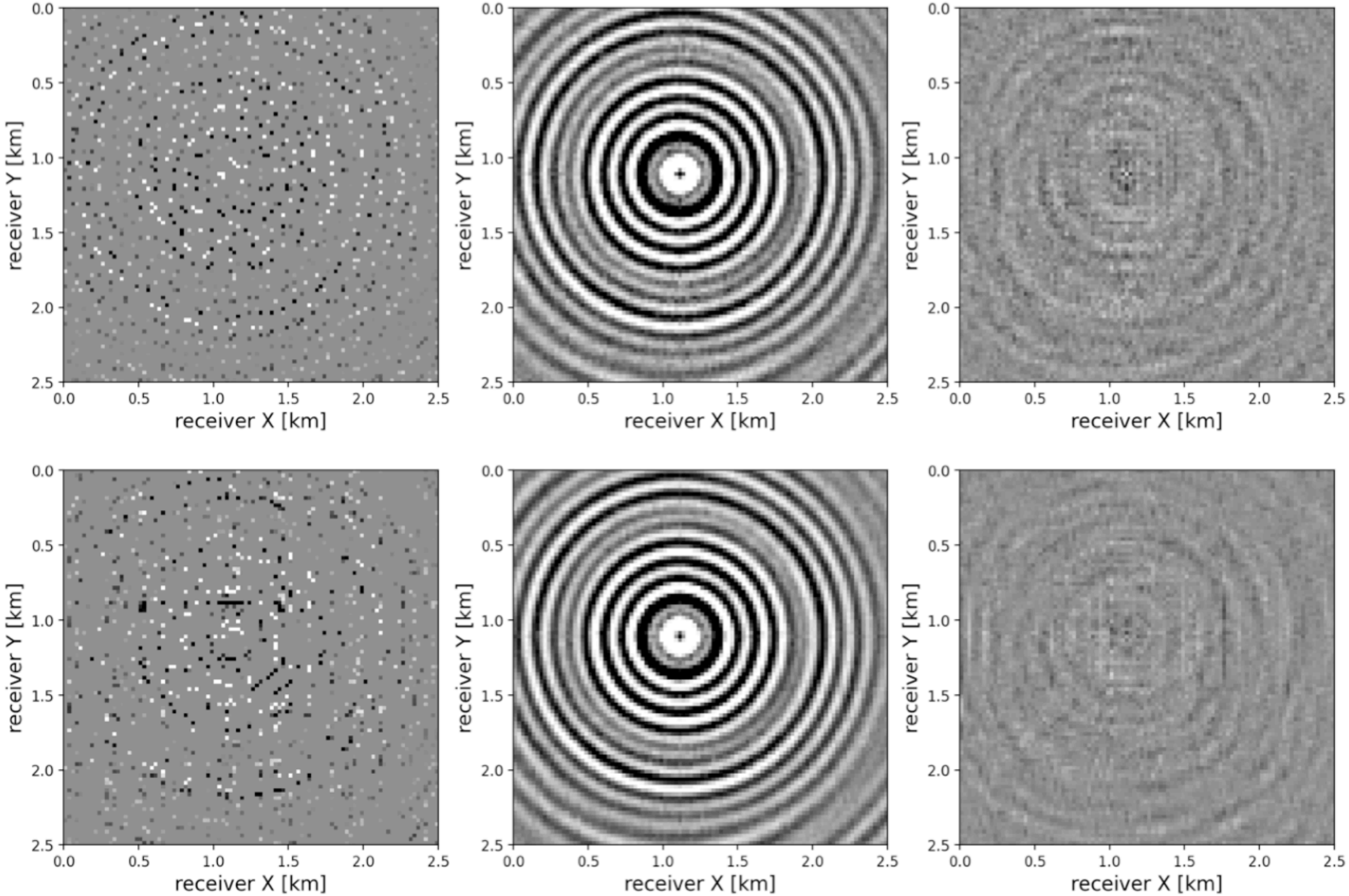

Contribution & conclusion

Proposed seismic survey design is

- simulation-free
- best suitable for wavefield reconstruction via matrix completion
- adaptable to 2D & 3D seismic survey designs

Optimized time-lapse acquisition design via spectral gap ratio minimization

Chapter 7

Oscar Lopez, Rajiv Kumar, Nick Moldoveanu and Felix J. Herrmann, “Graph Spectrum Based Seismic Survey Design”, 2020.
Mosher, C. C., S. T. Kaplan, and F. D. Janiszewski. "Non-uniform optimal sampling for seismic survey design." *74th EAGE Conference and Exhibition incorporating EUROPEC 2012*. European Association of Geoscientists & Engineers, 2012.
Ziyi Yin, Huseyin Tuna Erdinc, Abhinav Prakash Gahlot, Mathias Louboutin and Felix J. Herrmann. "De-risking geological carbon storage from high resolution time-lapse seismic to explainable leakage detection." *The leading edge. Just accepted in the January 2023 special section in seismic resolution*

Motivation

Seismic data

- expensive to acquire

Subsampling

- reduce costs
- increasingly employed in seismic data acquisition

Time-lapse seismic data

- crucial step for reservoir management
- play an important role for monitoring Geological Carbon Storage (GCS)
- offset the subsampling gains via replicate monitor and baseline surveys

Goal: propose a time-lapse seismic survey design

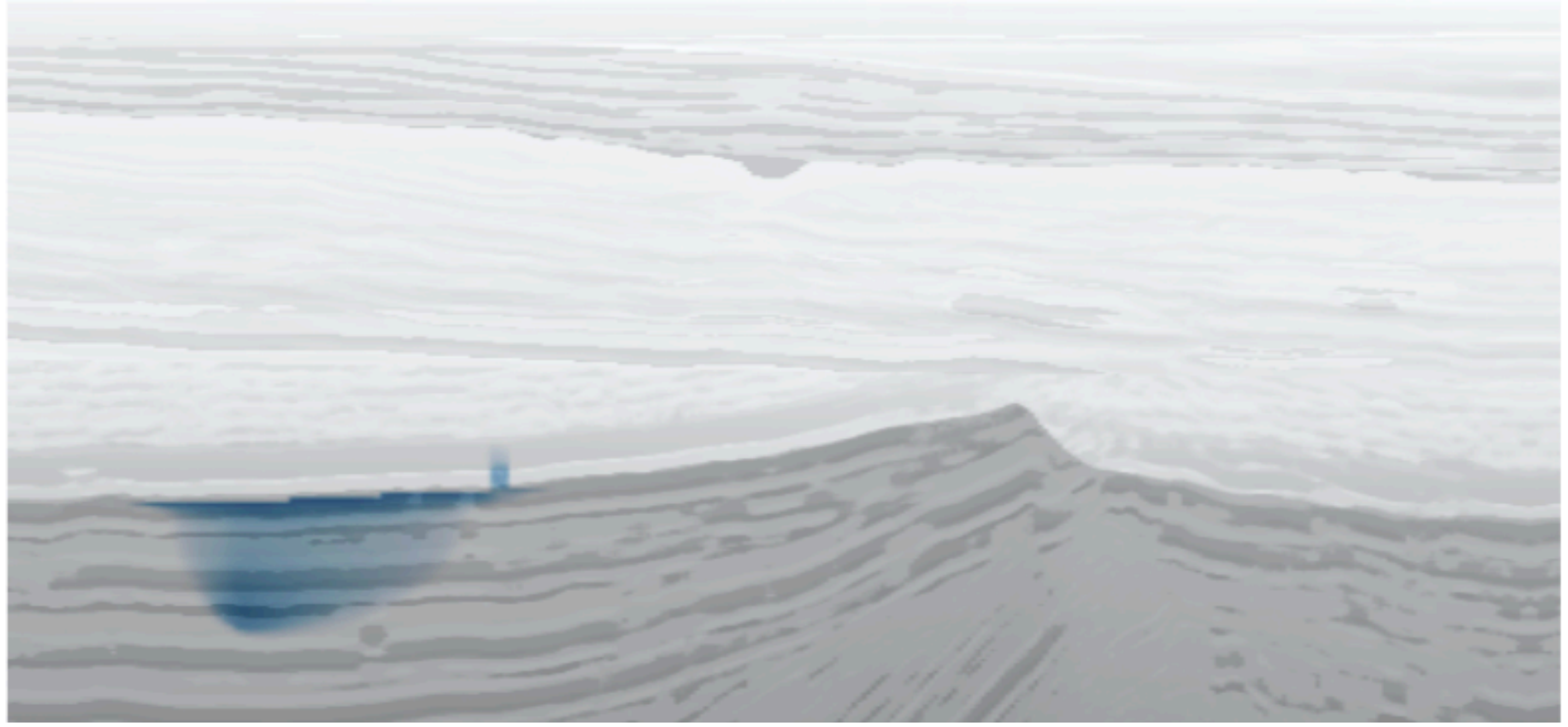

Image credit: Ziyi Yin

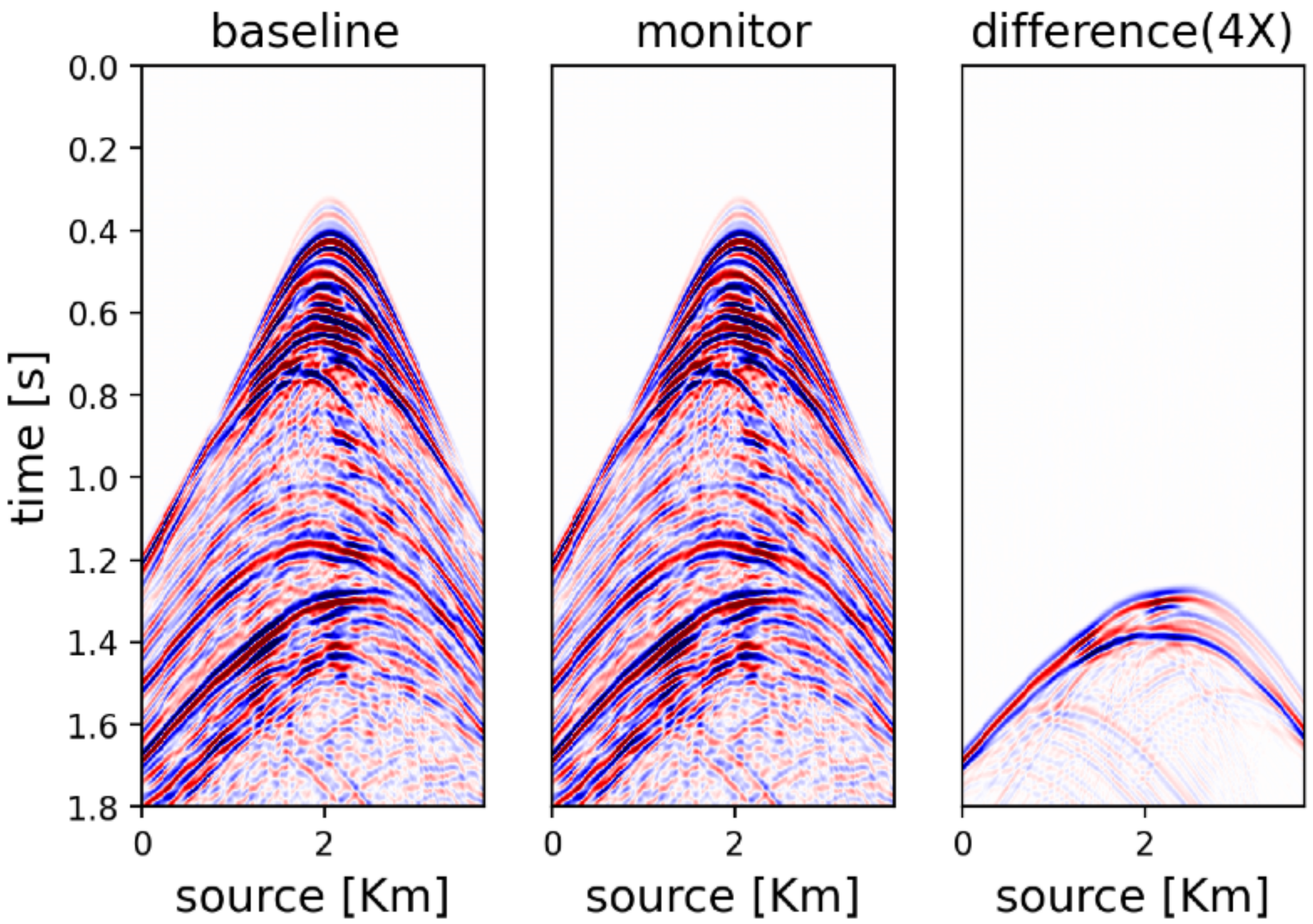

Time-lapse seismic acquisition
w/ multiple vintages

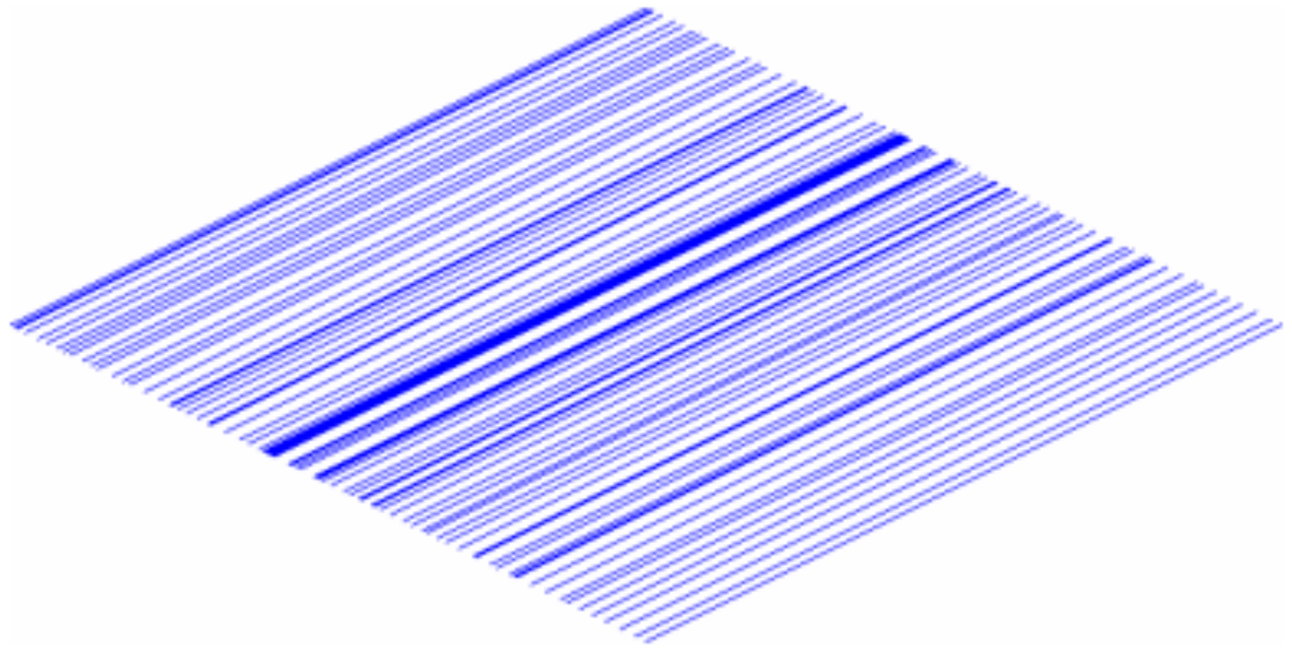

Baseline mask: $\mathbf{M}_1$

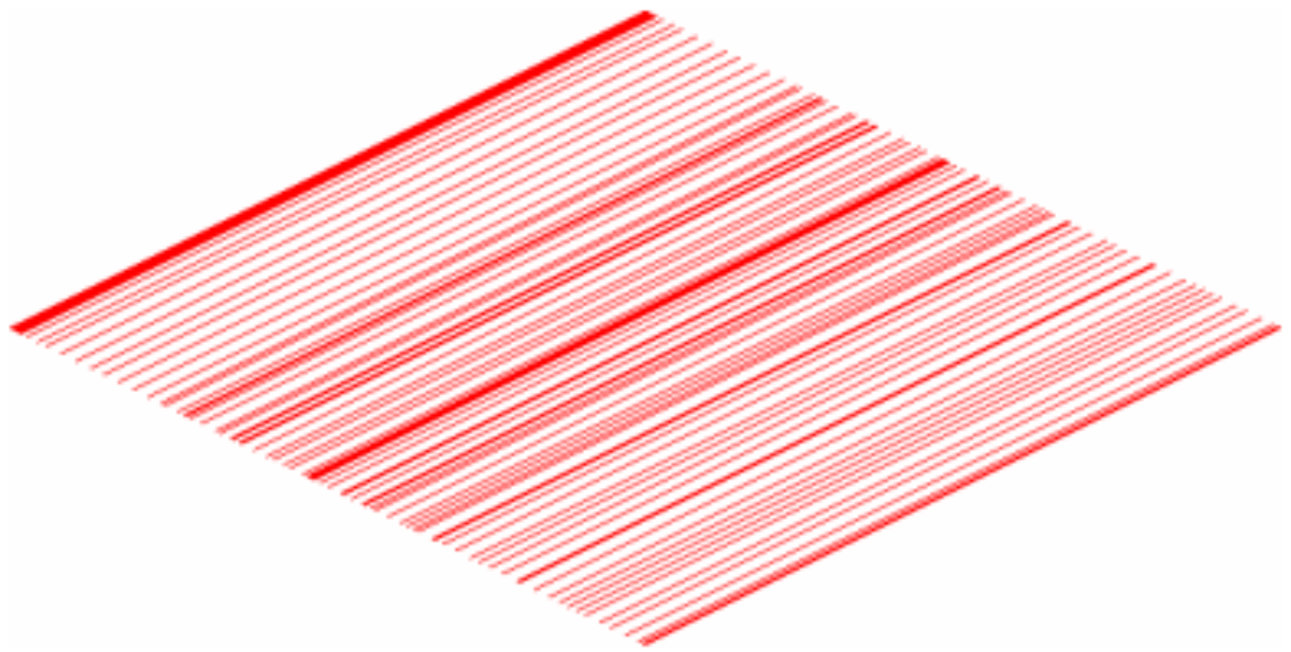

Monitor mask: $\mathbf{M}_2$

Oghenekohwo, Felix, Haneet Wason, Ernie Esser, and Felix J. Herrmann. "Low-cost time-lapse seismic with distributed compressive sensing—Part 1: Exploiting common information among the vintages." *Geophysics* 82, no. 3 (2017): P1-P13.

Kumar, Rajiv, et al. "Highly repeatable 3D compressive full-azimuth towed-streamer time-lapse acquisition—A numerical feasibility study at scale." *The Leading Edge* 36.8 (2017): 677-687.

Motivation

w/ joint recovery model (JRM)

$$\underbrace{\begin{bmatrix}\mathbf{b}_1\\ \mathbf{b}_2\end{bmatrix}}_{\mathbf{b}} = \underbrace{\begin{bmatrix}\mathscr{A}_1 & \mathscr{A}_1 & 0\\ \mathscr{A}_2 & 0 & \mathscr{A}_2\end{bmatrix}}_{\mathscr{A}} \underbrace{\begin{bmatrix}\mathbf{Z}_0\\ \mathbf{Z}_1\\ \mathbf{Z}_2\end{bmatrix}}_{\mathbf{z}}$$

$\mathbf{Z}_0$ ← **common component**

$\mathbf{Z}_1$, $\mathbf{Z}_2$ ← **innovation component**

- $\mathbf{b}_i$ subsampled data
- $\mathscr{A}_i$ sampling operator
- $\mathbf{X}_i$ to-be-recovered dense data
- $\mathbf{X}_i = \mathbf{Z}_0 + \mathbf{Z}_i \,, i \in 1,2$

- exploits common information between baseline & monitor
- benefits for non-replicated subsampling
- robust w.r.t noise

How to design JRM based masks?

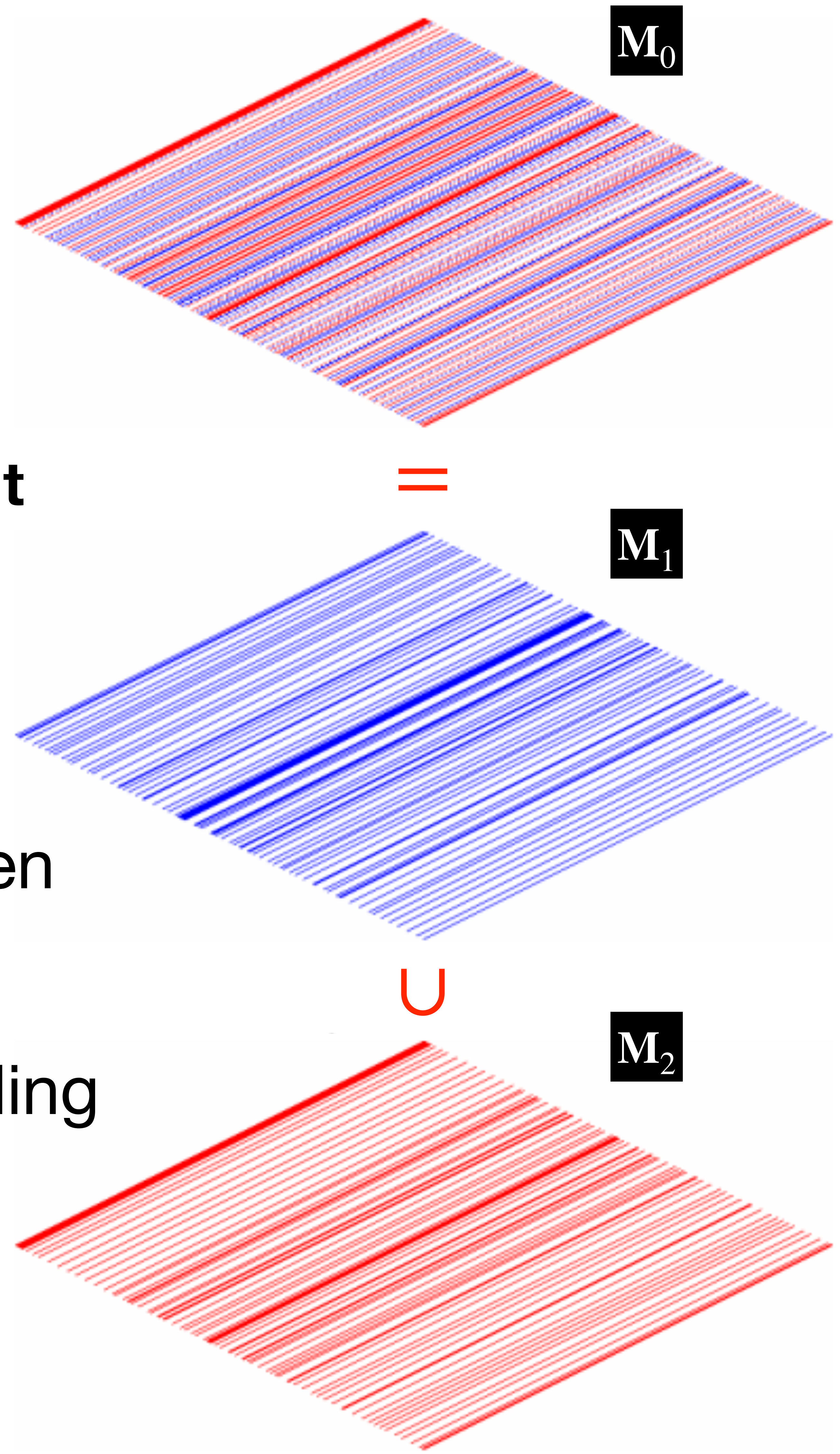

Oghenekohwo, Felix, Haneet Wason, Ernie Esser, and Felix J. Herrmann. "Low-cost time-lapse seismic with distributed compressive sensing—Part 1: Exploiting common information among the vintages." *Geophysics* 82, no. 3 (2017): P1-P13.

SLIM
ML4Seismic

Optimized problem

w/ joint recovery model (JRM) & two vintages

$$\underset{\mathbf{M_1},\mathbf{M_2}}{\text{minimize}} \quad \left\| \left[\mathscr{L}(\mathbf{M}_0), \sqrt{\frac{\#(\mathbf{M}_1)}{\#(\mathbf{M}_0)}} \mathscr{L}(\mathbf{M}_1), \sqrt{\frac{\#(\mathbf{M}_2)}{\#(\mathbf{M}_0)}} \mathscr{L}(\mathbf{M}_2) \right] \right\|_\infty$$

$$\text{subject to} \quad \mathbf{M}_1 \in \mathscr{C}^1, \mathbf{M}_2 \in \mathscr{C}^2$$

- $\sqrt{\frac{\#(\mathbf{M}_1)}{\#(\mathbf{M}_0)}}, \sqrt{\frac{\#(\mathbf{M}_2)}{\#(\mathbf{M}_0)}}$: balance the difference in spectral gap ratios, resulting from the difference subsampling numbers, between the common and innovation components.

Herrmann, Felix J., and Gilles Hennenfent. "Non-parametric seismic data recovery with curvelet frames." *Geophysical Journal International* 173.1 (2008): 233-248.

Optimal spectral gap ratio w/ simulated annealing

two vintages w/ JRM

Mask dimension: 300 X 300

Subsampling ratio: 25%

Source & receiver sampling interval: 12.5 m

Optimize the spectral gap ratios of given initial subsampling masks:

- jittered & $100\ \%$ replicated subsampling

Optimal a given mask

jittered & 100% replicated subsampling

● : baseline subsampled locations
● : monitor subsampled locations

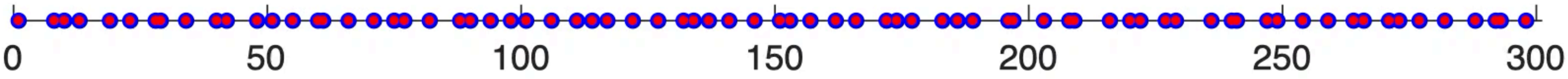

Baseline mask: M_1

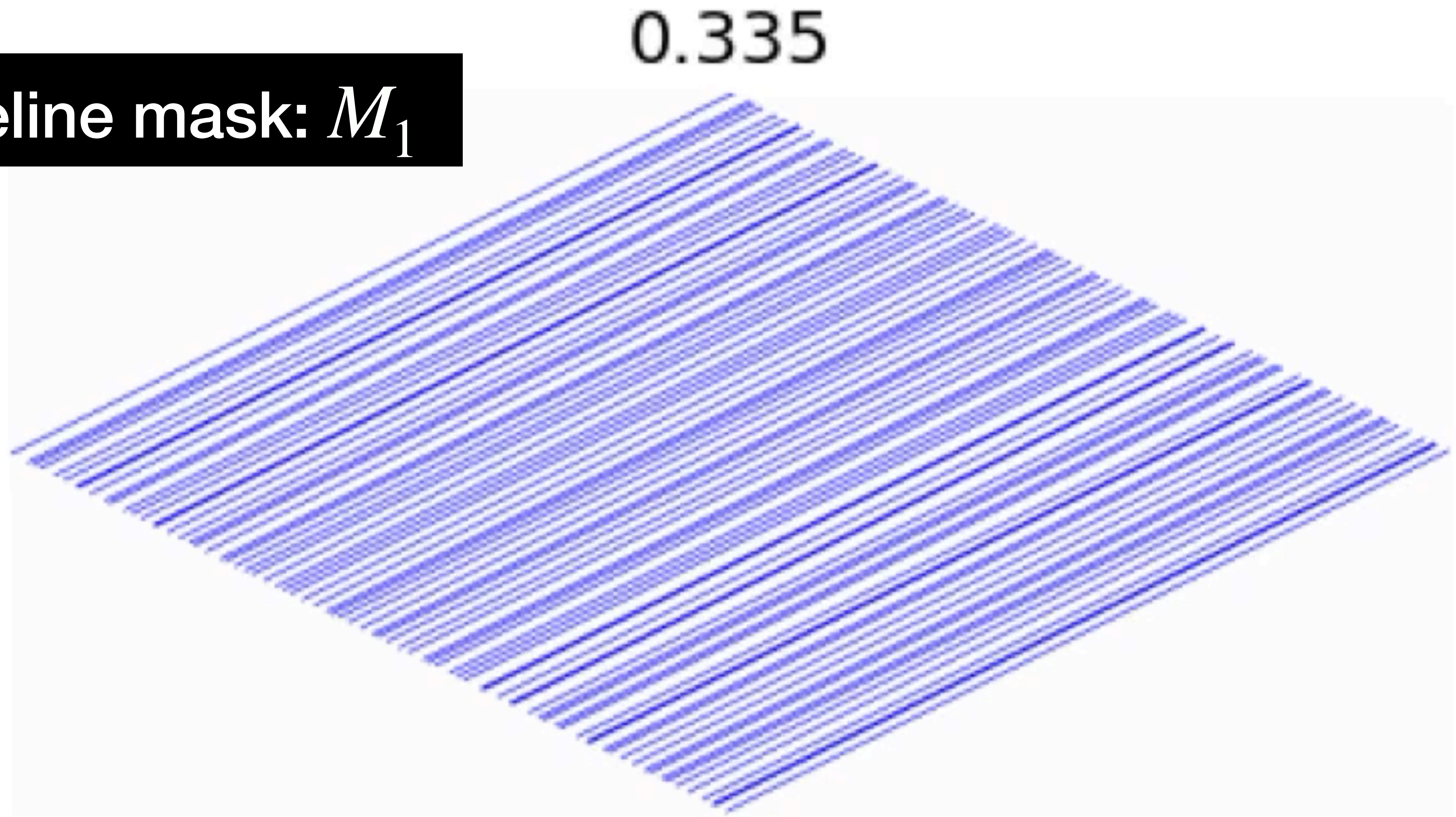

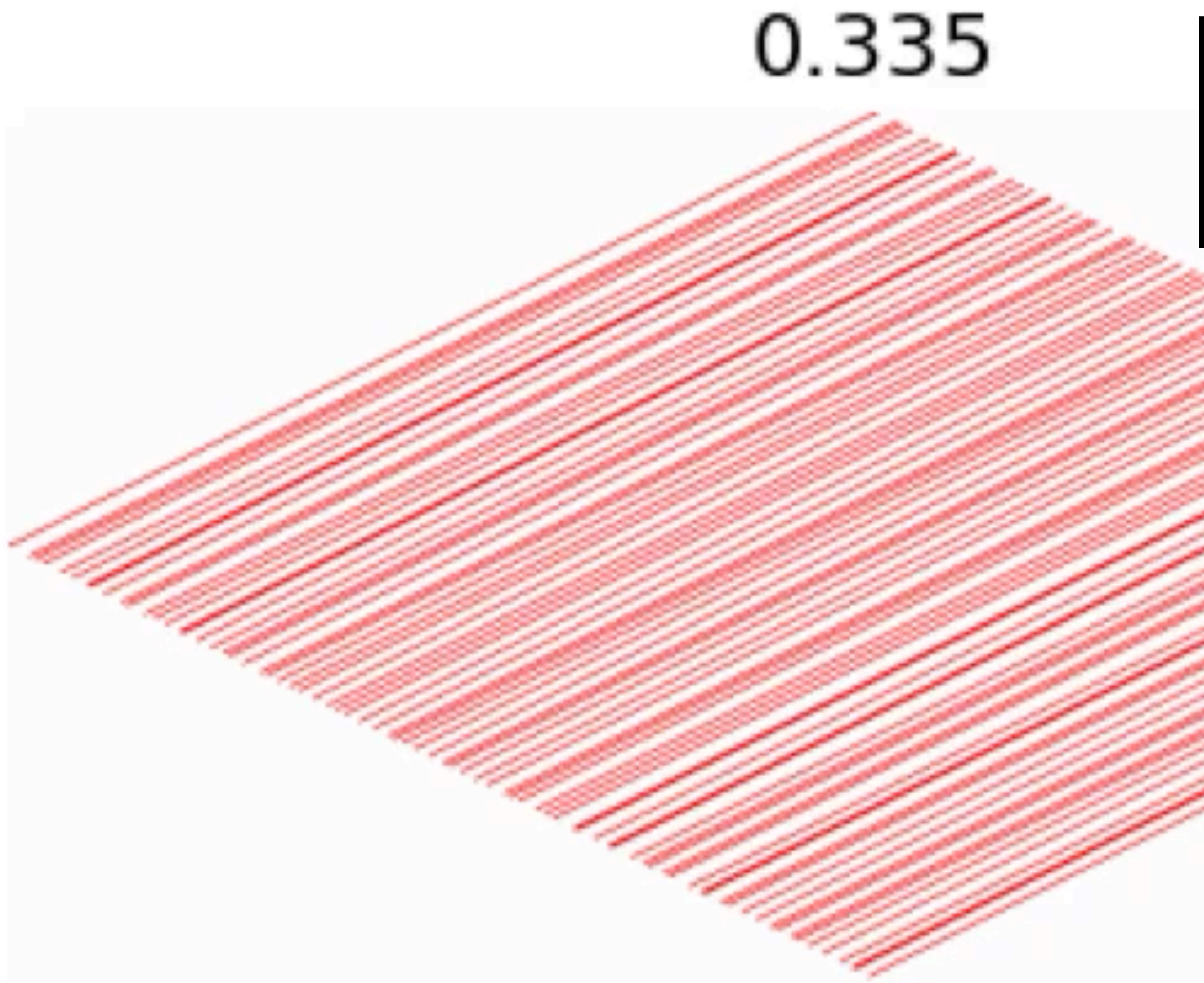

Mask common component:
$M_0 = M_1 \cup M_2$

Monitor mask: M_2

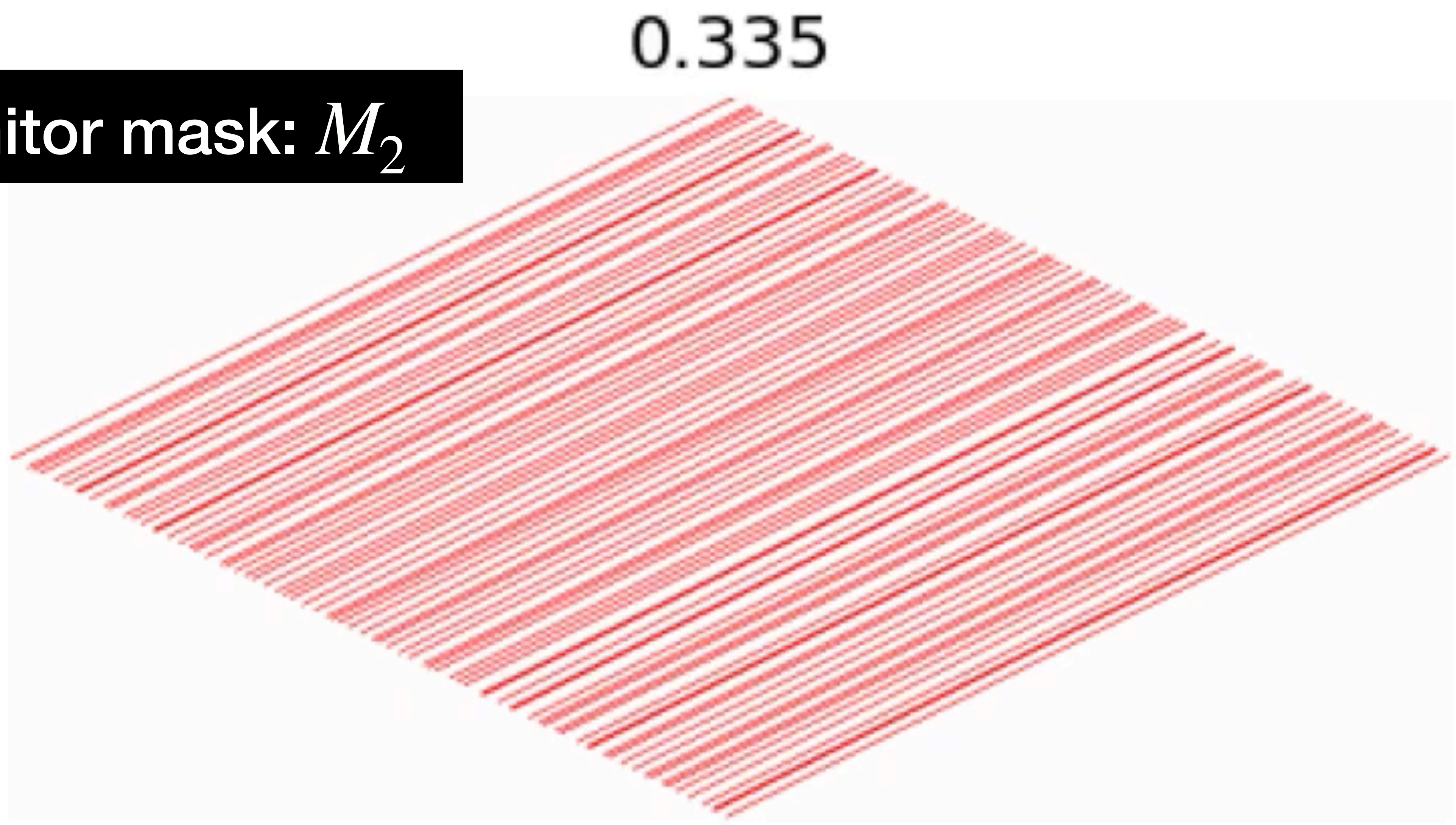

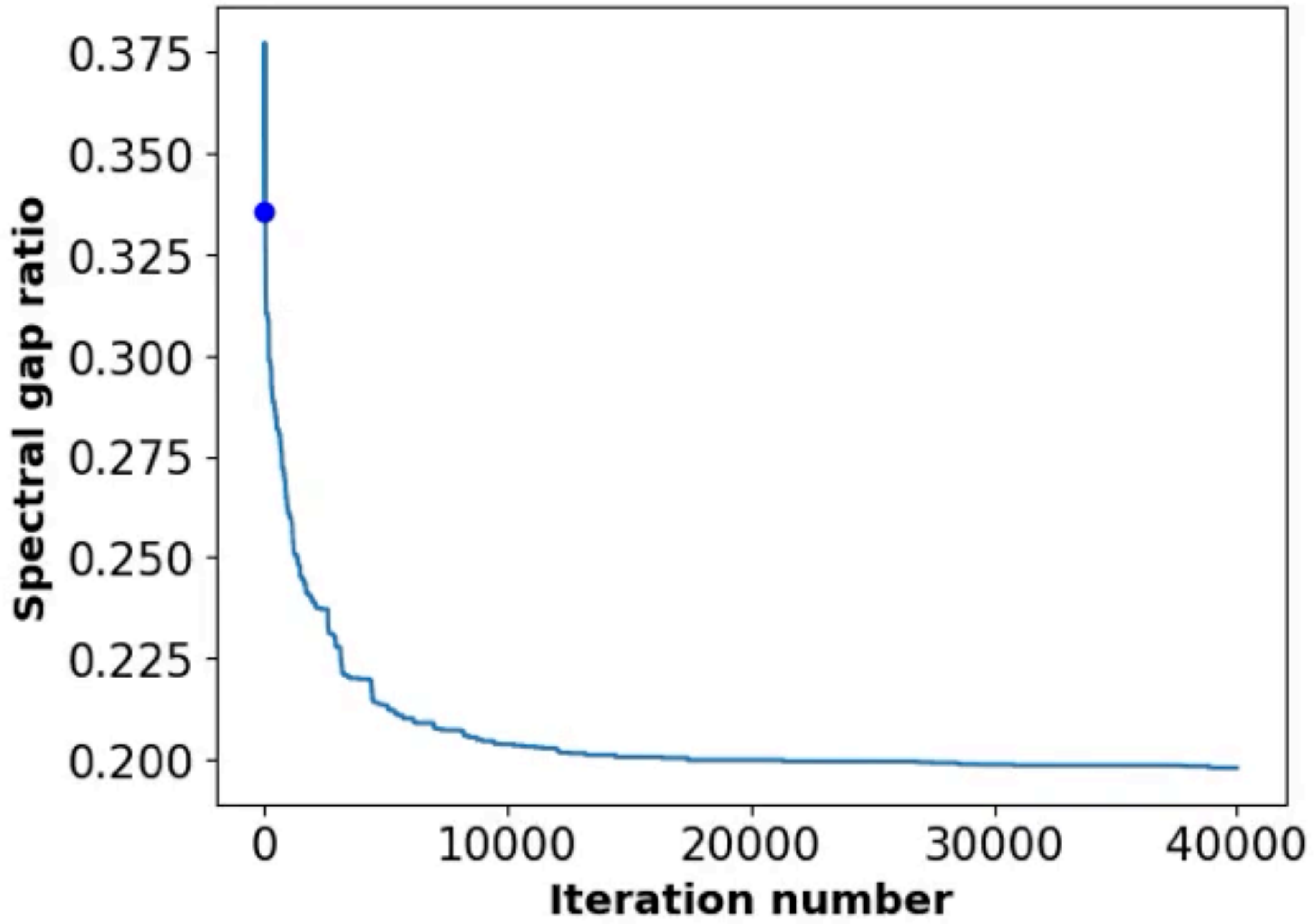

2D synthetic data example: BG

Data dimension: $300 \times 300 \times 901$ $(n_r \times n_s \times n_t)$

Dimension of each frequency slice: 300×300

Source sampling interval: 12.5 m

Receiver sampling interval: 12.5 m

Time sampling interval: 0.002 s

Observed data: ~75% missing sources

Animation

replicated jittered vs optimized

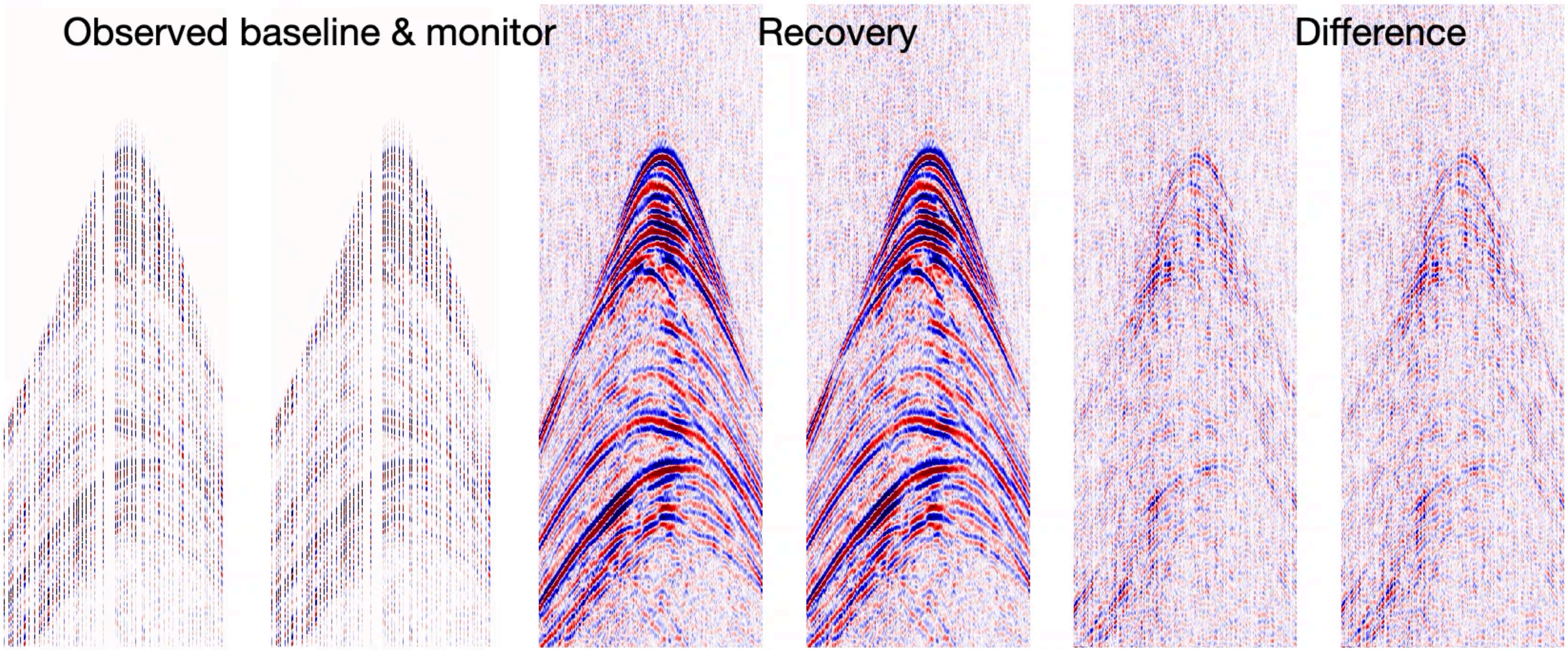

0.335

baseline SNR = 8.60 dB

monitor SNR = 8.73 dB

Spectral gap comparison vs. SNR comparison
w/ 30 independent experiments

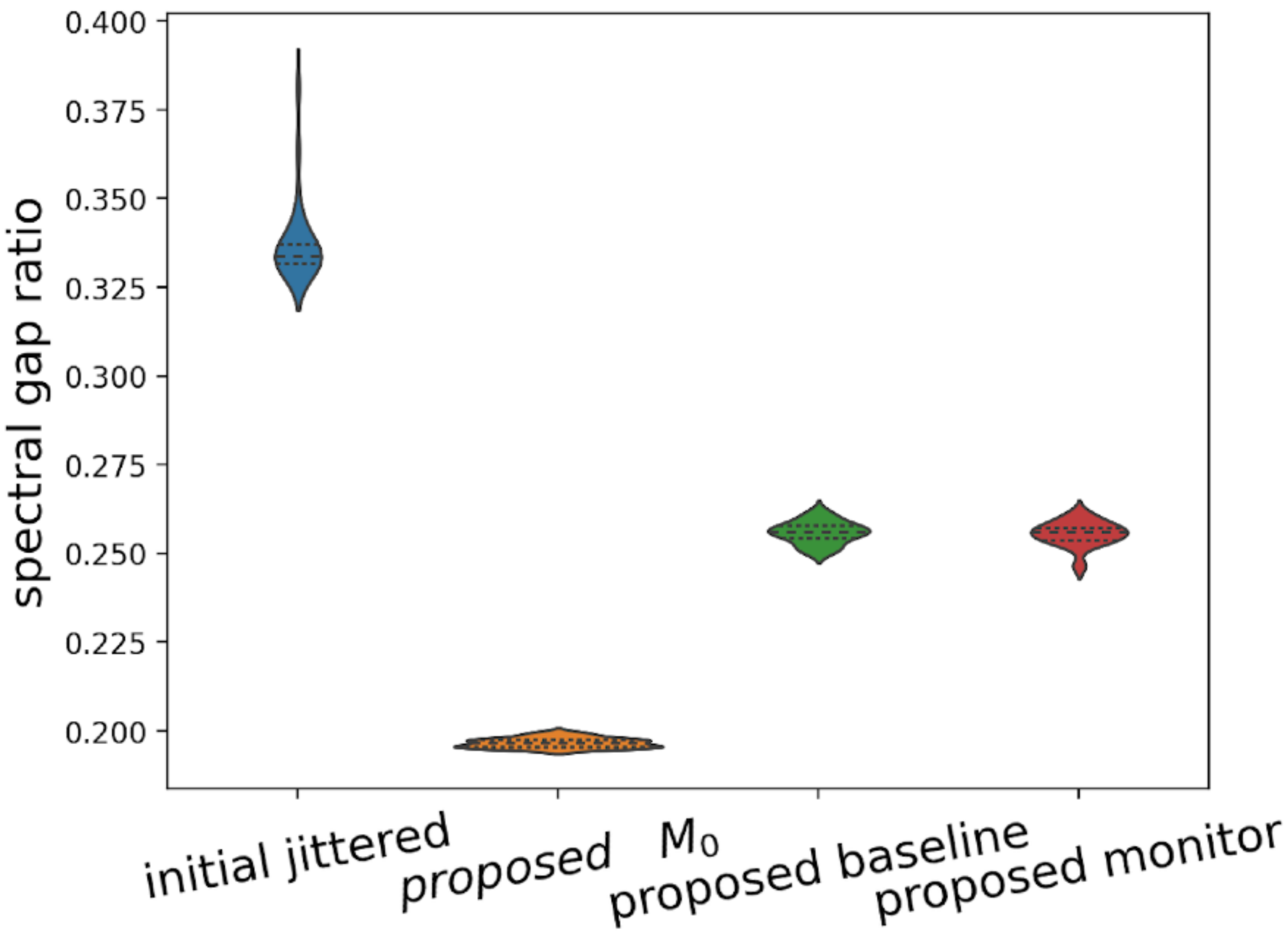

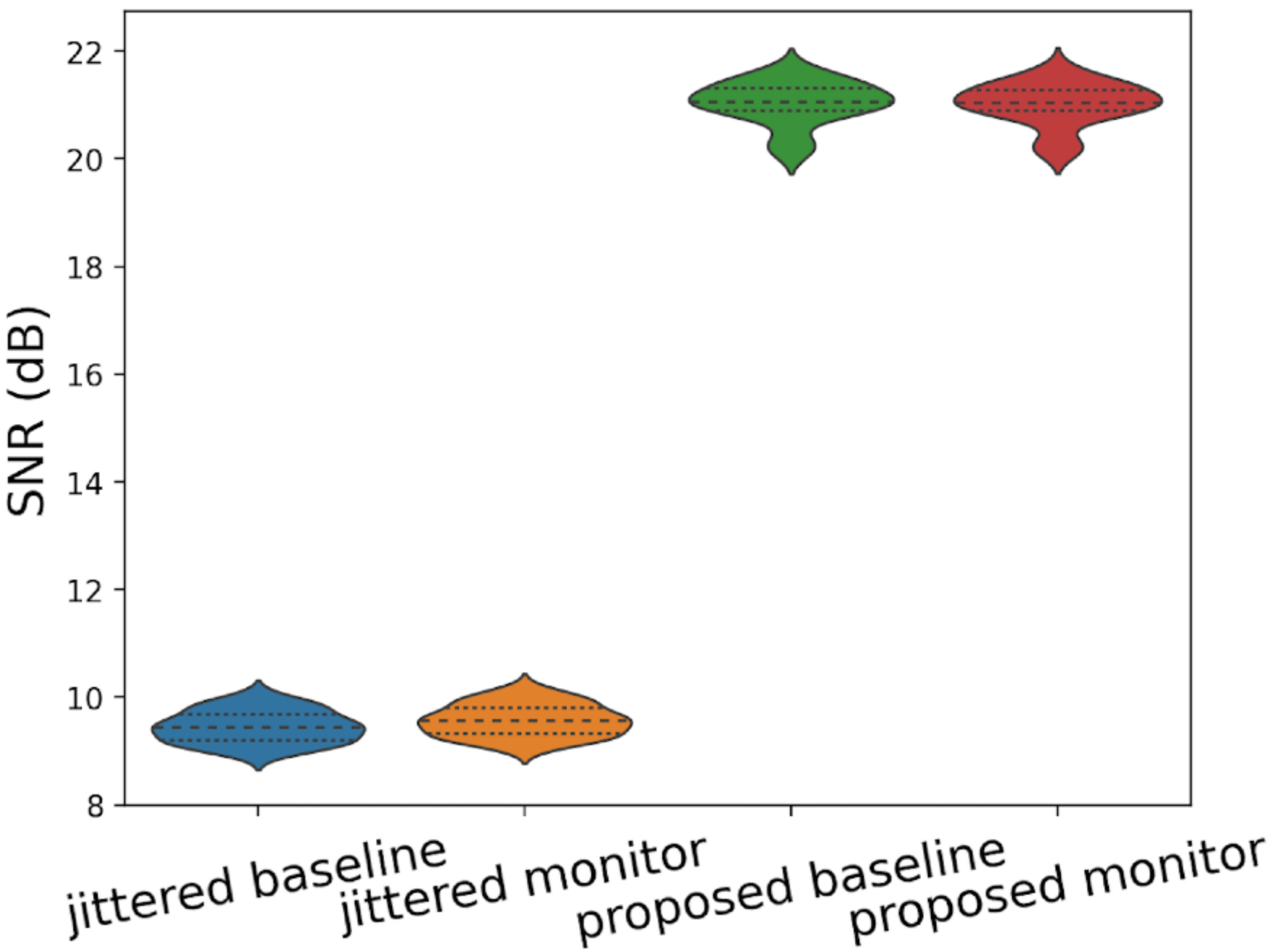

Conclusion

Proposed seismic survey design is

- simulation-free
- best suitable for wavefield reconstruction via matrix completion
- adaptable to multiple vintages' subsampling designs
    - prefer **non-replicated** subsampling locations

Large scale high-frequency wavefield reconstruction with recursively weighted matrix factorizations

Chapter 4

Motivations

2D seismic survey

- not collecting reflections outside the 2D plane
- small data volume
  - data dimension for one frequency slice, e.g. 355×355 $(n_r \times n_s)$

3D seismic survey

- capture 3D reflections
- large data volume
  - data dimension for one frequency slice, e.g. $201 \times 201 \times 41 \times 41$ $(n_{rx} \times n_{ry} \times n_{sx} \times n_{sy})$

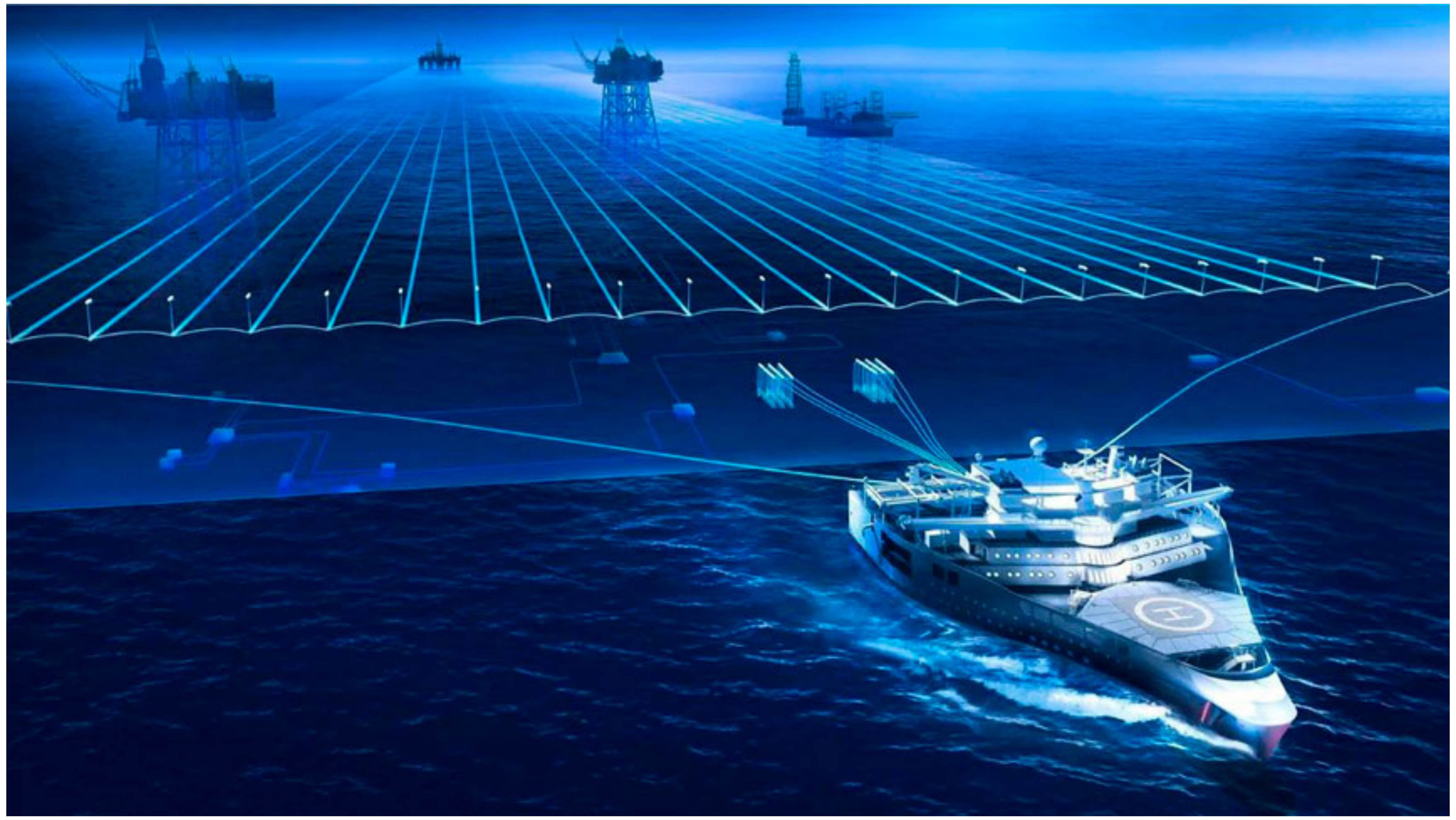

Motivations

Runtime comparison for one frequency slice w/ dimension 8241×8241 $(201 \times 41 = 8241)$

Methods	SNRs (dB)	Times (hours)	Iterations
Weighted method	16.28	10.34	130
Weighted method (efficient)	16.16	4.19	150

3D seismic survey

- one data volume w/ hundreds of frequency slices
- bring computational challenges

Aravkin, A., Kumar, R., Mansour, H., Recht, B., and Herrmann, F. J. “Fast methods for denoising matrix completion formulations, with applications to robust seismic data interpolation.” SIAM Journal on Scientific Computing, 2014.
Zhang, Yijun, et al. "Wavefield recovery with limited-subspace weighted matrix factorizations." *SEG International Exposition and Annual Meeting*. OnePetro, 2020

Question: Is it possible to parallelize the new method and increase its efficiency when solving 3D problems?

Parallel matrix completion

Parallel matrix completion

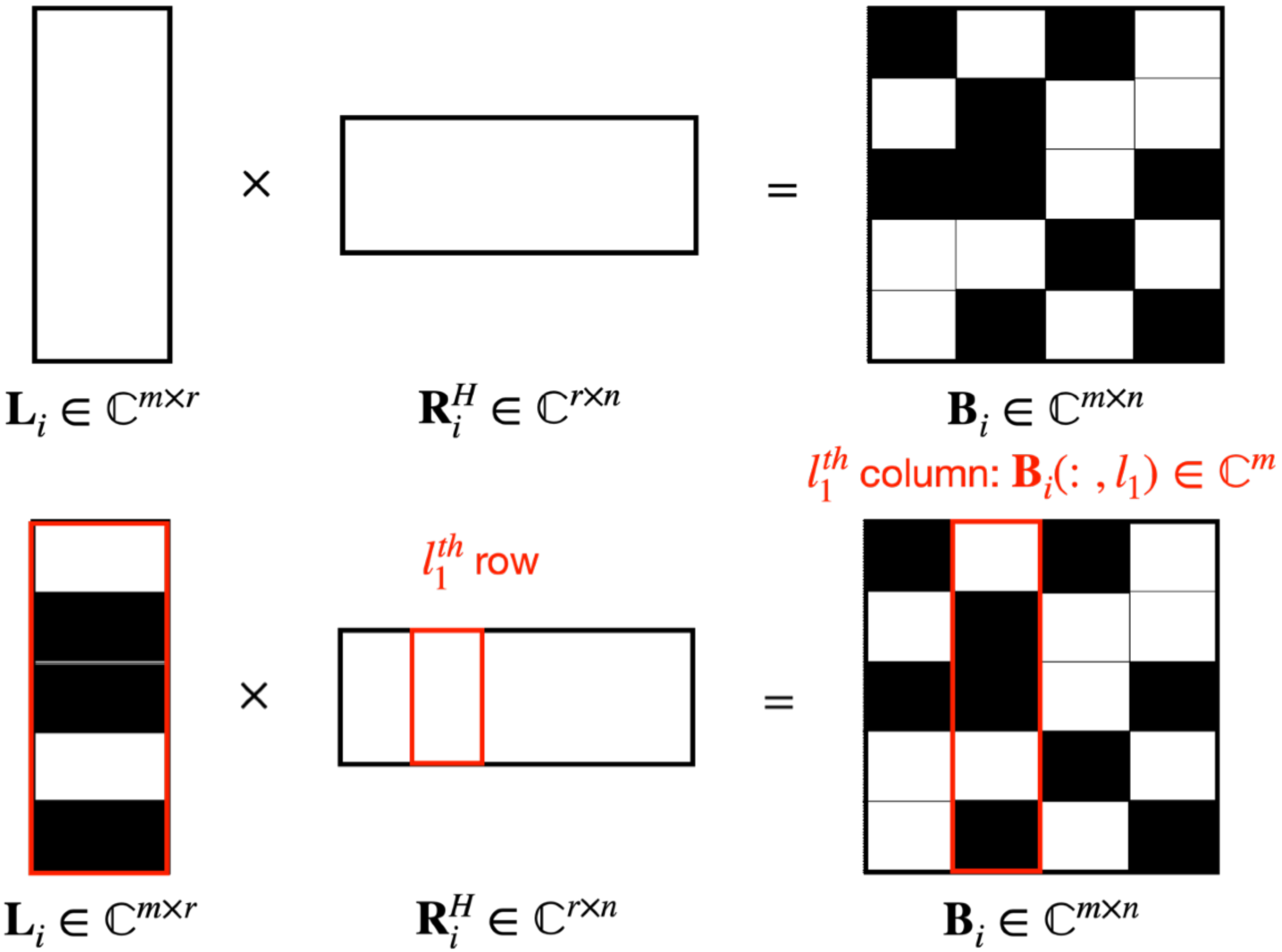

Lopez, Oscar, Rajiv Kumar, and Felix J. Herrmann. "Rank minimization via alternating optimization-seismic data interpolation." In *77th EAGE Conference and Exhibition 2015*, vol. 2015, no. 1, pp. 1-5. European Association of Geoscientists & Engineers, 2015.

Lopez, Oscar, Rajiv Kumar, and Felix J. Herrmann. "Rank minimization via alternating optimization-seismic data interpolation." In *77th EAGE Conference and Exhibition 2015*, vol. 2015, no. 1, pp. 1-5. European Association of Geoscientists & Engineers, 2015.
Recht, Benjamin, and Christopher Ré. "Parallel stochastic gradient algorithms for large-scale matrix completion." *Mathematical Programming Computation* 5, no. 2 (2013): 201-226.

SLIM

Parallel matrix completion

Alternating optimization between minimizing rows via row-by-row decoupled computing **Fixed $\mathbf{L}$, update $\mathbf{R}$**

$$\underset{\mathbf{v}\in\mathbb{C}^{\mathbf{r}\times 1}}{\text{minimize}} \quad \frac{1}{2}\|\mathbf{v}\|^2 \quad \text{subject to} \quad \|\mathscr{A}_{l_1}(\mathbf{L}\mathbf{v}) - \mathbf{B}(:,l_1)\| \leq \tau$$

and minimizing columns via the column-by-column decoupled computation **Fixed $\mathbf{R}$, update $\mathbf{L}$**

$$\underset{\mathbf{u}\in\mathbb{C}^{\mathbf{r}\times 1}}{\text{minimize}} \quad \frac{1}{2}\|\mathbf{u}\|^2 \quad \text{subject to} \quad \|\mathscr{A}_{l_2}((\mathbf{R}\mathbf{u})^H) - \mathbf{B}(l_2,:)\| \leq \tau$$

- $\mathbf{v} = \mathbf{R}(l_1,:)^H, \mathbf{u} = \mathbf{L}(l_2,:)^H, l_1 = 1,\cdots,n, l_2 = 1,\cdots,m$
- $\mathbf{L} \in \mathbb{C}^{m\times r}$
- $\mathbf{R} \in \mathbb{C}^{n\times r}$
- $\mathbf{X} = \mathbf{L}\mathbf{R}^H$
- Subsampling operators $\mathscr{A}_{l_1}$ and $\mathscr{A}_{l_2}$ perform operations on columns/rows

Question: Is it possible to parallelize the new method and increase its efficiency when solving 3D problems?

Answer: Weighted parallel matrix factorization

SLIM

Weighted parallel matrix completion

Alternating optimization between minimizing rows via row-by-row decoupled computing

$$\underset{\bar{\mathbf{v}} \in \mathbb{C}^{r \times 1}}{\text{minimize}} \quad \frac{1}{2} \| \bar{\mathbf{v}} \|^2 \quad \text{subject to} \quad \| \mathscr{A}_{l_1}(\widehat{\mathbf{Q}} \bar{\mathbf{L}} \bar{\mathbf{v}}) - w_1 w_2 \mathbf{B}(:, l_1) \| \leq w_1 w_2 \tau$$

and minimizing columns via the column-by-column decoupled computation

$$\underset{\bar{\mathbf{u}} \in \mathbb{C}^{r \times 1}}{\text{minimize}} \quad \frac{1}{2} \| \bar{\mathbf{u}} \|^2 \quad \text{subject to} \quad \| \mathscr{A}_{l_2}((\bar{\mathbf{R}} \bar{\mathbf{u}})^H \widehat{\mathbf{W}}) - w_1 w_2 \mathbf{B}(l_2, :) \| \leq w_1 w_2 \tau$$

- $\bar{\mathbf{v}} = \bar{\mathbf{R}}(l_1, :)^H, \bar{\mathbf{u}} = \bar{\mathbf{L}}(l_2, :)^H, l_1 = 1, \cdots, n, l_2 = 1, \cdots, m$
- $\widehat{\mathbf{Q}} = \mathbf{U}\mathbf{U}^H + w_1 \mathbf{U}^{\perp} \mathbf{U}^{\perp^H} = w_1 \mathbf{Q}^{-1}$
- $\widehat{\mathbf{W}} = \mathbf{V}\mathbf{V}^H + w_2 \mathbf{V}^{\perp} \mathbf{V}^{\perp^H} = w_2 \mathbf{W}^{-1}$
- $\mathbf{L} = \frac{1}{w_1} \widehat{\mathbf{Q}} \bar{\mathbf{L}}, \ \mathbf{R} = \frac{1}{w_2} \widehat{\mathbf{W}} \bar{\mathbf{R}}$

Weighted minimization

Via alternating minimization

Input: Observed data $\mathbf{B}$, rank r, acquisition mask $\mathscr{A}$,priors $\widehat{\mathbf{Q}}$, $\widehat{\mathbf{W}}$ & initial guess $\bar{\mathbf{L}}^{(0)}$

1. for $k = 0,1,2,\cdots, N-1$ // solve for rows of $\mathbf{R}$ & $\mathbf{L}$ in parallel

2. $\left(\bar{\mathbf{R}}^{(k+1)}(l_1, :)\right)^H := \arg\min_{\bar{\mathbf{v}}} \quad \frac{1}{2} \| \bar{\mathbf{v}} \|^2$ s. t. $\|\mathscr{A}_{l_1}(\widehat{\mathbf{Q}}\bar{\mathbf{L}}^{(k)}\bar{\mathbf{v}}) - w_1 w_2 \mathbf{B}(:, l_1)\| \leq w_1 w_2 \tau$

3. $\left(\bar{\mathbf{L}}^{(k+1)}(l_2, :)\right)^H := \arg\min_{\bar{\mathbf{u}}} \quad \frac{1}{2} \| \bar{\mathbf{u}} \|^2$ s. t. $\|\mathscr{A}_{l_2}((\bar{\mathbf{R}}^{(k+1)}\bar{\mathbf{u}})^H \widehat{\mathbf{W}}) - w_1 w_2 \mathbf{B}(l_2, :)\| \leq w_1 w_2 \tau$

4. end for

5. $\mathbf{L} = \frac{1}{w_1} \widehat{\mathbf{Q}} \bar{\mathbf{L}}$

6. $\mathbf{R} = \frac{1}{w_2} \widehat{\mathbf{W}} \bar{\mathbf{R}}$

Output: Recovered wavefield in factored form $\{\mathbf{L}, \mathbf{R}\}$

Runtime comparison

By working with 8 parallel workers (2 threads each) in the Cloud, a significantly faster runtime ($83\times$) is achieved compare w/ the original weighted method

Runtime comparison for one frequency slice w/ dimension 8241×8241

Methods	SNRs (dB)	Times (hours)	Iterations
Weighted method	16.28	10.34	130
Weighted method (efficient)	16.16	4.19	150
Parallel weighted	**16.33**	**0.13**	5 alternations & 40 inner iterations

Synthetic Compass model data: 3D example

Synthetic Compass model data

3D example

Data dimension: $201 \times 201 \times 41 \times 41 \times 501$ $(n_{rx} \times n_{ry} \times n_{sx} \times n_{sy} \times n_t)$

Dimension of each frequency slice: 8241×8241

Source sampling interval: 150 m

Receiver sampling interval: 25 m

Time sampling interval: 0.01s

Observed data: $90\ \%$ missing receivers

Scenarios compared

Scenarios

- w/o using any prior information (conventional)

- using recursive prior information (recursively weighted)

Frequency slice (one shot) (15Hz)

Fully sampled data
~15 Hz slice

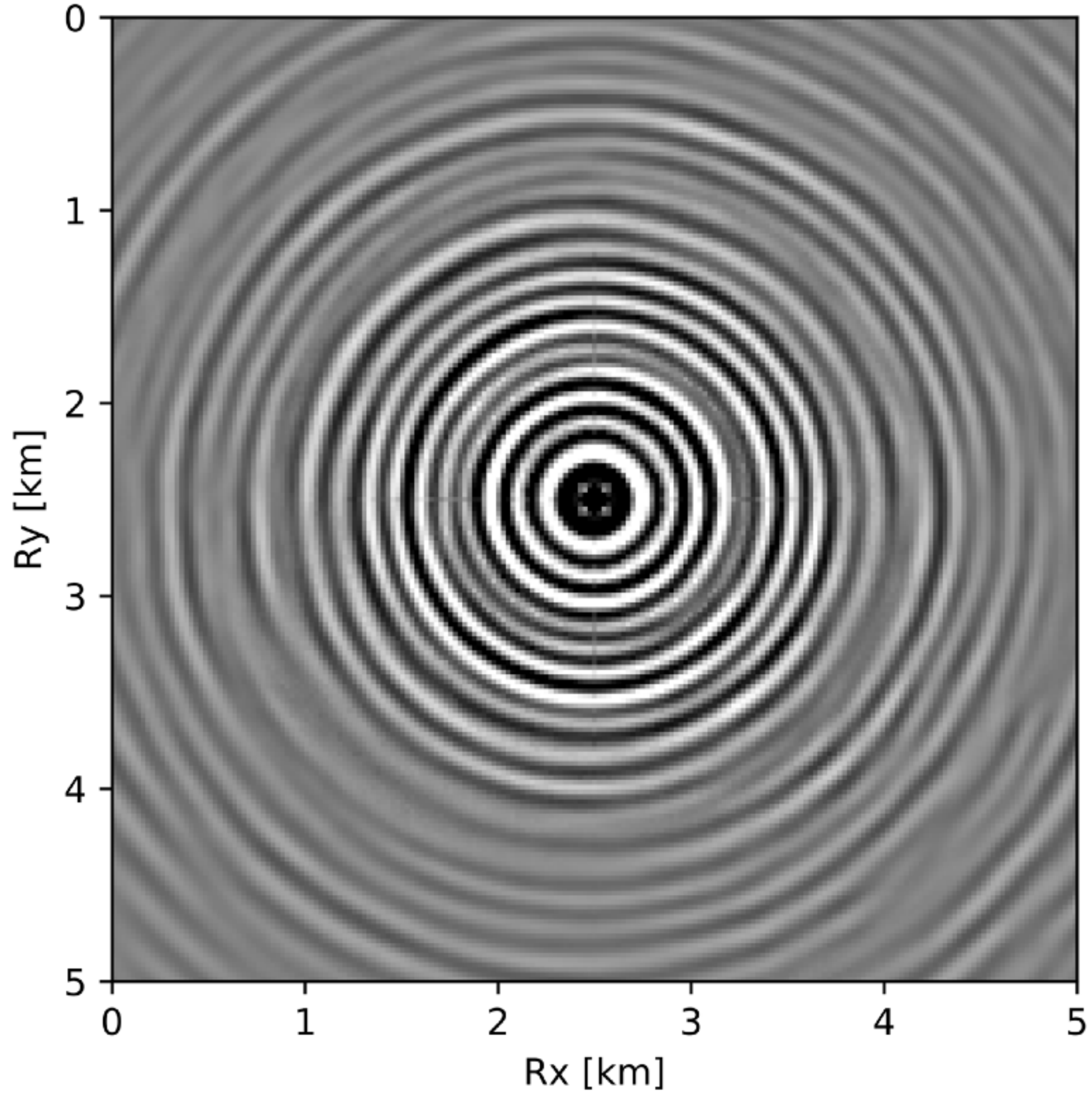

Observed data

90 % jittered subsampling

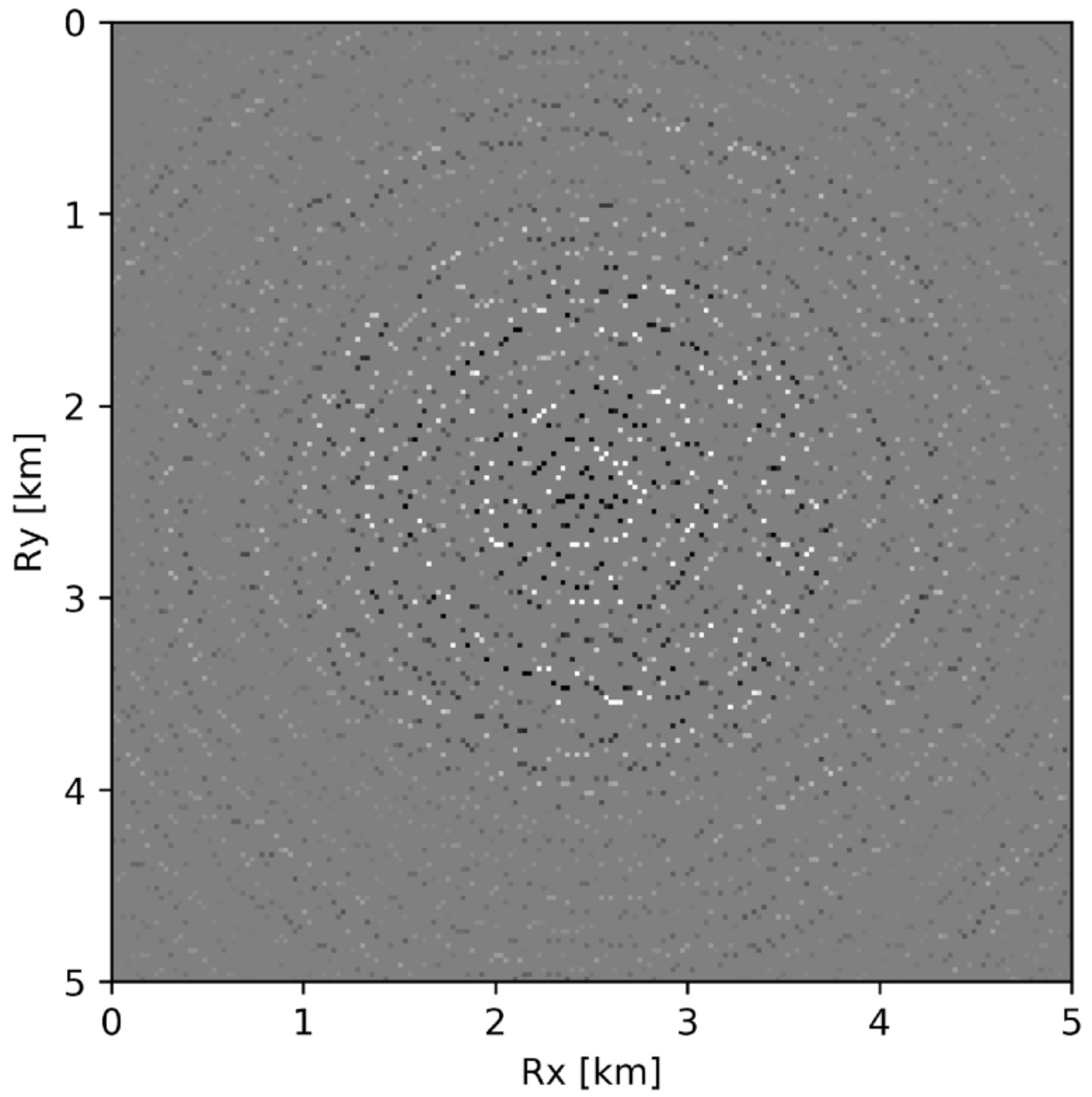

Herrmann, Felix J., and Gilles Hennenfent. "Non-parametric seismic data recovery with curvelet frames." *Geophysical Journal International* 173.1 (2008): 233-248.

Recovery
w/ conventional matrix completion

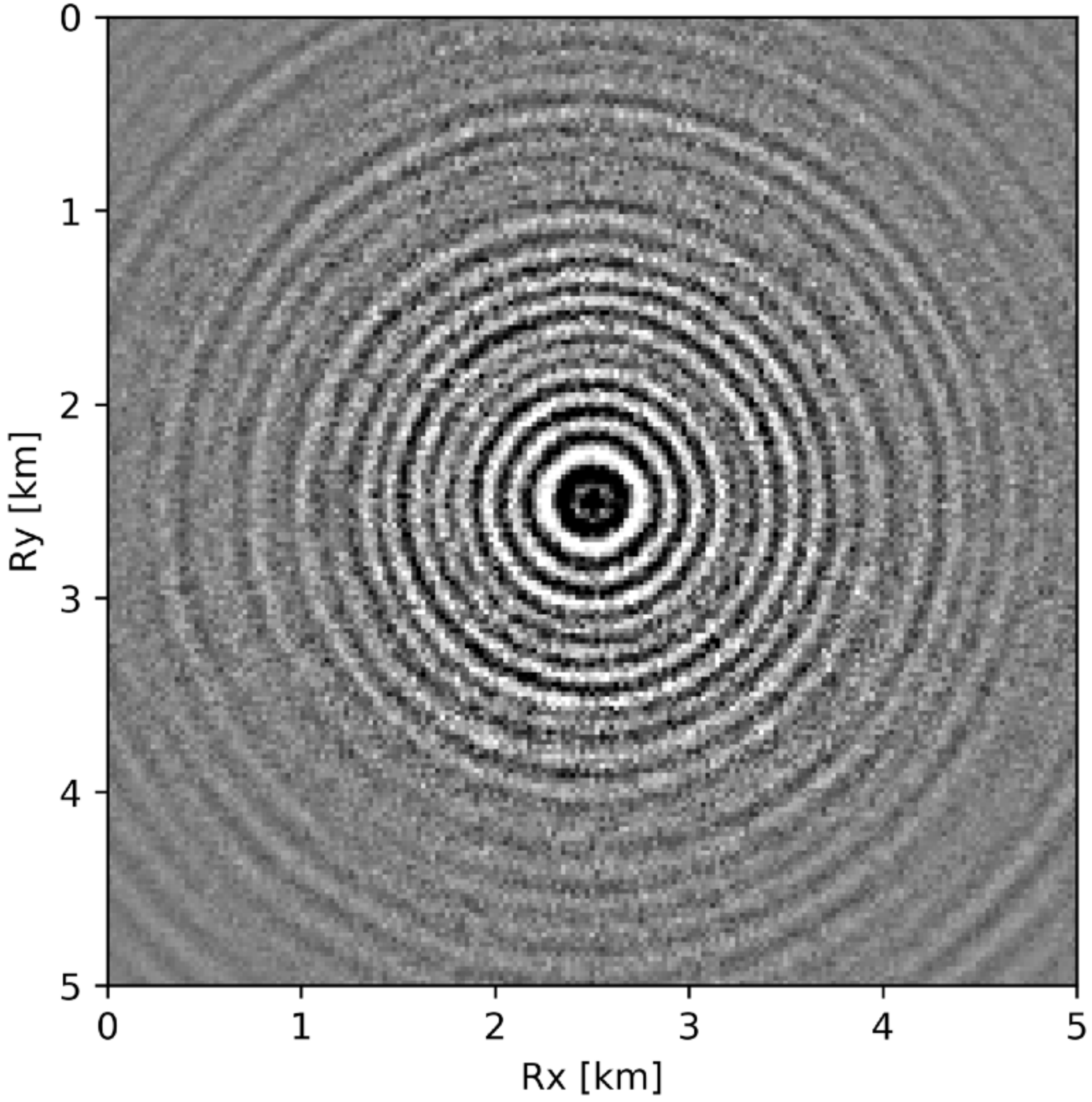

SNR = 3.7 dB
Rank = 228

Recovery
w/ recursively weighted matrix completion

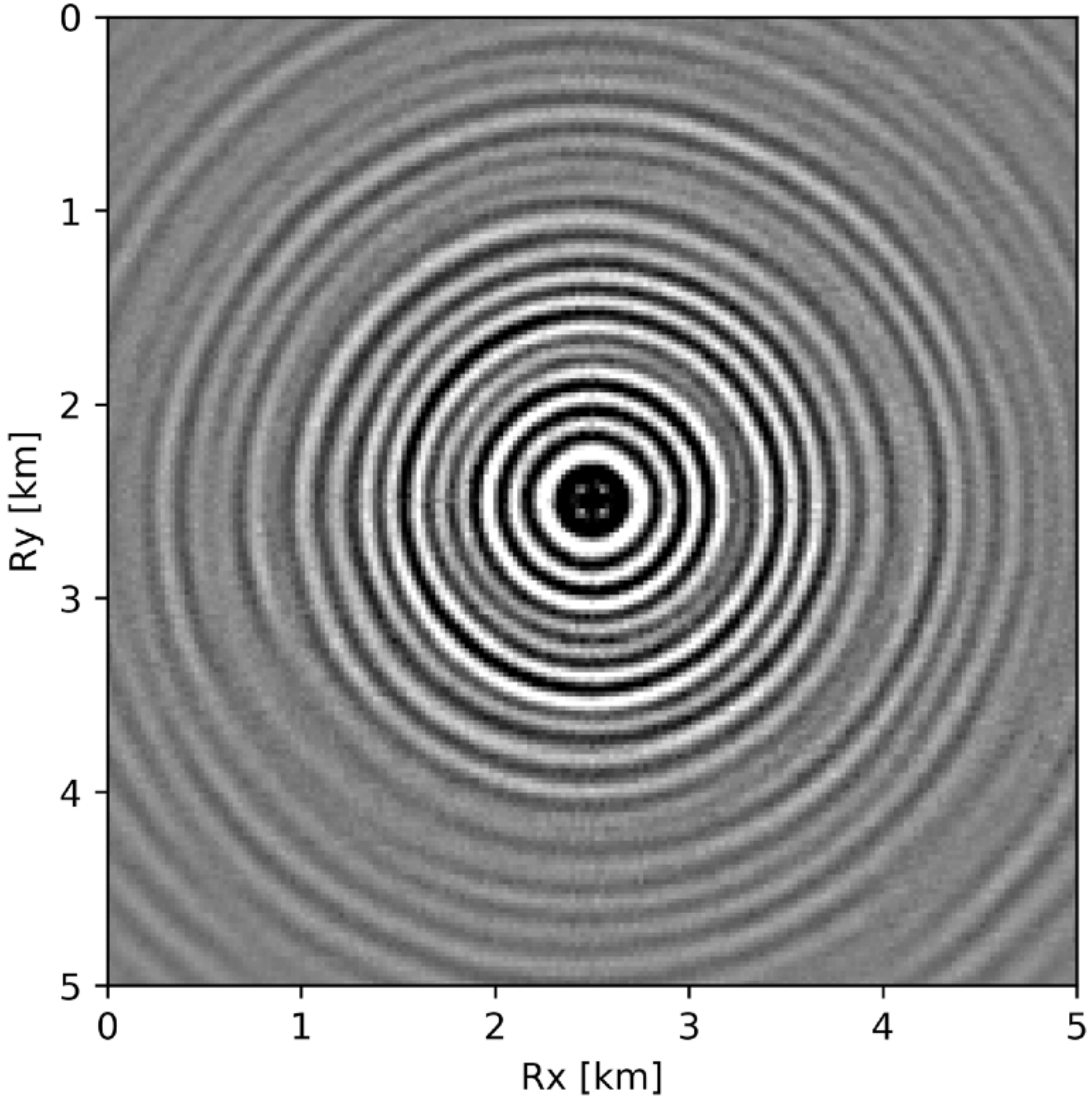

SNR = 12.5 dB
Rank = 228

Difference: True - Recovery
w/ conventional matrix completion

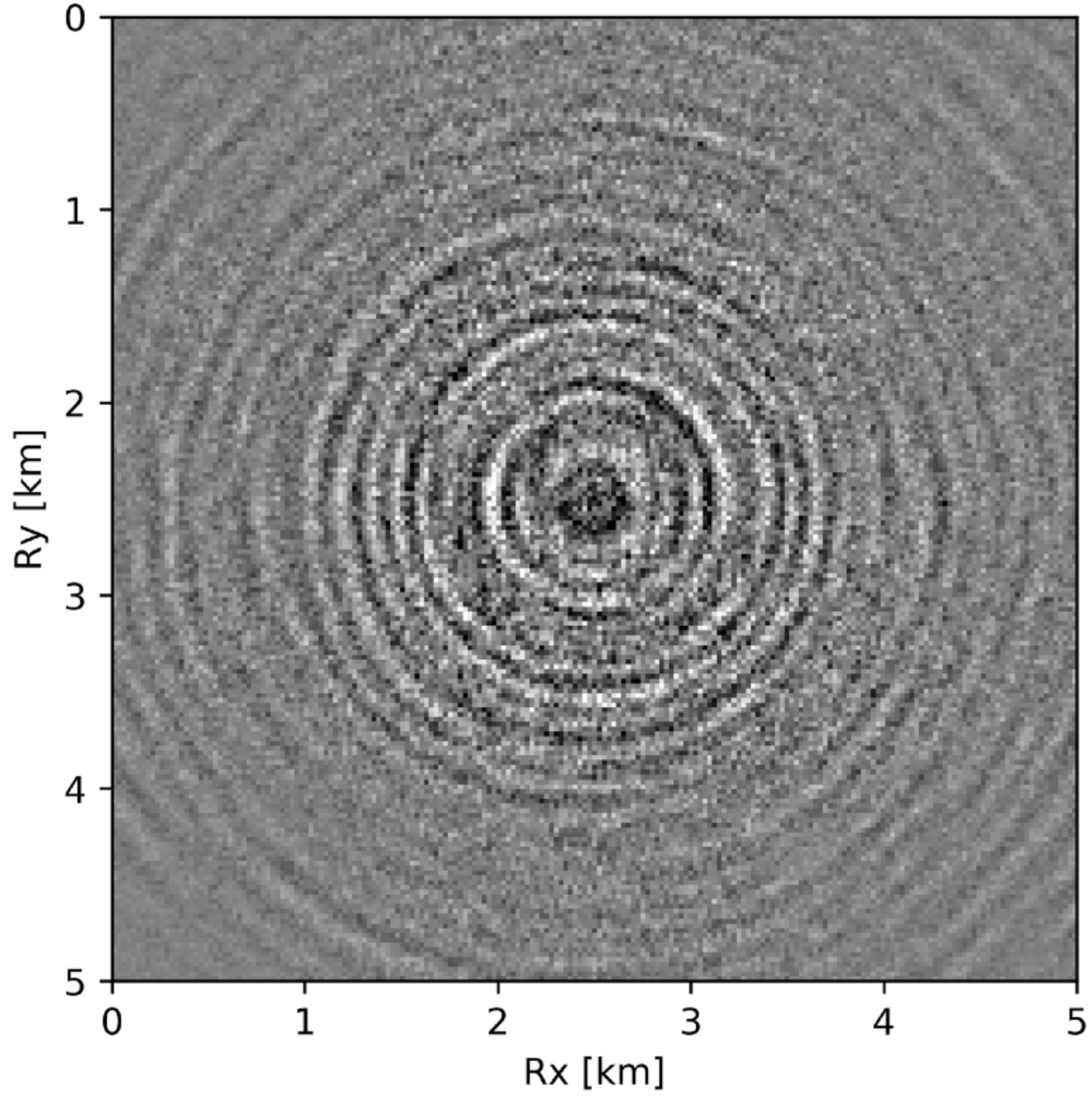

SNR = 3.7 dB
Rank = 228

Difference: True - Recovery
w/ recursively weighted matrix completion

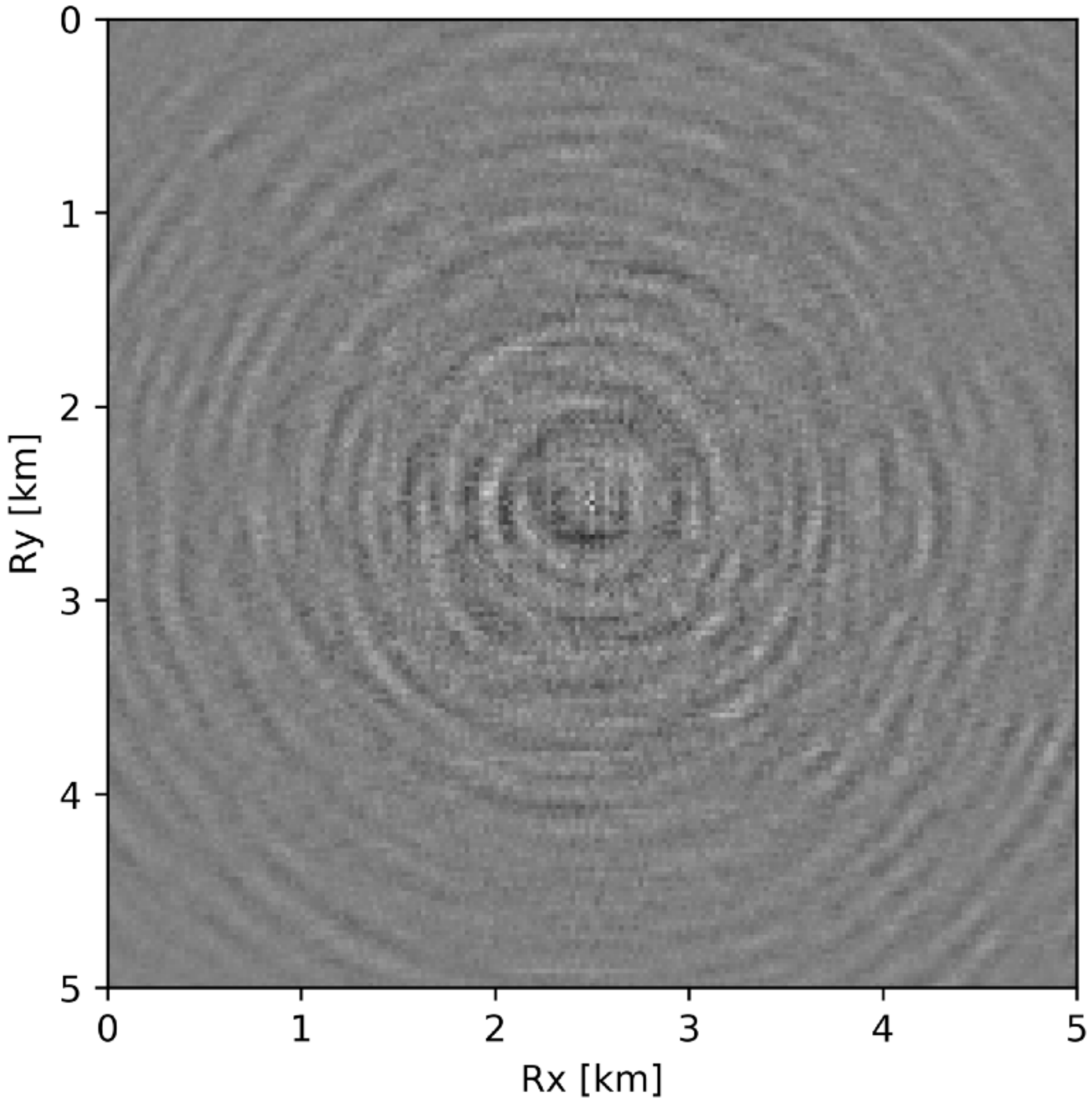

SNR = 12.5 dB
Rank = 228

Frequency-wavenumber (f-k) spectrum comparison (one shot)

Fully sampled data

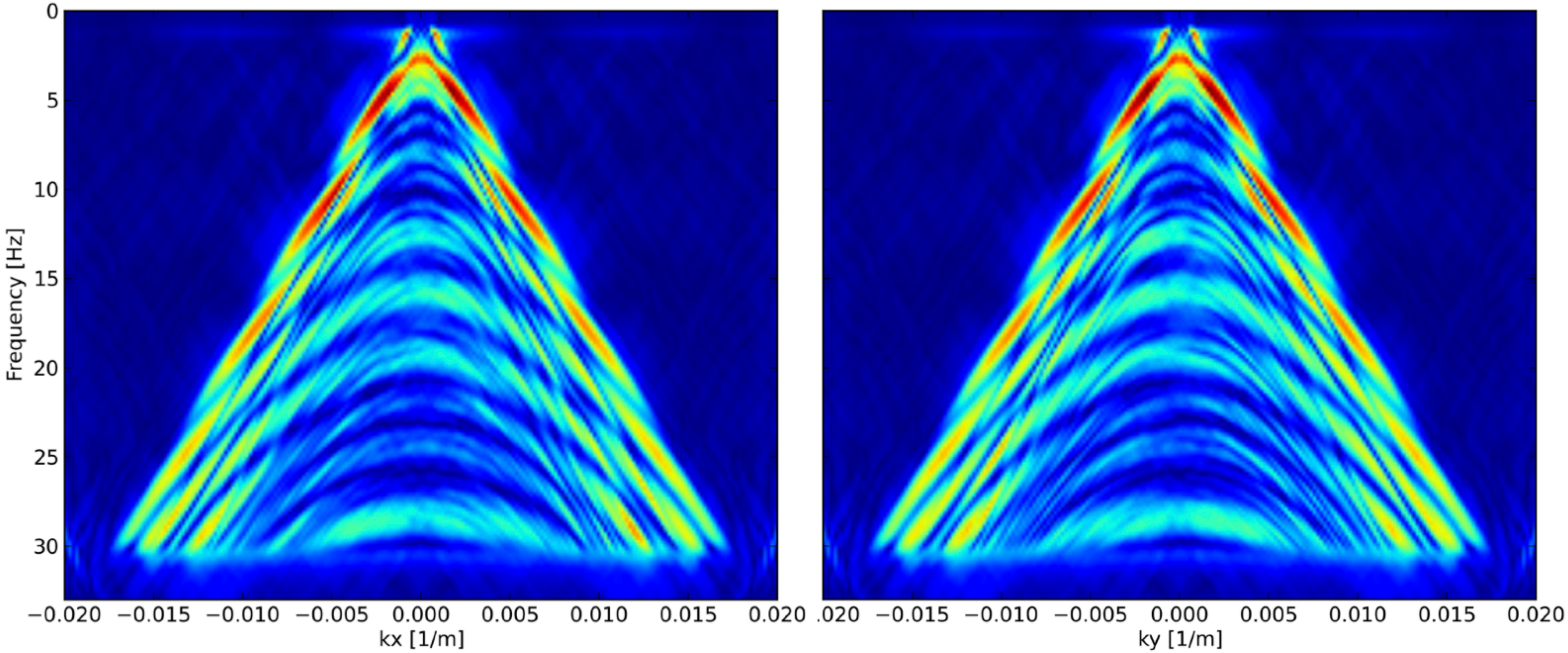

Observed data
90 % jittered subsampling

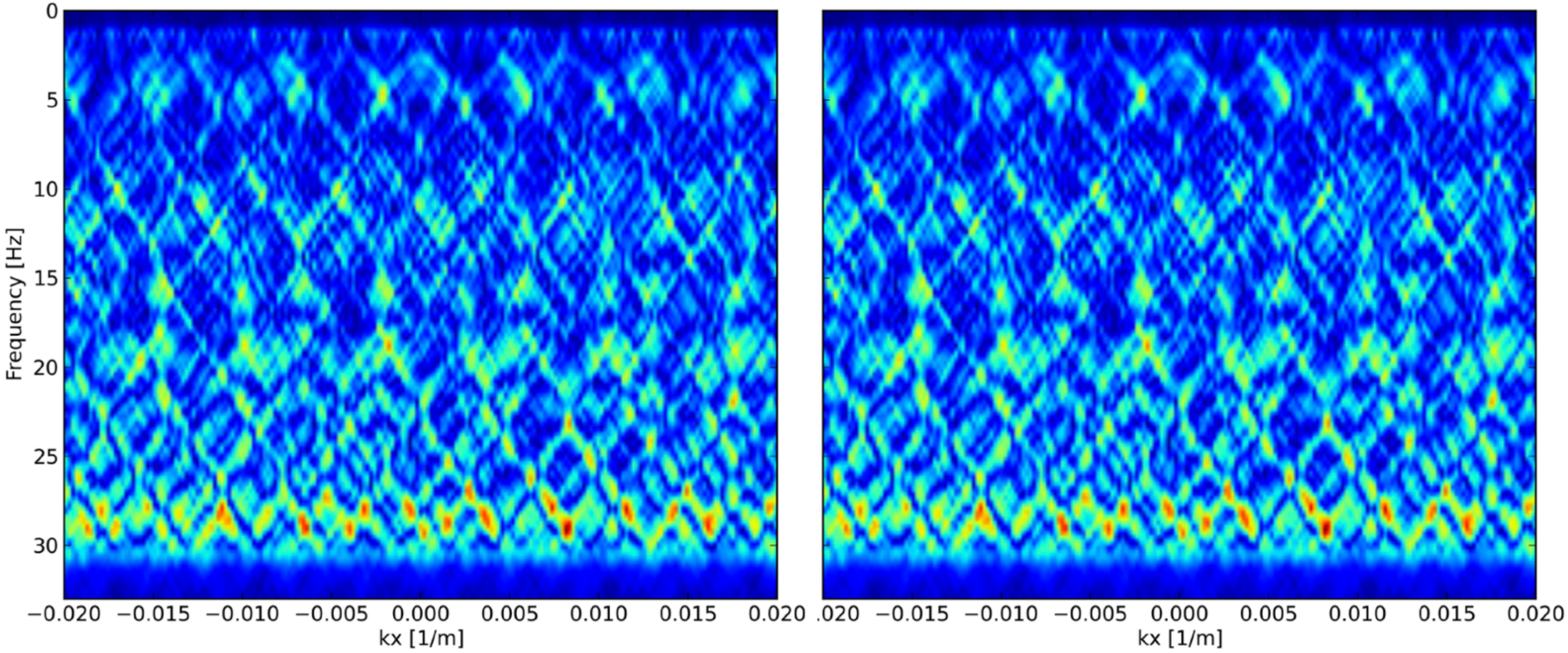

Recovery
w/ conventional matrix completion

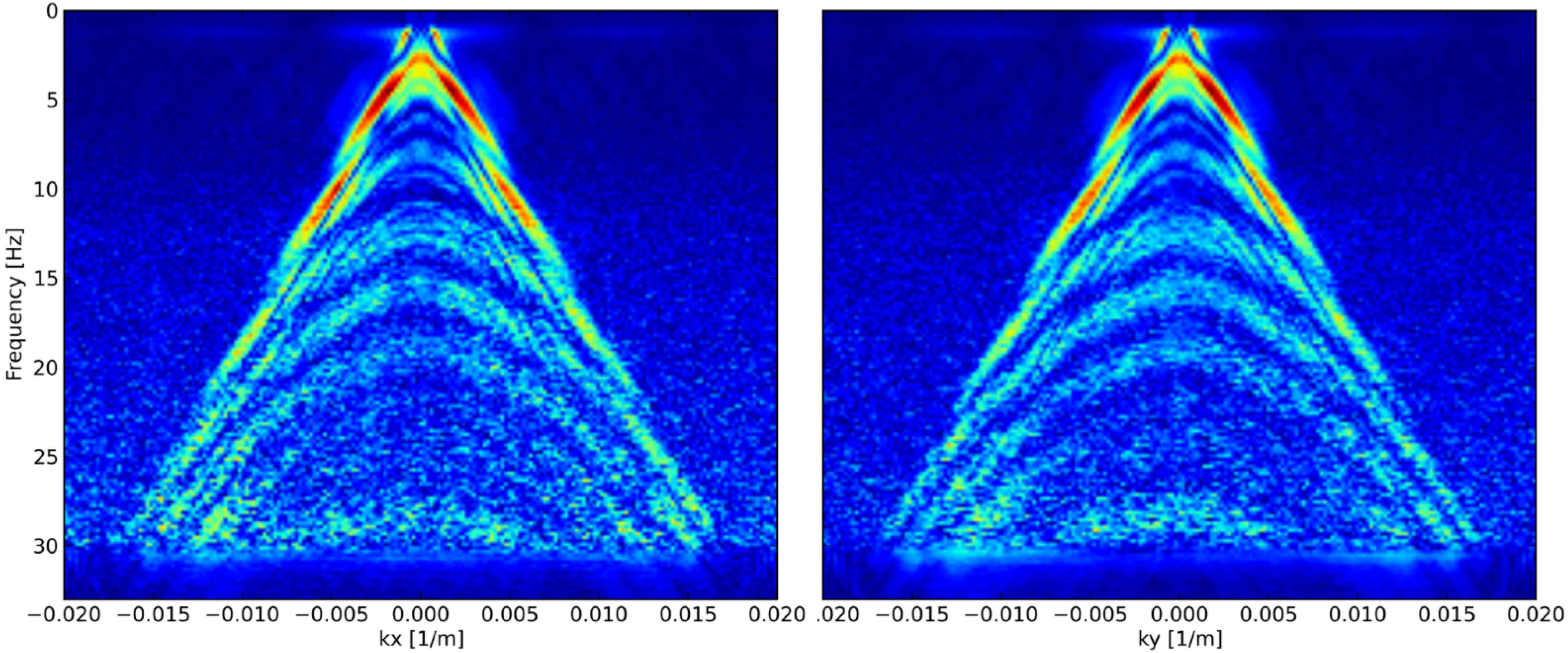

Recovery
w/ recursively weighted matrix completion

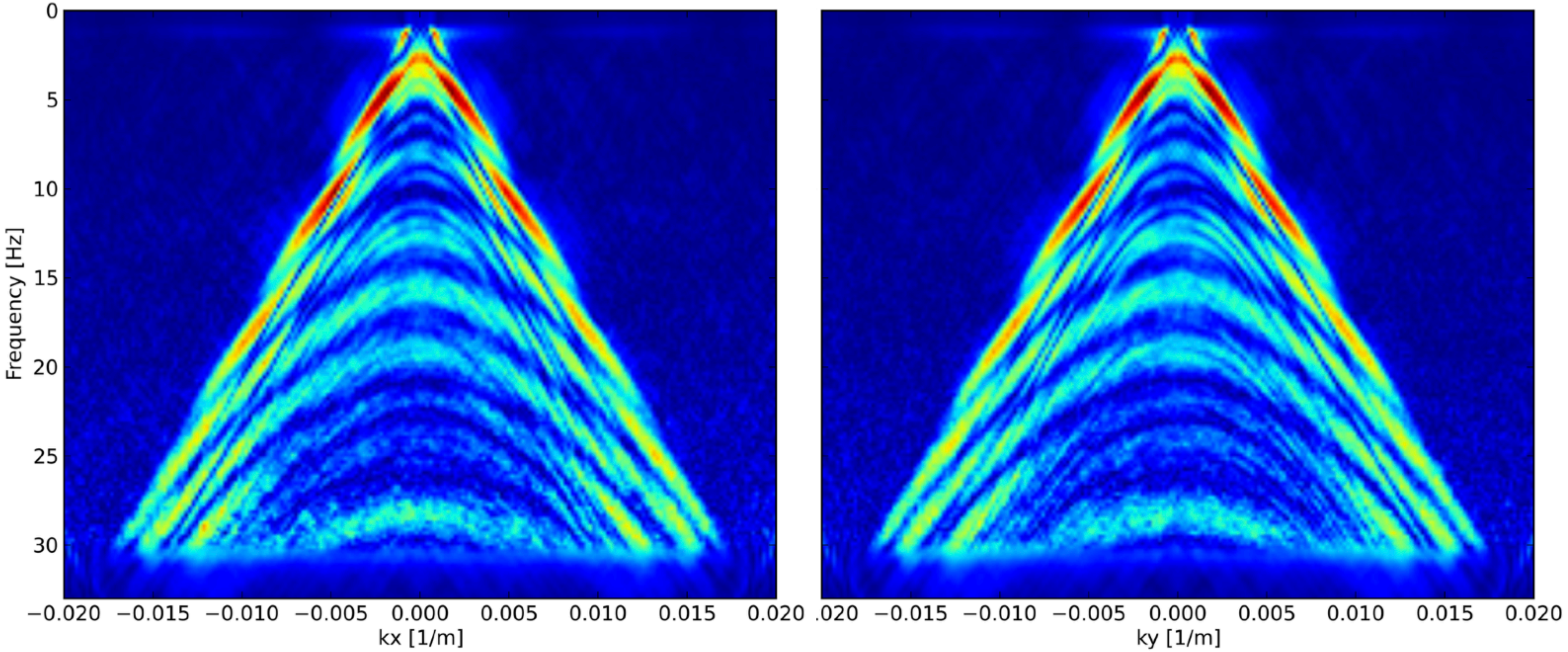

Contribution

Proposed a parallel weighted matrix completion for larger weights

Improved the reconstruction of higher frequency slices

Conclusions and future work

The weighted parallel matrix completion

- be implemented for larger weights
- achieves a significantly faster runtime, while maintaining similar SNRs

The recursively weighted parallel strategy

- improves SNR at higher frequencies

Extend this methodology of parallelism even with low weight values

A practical workflow for land seismic wavefield recovery with weighted matrix factorization

Chapter 5

Motivations

Weighted matrix completion for higher frequencies

- application to land data is hampered by ground roll

Ground roll corresponding to Rayleigh-type surface waves

- slow & aliased
- strong amplitude

Dominate the reconstruction at the expense of weaker body waves

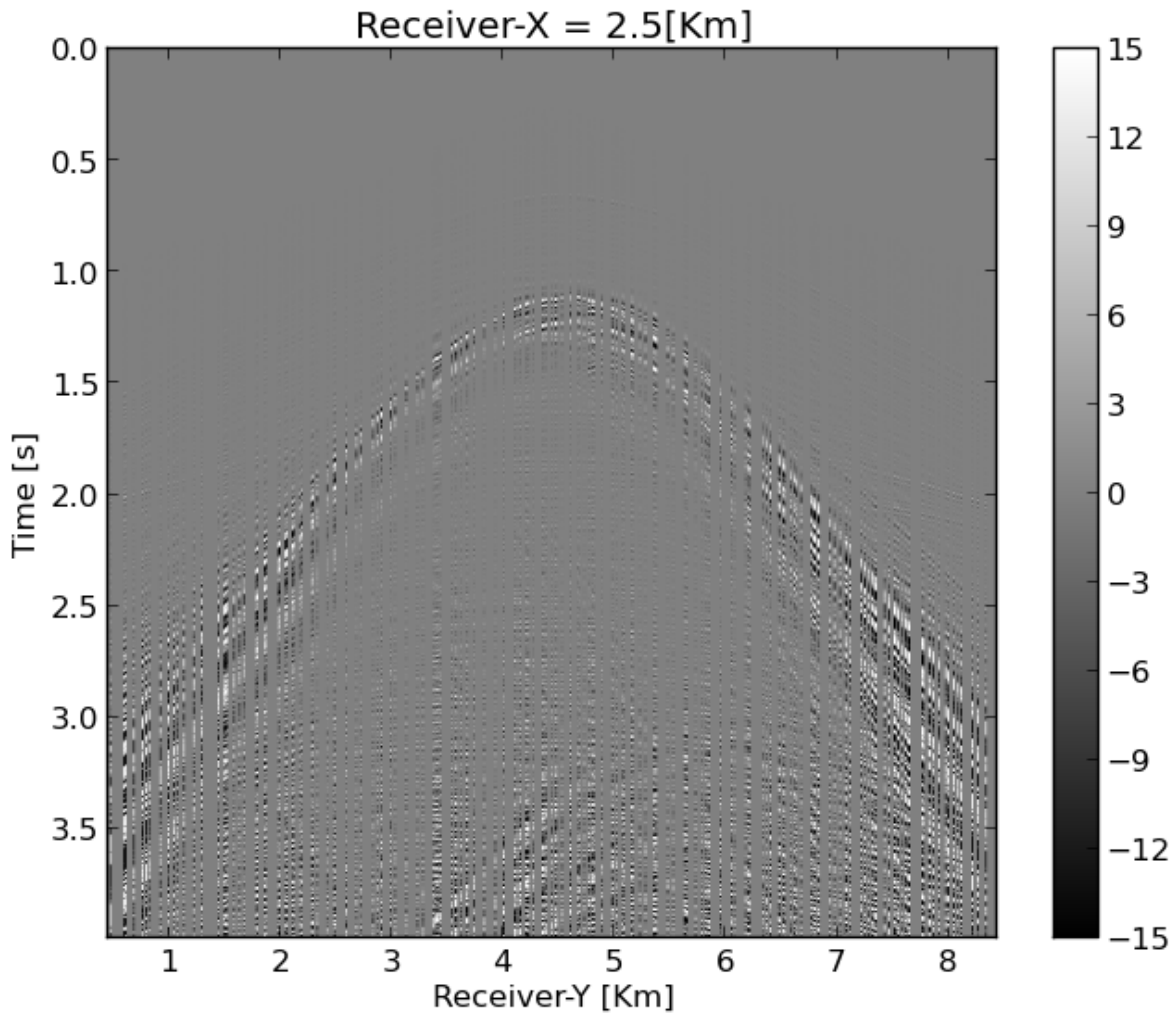

Van De Coevering, Norbert, Klaas Koster, and Rob Holt. "A scepVc's view of VVAz and AVAz." *SEG Technical Program Expanded Abstracts 2019*.
Tan, JusVn, et al. "SEAM Phase II Barre` model classic data study: Processing, imaging, and a`ributes analysis." *SEG Technical Program Expanded Abstracts 2019.*

Blind study on 3D SEAM Barrett dataset

Data dimension: 80 x 21 x 641 x 641 x 667
$(n_{rx} \times n_{ry} \times n_{sx} \times n_{sy} \times n_t)$

Receiver sampling interval: 12.5 m

Source sampling interval: 25 m in the shot line direction and 100 m in the perpendicular direction

Time sampling interval: 0.006 s

Subset of dataset:

- Benchmark for land data
- Contains realistic surface waves

https://www.researchgate.net/publication/

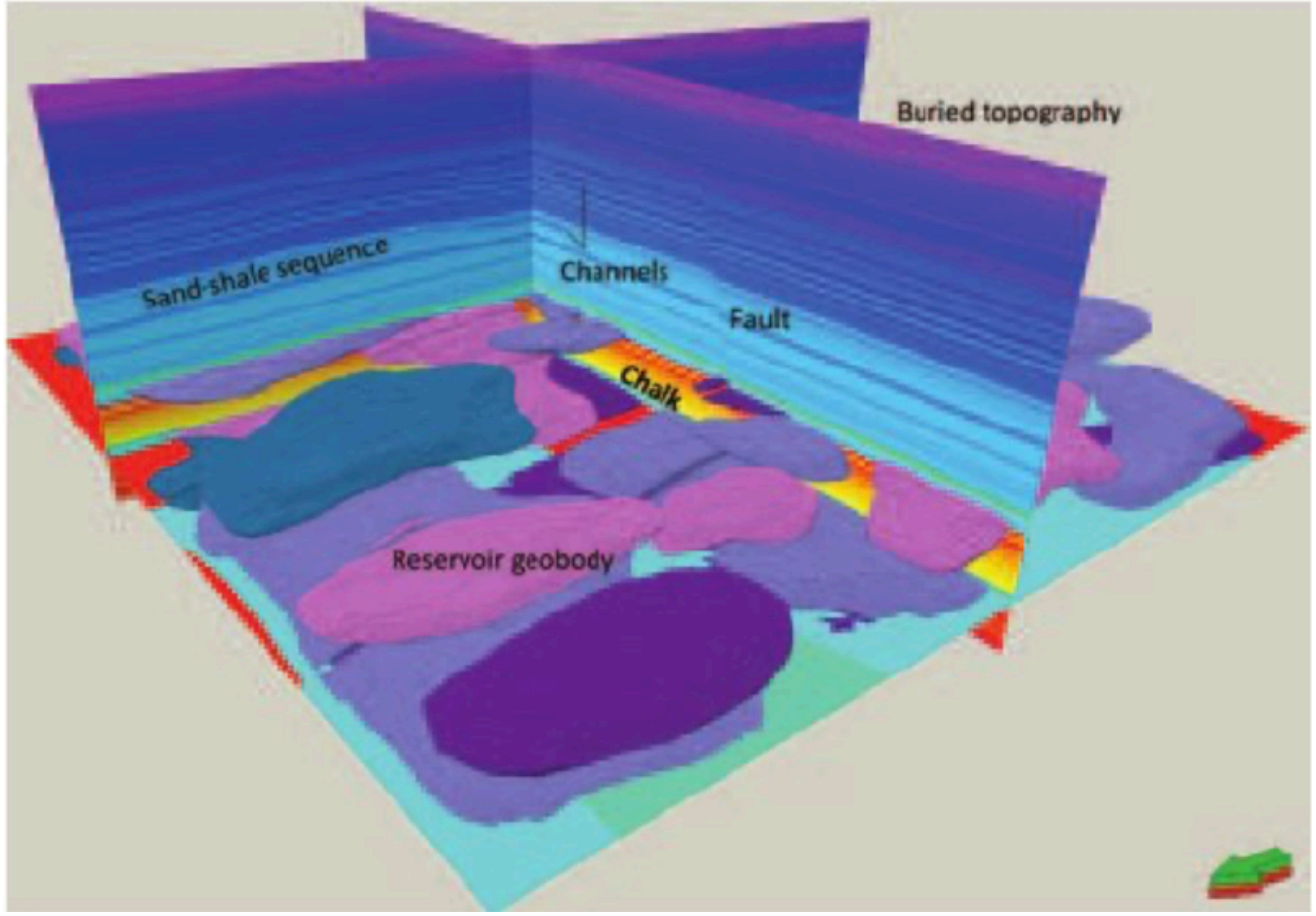

Acquisition geometry

w/ ~$75\ \%$ missing receivers, 21 source lines

A subset consists of 21 source lines (red lines in the center area)

Each source line contains 80 sources

The 8×8 km receiver aperture moves with the source location

- neighboring shots share most randomly sampled receivers (black dots in the figure)
- some drop-off and others add (red and blue rectangles in the figure)

Acquisition geometry for the observed dataset

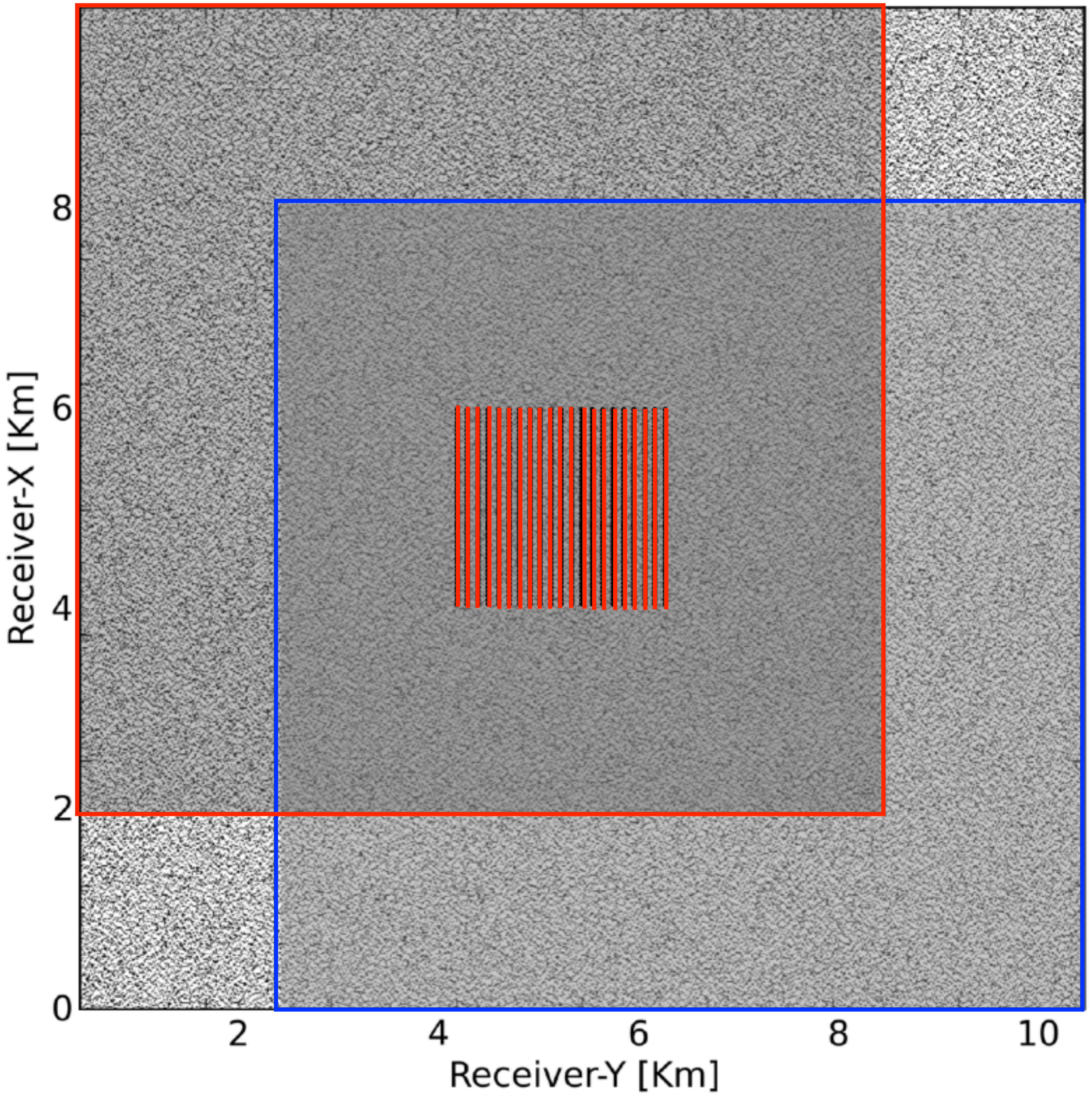

Observed data in time domain (one shot)

w/ ~75 % missing receivers

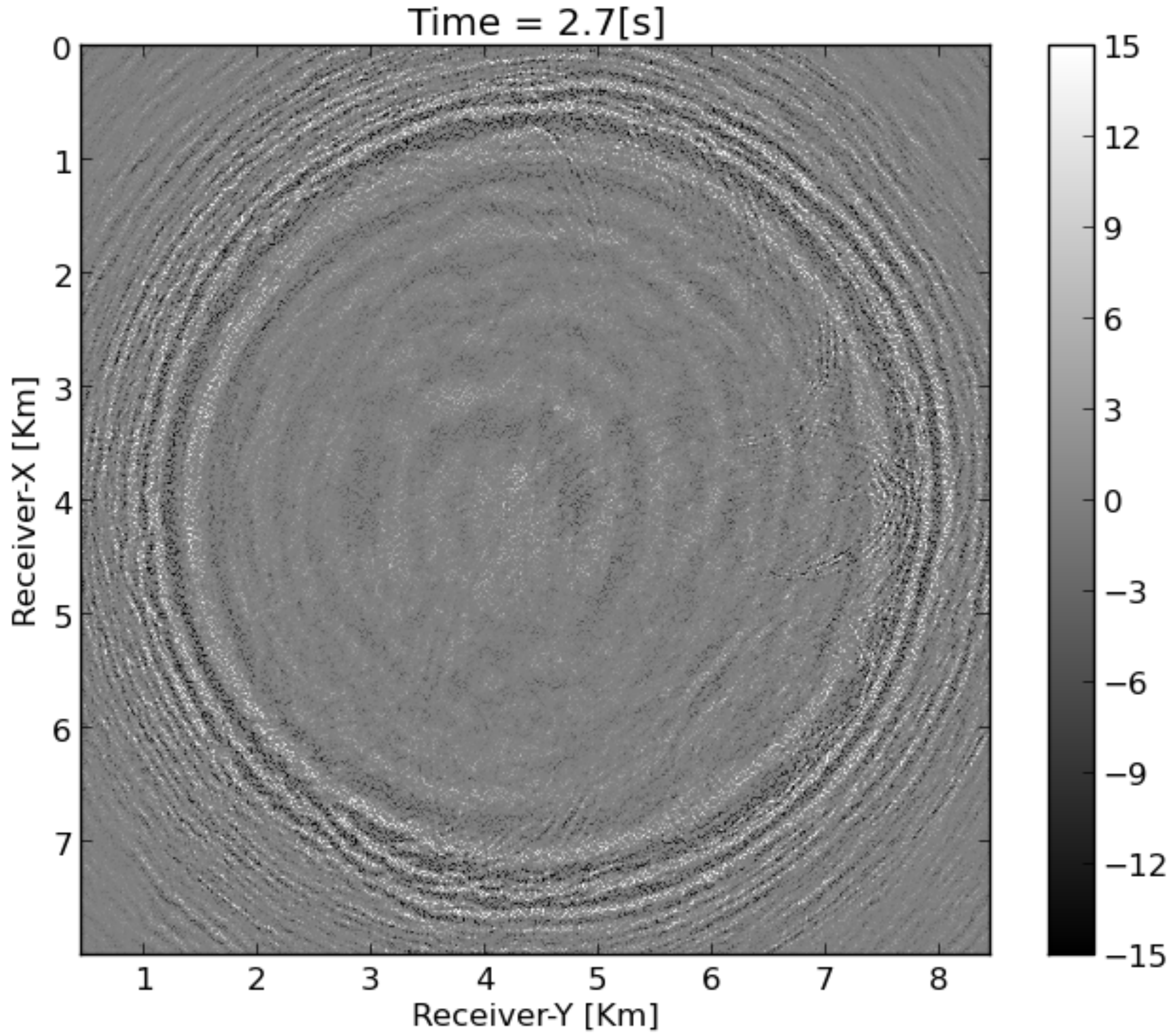

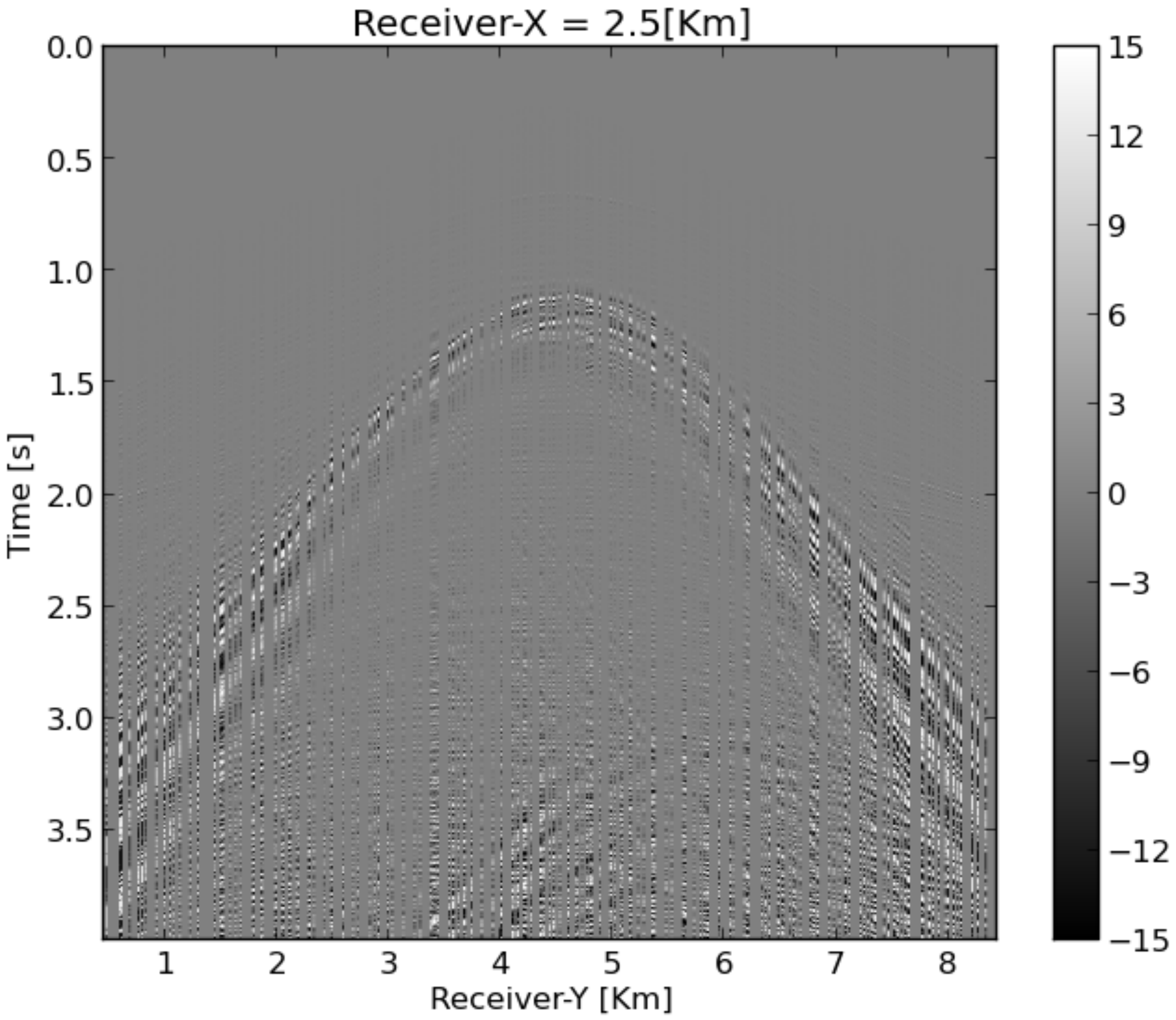

An automatic gain control (AGC) is applied to this observed dataset.

Observed data in time domain (one shot)
w/ ~75 % missing receivers

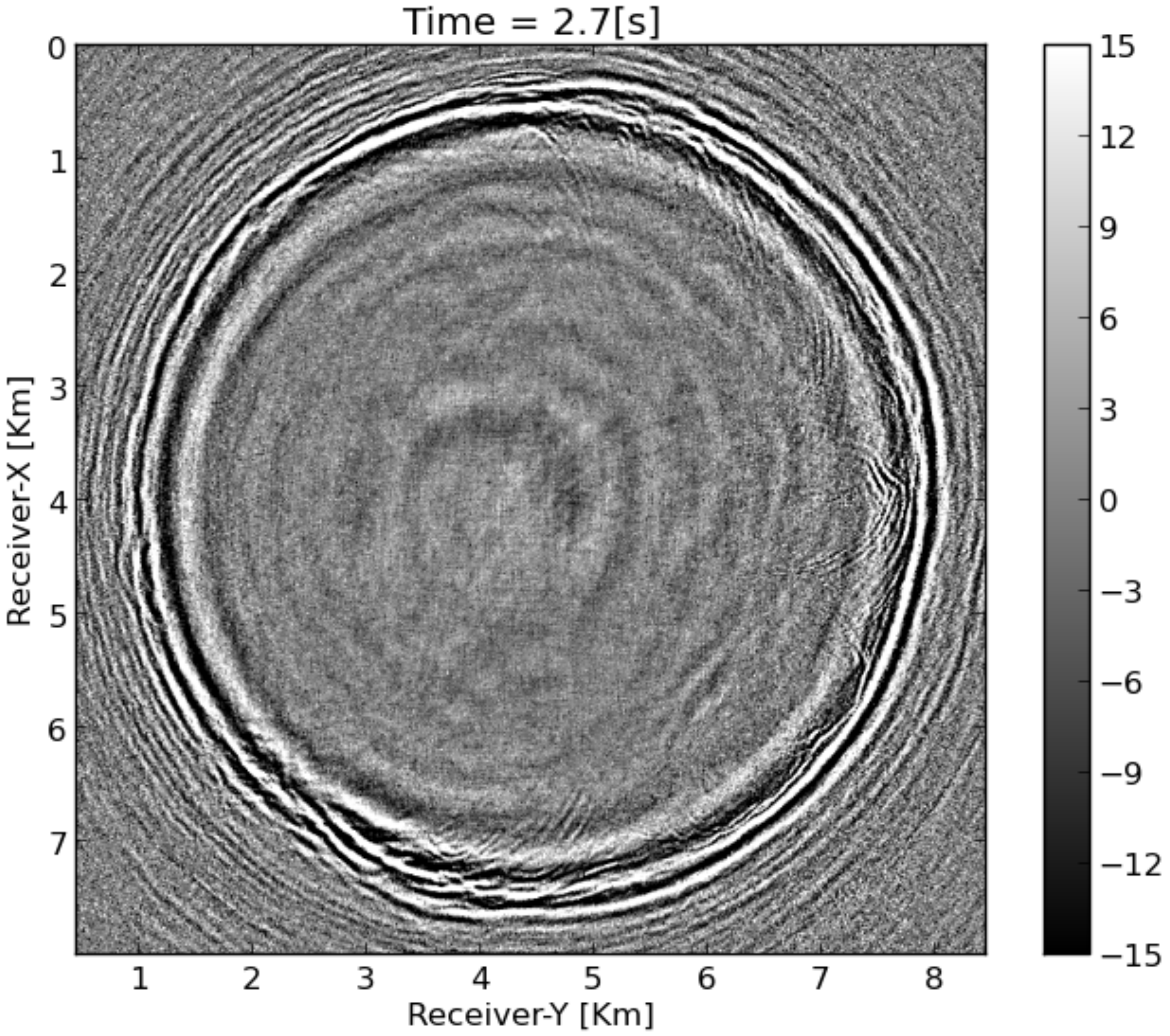

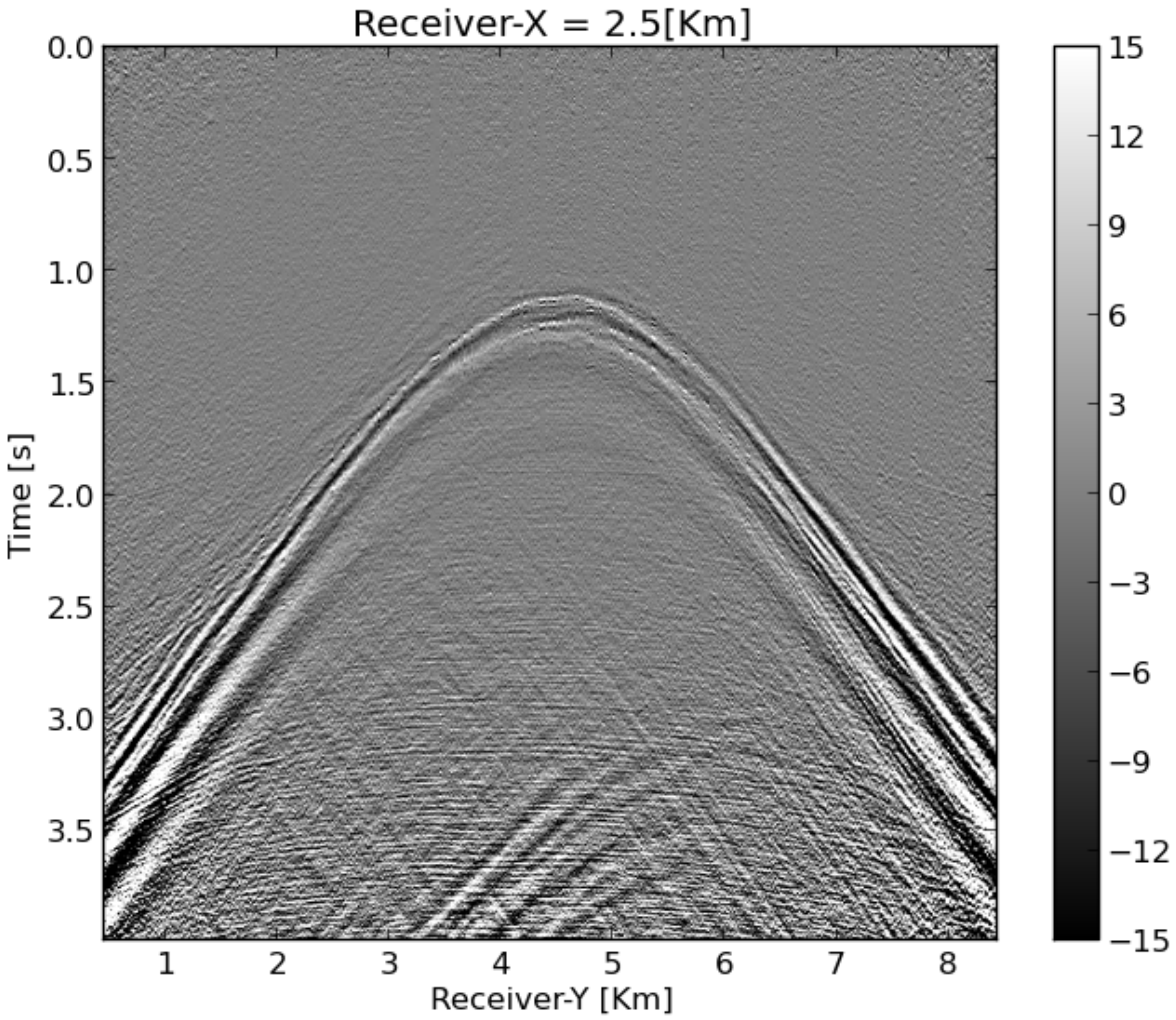

Question

How can we use the weighted matrix factorization on land data while avoiding the impact of ground roll?

Answer:

- Reconstruct the body and surface (ground roll) waves separately.

Why separation?

Answer:

- Reduce the effect of the strong aliased ground roll on the body wave reconstruction.
- The ground roll could be separated from the body wave, at least in an approximate sense.

Proposed workflow

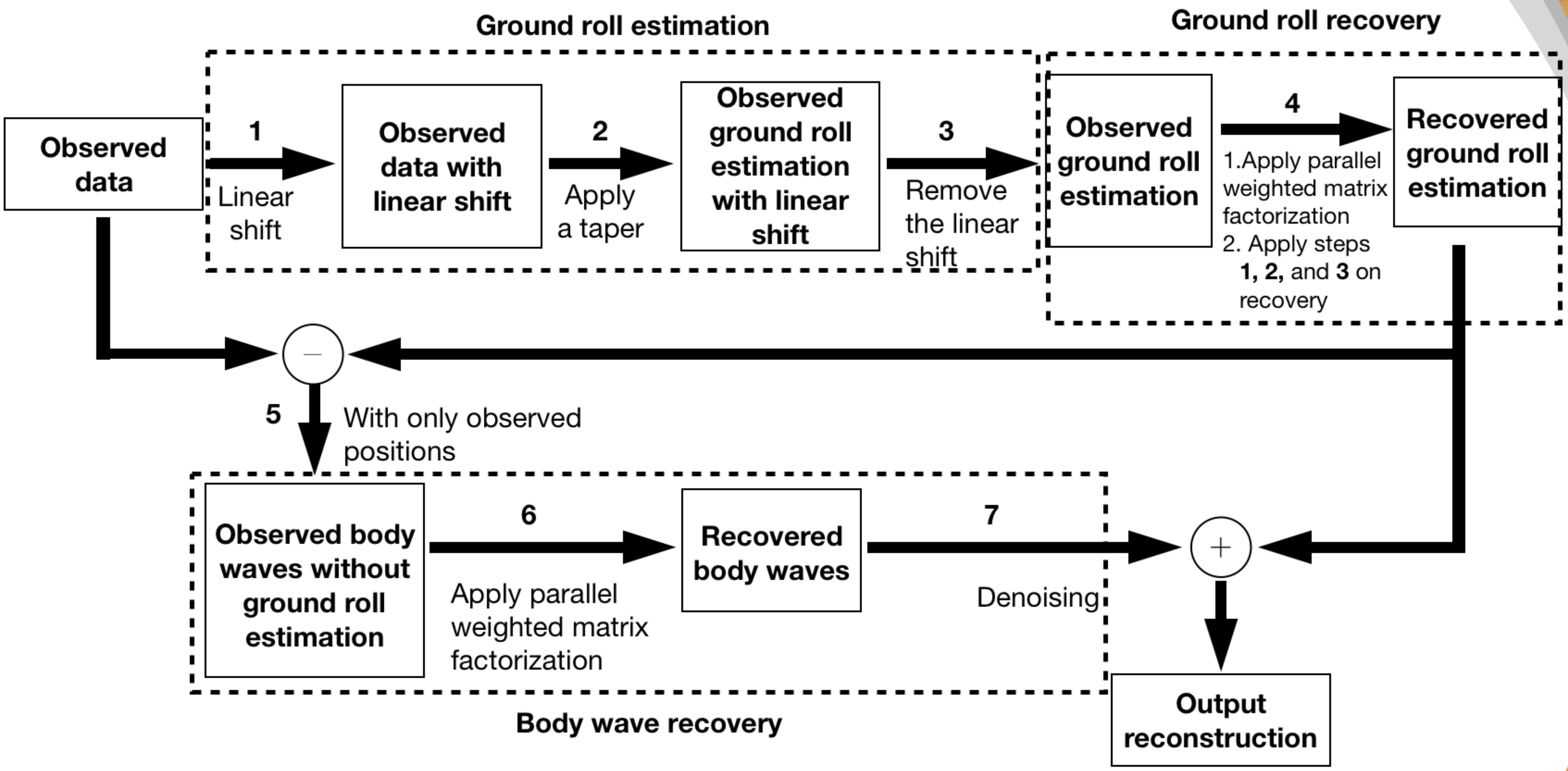

Final reconstructed result in time domain

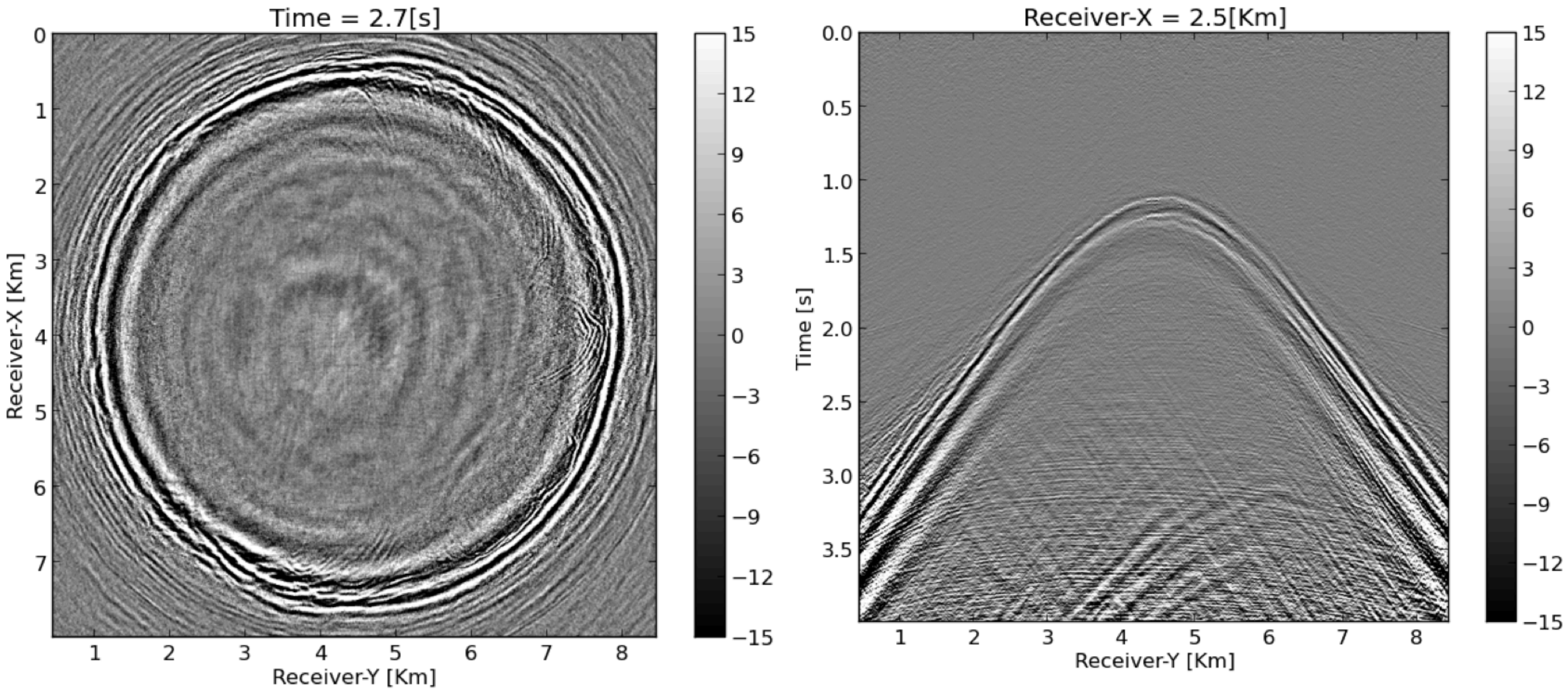

QC

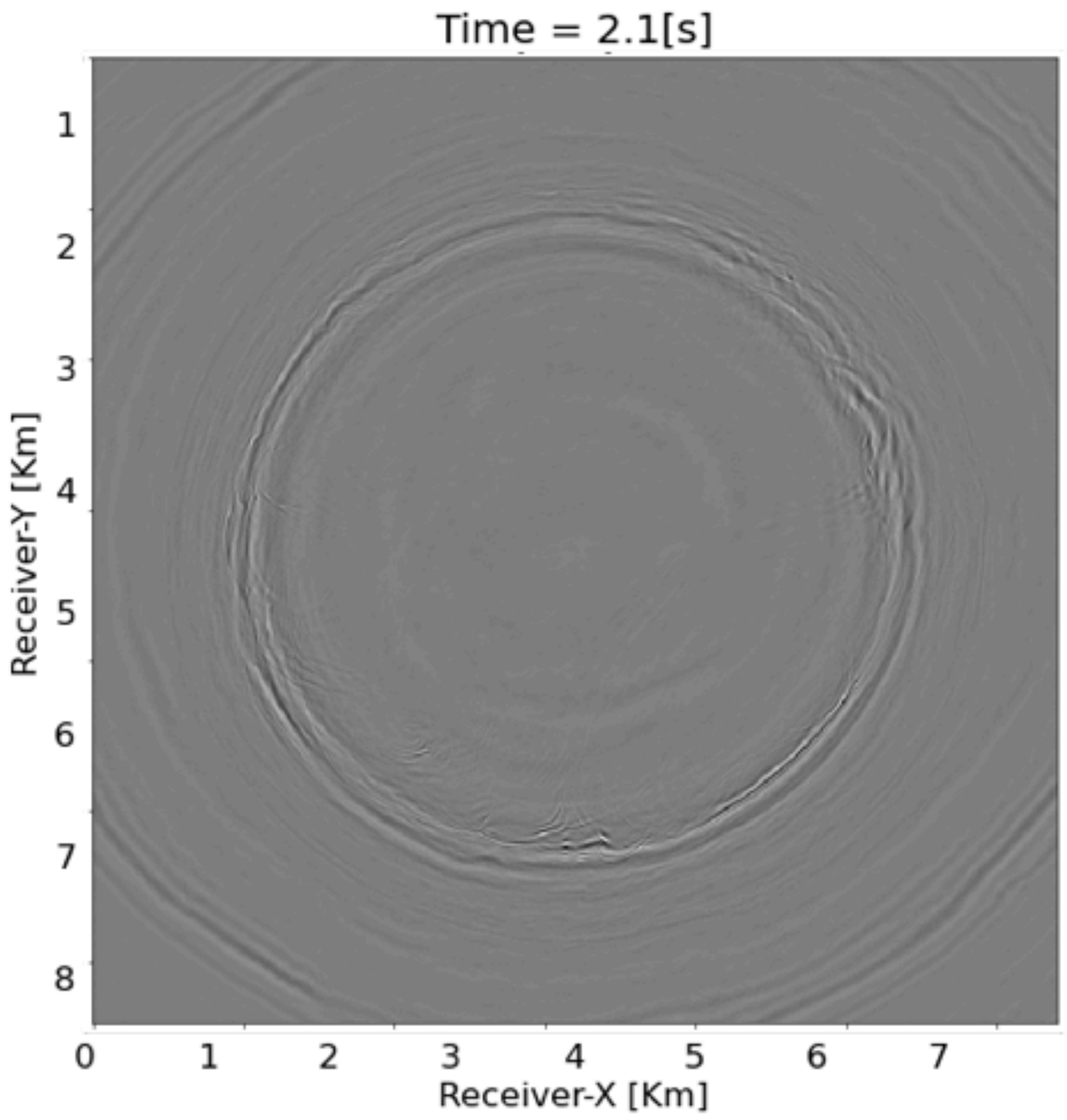

Ground truth

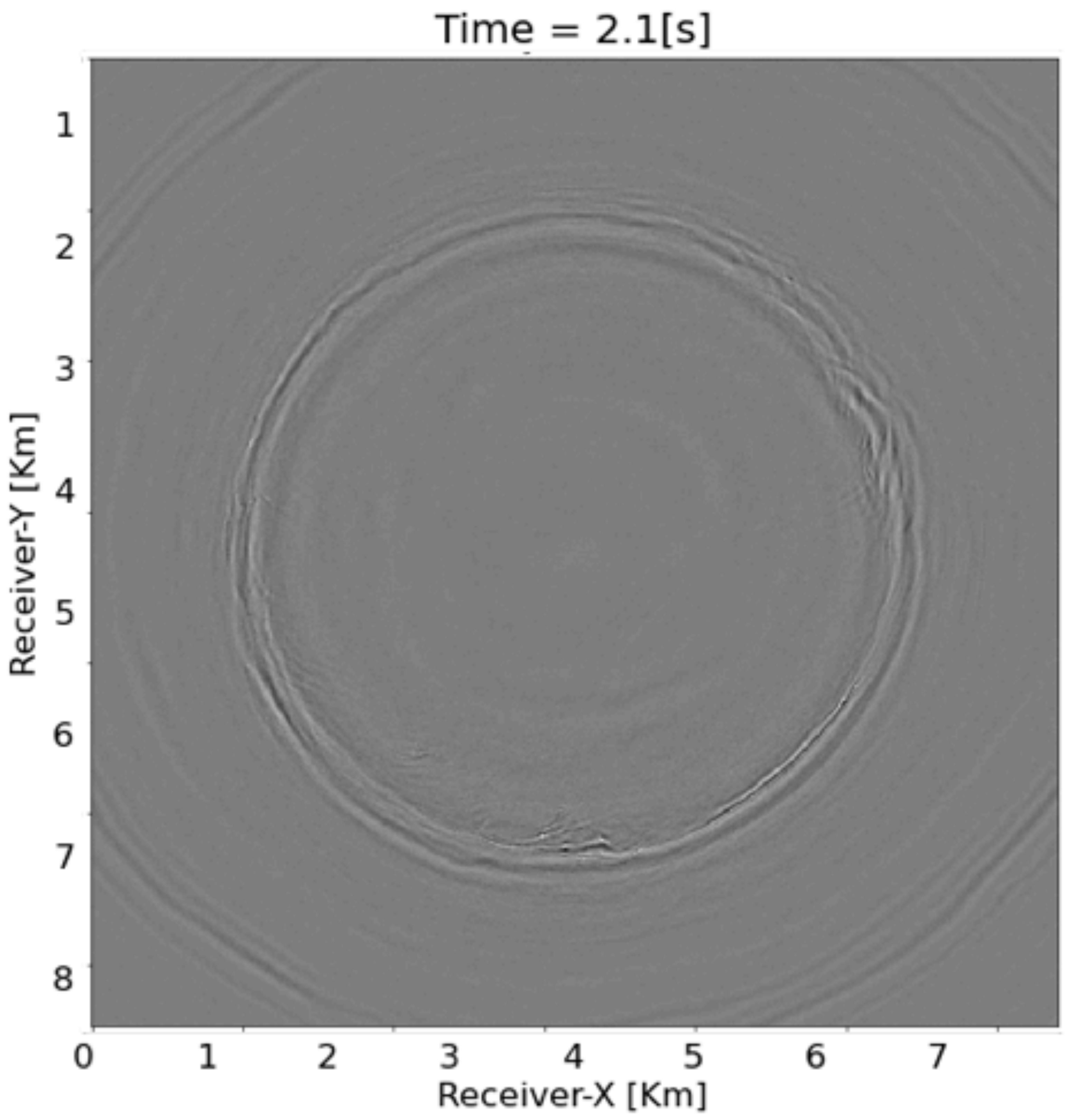

Recovered data

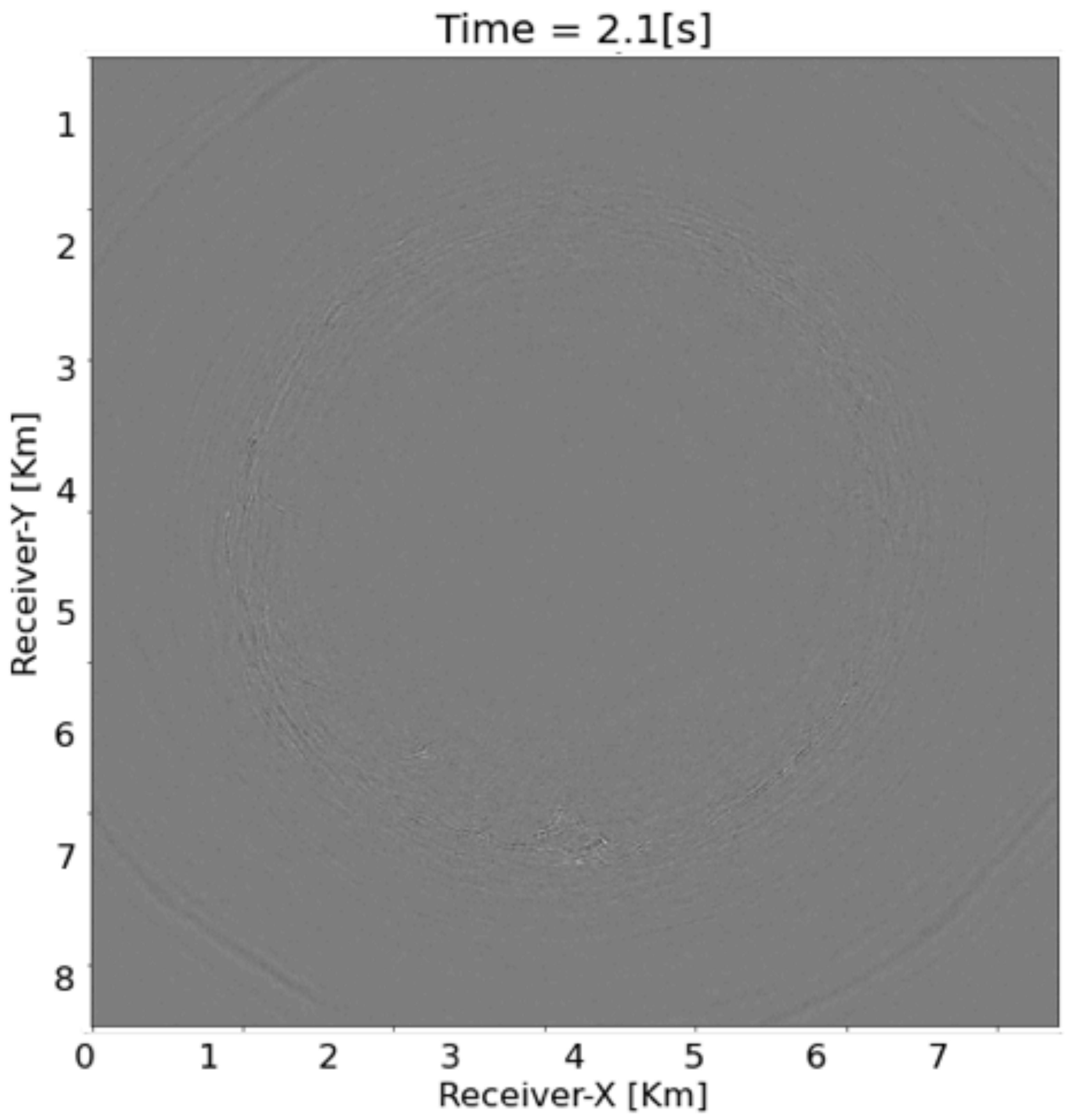

Difference

Contribution and conclusion

We mitigate the effects of the strongly aliased ground roll by employing the proposed separation.

Furthermore, the proposed workflow successfully recovers body waves (reflections and diffractions).

Acknowledgement

I would like to thank my PhD advisor Professor Felix J. Herrmann for his support and guidance.

I would like to thank Professor Ghassan AlRegib, Professor Zhigang Peng, Professor Faramarz Fekri and Professor Oscar Lopez for their support of my doctoral training.

I would also like to thank my colleagues and researchers at SLIM for their support and collaboration.

SLIM

Acknowledgement

This research is carried out with the support of Georgia Research Alliance and partners of the ML4Seismic Center.

I would like to express my gratitude to Georgia Institute of Technology for funding this study.

I would also like to thank Occidental for providing the dataset, as well as Klaas Koster for his professional help.

Thank you for your attention!!